



T.R.

**ONDOKUZ MAYIS UNIVERSITY
INSTITUTE OF HEALTH SCIENCES
DEPARTMENT OF HISTOLOGY AND EMBRYOLOGY**

**POSSIBLE EFFECTS OF GARLIC AND MOMORDICA
CHARANTIA ON RAT CEREBELLUM AFTER
EXPOSURE TO 900 MHZ ELECTROMAGNETIC FIELD**

DOCTORAL THESIS

Fathelrahman Idris Gasmelseed ALI

**Samsun
November-2019**



T.R.

**ONDOKUZ MAYIS UNIVERSITY
INSTITUTE OF HEALTH SCIENCES
DEPARTMENT OF HISTOLOGY AND EMBRYOLOGY**

**POSSIBLE EFFECTS OF GARLIC AND MOMORDICA
CHARANTIA ON RAT CEREBELLUM AFTER
EXPOSURE TO 900 MHZ ELECTROMAGNETIC FIELD**

DOCTORAL THESIS

Fathelrahman Idris Gasmelseed ALI

Supervisor

Prof. Dr. Suleyman KAPLAN

Samsun

November-2019

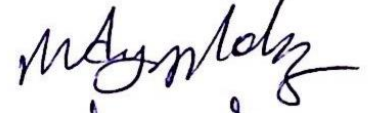
T.R.
ONDOKUZ MAYIS UNIVERSITY
INSTITUTE OF HEALTH SCIENCES

The thesis prepared by Fathelrahman Idris Gasmelseed Ali entitled "Possible effects of garlic and *Momordica charantia* on rat cerebellum after exposure to 900 MHz electromagnetic field" has been supervised by Prof. Dr. Suleyman Kaplan and accepted by the committee members as PhD thesis of the Department of Histology and Embryology, following the examination on the date 29/11/2019.

Chairman: Prof. Dr. Suleyman Kaplan, Ondokuz Mayıs University



Member: Prof. Dr. Mustafa Ayyıldız, Ondokuz Mayıs University



Member: Prof. Dr. Abdurrahman Aksoy, Ondokuz Mayıs University



Member: Prof. Dr. Berrin Zuhale Altunkaynak, Okan University



Member: Assist. Prof. Seda Karabulut, Medipol University



CONFIRMATION

This thesis has been approved by the committee members that already stated above and determined by the Institute Executive Board.

.... / /

Prof. Dr. Ahmet Uzun
Director of Institute of Health Sciences

ACKNOWLEDGEMENTS

First of all, I would like to express from the bottom of my heart my special thanks and appreciation to my supervisor Professor Suleyman Kaplan who supported me throughout my PhD journey with his constant support, precious advice, and excellent supervision. Not only he has been wonderful mentor but offered me good experience in the field of stereology and electromagnetic field at Ondokuz Mayıs University, Samsun, Turkey.

I would like to express my heartfelt thanks and sincere gratitude to Professor Berrin Zuhale Altunkaynak for her kind help and cooperation. My deep thanks to Associate Professor Mehmet Emin Onger for his valuable advice and cooperation. I would like to express my gratitude to Associate Professor Bahattin Avcı and Research Assistant Sebati Sinan Urkmez for allowing me to conduct the biochemical analysis in my study in the biochemistry department and for their help. I have no words to express my sincere thanks and appreciation to my colleague Gamze Altun who helped and guided me from the beginning to the end of my thesis. A special gratitude to my colleague Dr. Ömür Gülsüm Deniz for her valuable help and excellent support throughout my works. I am also very thankful to all PhD students specially, Kıymet Kubra Yurt, Elvide Gizem Kivrak, Adem Kocaman, Isinsu Aydın, Erkan Erener and Burcu Delibaş for their cooperation and supports. Without the help of these colleagues, this thesis would not have been possible.

I would like to thank everyone in the Department of Histology and Embryology, for their help, support and for allowing me to obtain all the needs for my thesis.

I would like to thank the Khartoum University, they allowed and supported me for my PhD study to be done in the Ondokuz Mayıs University.

Finally, I express my warm gratitude to my parents (Idris and Nadia), sisters and brothers for their support, care and encouragement to complete my work. I dedicate this thesis to them.

ÖZET

900 MHZ ELEKTROMANYETİK ALANA MARUZ KALMIŞ SIÇAN BEYİNCİĞİ ÜZERİNE MOMORDICA CHARANTIA VE SARIMSAĞIN MUHTEMEL ETKİLERİNİN ARAŞTIRILMASI

Amaç: Bu çalışmanın amacı, 900 MHz'lik elektromanyetik alan (EMA) maruziyeti sonrası antioksidan özelliği bulunan sarımsak (Sar) ve *Momordica charantia*'nın (Kudret narı-MC) sıçan beyinciği üzerindeki etkisini araştırmaktır.

Materyal ve Metot: Çalışma, 56 adet 12 haftalık erişkin erkek Wistar albino sıçan üzerinde yapıldı. Hayavanlar, her biri 7 sıçandan oluşan 8 gruba ayrıldı: EMA grubu, EMA+Sar grubu, EMA+MC grubu, EMA+Sar+MC grubu, Sar grubu, MC grubu, Sham grubu and Kontrol (Kont) grubu. EMA, EMA+Sar, EMA+MC, EMA+Sar+MC gruplarındaki sıçanlar, 28 gün boyunca günde 1 saat 900 MHz EMA'ya maruz bırakıldı. Her sıçan beyinciğindeki Purkinje hücrelerinin sayısının hesaplanması için stereolojik teknikler uygulandı. Oksidatif stresi değerlendirmek için süperoksit dismutaz (SOD) ve katalaz (CAT) enzim analizleri yapıldı.

Bulgular: EMA grubu ile Kont grubu toplam Purkinje hücre sayısı bakımından karşılaştırıldığında anlamlı bir fark gözlenmedi ($p>0,05$). Ancak, toplam Purkinje hücresi sayısı, EMA+MC ve EMA+Sar+MC gruplarında EMA grubuna göre anlamlı derecede daha yüksekti ($p<0,05$). Sar grubundaki Purkinje hücrelerinin sayısı, EMA ve sham gruplarından anlamlı derecede yüksekti ($p<0,01$). EMA grubundaki SOD aktivitesi, EMA+Sar grubuna göre ($p<0,05$) ve EMA+MC, EMA+Sar+MC, Sar ve MC gruplarına göre anlamlı derecede düşüktü ($p<0,01$). EMA ve Kont grupları arasında SOD aktivitesinde anlamlı bir fark saptanmadı ($p>0,05$). EMA grubundaki CAT enzim aktivitesinin, Sar grubundan anlamlı derecede düşük olduğu gözlemlendi ($p<0,05$) ve diğer gruplar arasında anlamlı fark saptanmadı ($p>0,05$).

Sonuç: 900 MHz'lik EMA'ya maruz kalma, erkek sıçan beyinciğindeki Purkinje hücrelerinin sayısının ve morfolojisini etkilemektedir. MC veya Sar ve MC' nin birlikte kullanılması, Purkinje hücreleri üzerinde koruyucu bir etkiye sahip olabilir.

Anahtar Kelimeler: Elektromanyetik alan; Beyincik; Sarımsak; *Momordica charantia*; Purkinje hücreleri; Stereoloji

Fathelrahman Idris Gasmelseed Ali, Doktora Tezi
Ondokuz Mayıs Üniversitesi - Samsun, Kasım-2019

ABSTRACT

POSSIBLE EFFECTS OF GARLIC AND MOMORDICA CHARANTIA ON RAT CEREBELLUM AFTER EXPOSURE TO 900 MHZ ELECTROMAGNETIC FIELD

Aim: The aim of the study was to investigate the possible effects of garlic (GL) and *Momordica charantia* (bitter melon-MC) on rat cerebellum that exposed to 900 MHz electromagnetic field (EMF).

Material and Methods: The experiment was done on fifty-six male Wistar albino rats, 12-week-old. The rats were divided into eight groups, 7 rats in each group: EMF group, EMF+GL group, EMF+MC group, EMF+GL+MC group, GL group, MC group, sham group and a control (Cont) group. The rats in EMF, EMF+GL, EMF+MC, EMF+GL+MC groups were exposed to 900 MHz EMF for 1 hour/day for 28 days. Stereological techniques were used to estimate Purkinje cells number in the rat cerebellum. Superoxide dismutase (SOD) and catalase (CAT) enzyme assays were done to evaluate the oxidative stress.

Results: There is no significant difference in terms of total Purkinje cell number between the EMF and the Cont groups ($p>0.05$). However, the total number of Purkinje cells was significantly higher in EMF+MC and EMF+GL+MC groups compared to EMF group ($p<0.05$). The GL group had significantly higher Purkinje cells' number than EMF and sham groups ($p<0.01$). SOD activity decreased significantly in EMF group compared to EMF+GL group ($p<0.05$), and compared to EMF+MC, EMF+GL+MC, GL and MC groups ($p<0.01$). There was no significant difference in SOD activity between the EMF and Cont groups ($p>0.05$). The CAT enzyme activity in the EMF group was significantly lower than in the GL group ($p<0.05$) and there were no any significant differences between other groups ($p>0.05$).

Conclusion: The exposure to 900 MHz EMF affects the Purkinje cells in male rat cerebellum. MC or using GL and MC together may have a protective effect on the Purkinje cells. GL alone doesn't seem to have a protective effect.

Keywords: Electromagnetic field; Cerebellum; Garlic; *Momordica charantia*; Purkinje cells; Stereology

Fathelrahman Idris Gasmelseed Ali, Ph.D. Thesis
Ondokuz Mayıs University- Samsun, November-2019

List of abbreviations

A β : β -amyloid

AD: Alzheimer's disease

ALS: Amyotrophic Lateral Sclerosis

BBB: Blood Brain Barrier

CAT: Catalase

CE: Coefficient of Error

CNS: Central Nervous System

Cont: Control

CV: Coefficient of Variation

DPPH: 2,2-diphenyl-1-picrylhydrazyl

EHF: Extremely High Frequency

ELF: Extremely Low Frequency

EMF: Electromagnetic Field

EMFs: Electromagnetic Fields

ERK: Extracellular signal-regulated kinases

FRAP: Ferric iron Reduction Antioxidant Power

GABA: Gamma Aminobutyric Acid

GAE: Gallic Acid Equivalent

GFAP: Glial Fibrillary Acidic Protein

GHz: Gigahertz

GL: Garlic

GPx: Glutathione Peroxidase

GRAS: Generally Recognized as Safe

GSH: Glutathione

GSM: Global System for Mobile Communications

H₂O₂: Hydrogen peroxide

IARC: International Agency for Research on Cancer

ITU: International Telecommunication Union

JNK3: c-Jun N-terminal Kinase 3
kHz: Kilohertz
LD₅₀: Lethal dose, 50%
LF: Low Frequency
MAPK: Mitogen Activated Protein Kinases
MC: *Momordica charantia*
MDA: Malondialdehyde
MHz: Megahertz
mT: Millitesla
NADH: Nicotinamide Adenine Dinucleotide (reduced form)
NMDA: N-methyl-D-aspartate
NO: Nitric oxide
Nrf2: Nuclear factor erythroid 2-related factor 2
O₂⁻: Superoxide anion
ROS: Reactive Oxygen Species
rpm: Revolutions per minute
SAR: Specific Absorption Rate
SD: Standard Deviation
SH-: Sulfanyl group
SOD: Superoxide Dismutase
SRS: Systematic Random Sampling
STEM: Scanning Transmission Electron Microscope
TPTZ: 2,4,6-tripyridyl-s-triazine
UHF: Ultra High Frequency
UV: Ultraviolet
VHF: Very High Frequency
VLf: Very Low Frequency
WHO: World Health Organization
µm: Micrometer

CONTENTS	
ÖZET	iv
ABSTRACT	v
ABBREVIATIONS	vi
CONTENTS	viii
INTRODUCTION	1
2. GENERAL INFORMATION	7
2.1. Electromagnetic Field.....	7
2.2. Electromagnetic Field Frequency.....	7
2.3. Sources of the Electromagnetic Field.....	7
2.4. Propagation of the Electromagnetic Fields.....	8
2.5. Types of Electromagnetic Radiations.....	8
2.6. Electromagnetic Field Spectrum.....	9
2.7. Effects of Electromagnetic Fields on Human Health.....	10
2.8. Biological Effects of Electromagnetic Fields.....	11
2.9. Impact of Mobile Phone Radiation on the Cerebellum.....	12
2.10. Cerebellum.....	13
2.10.1. Anatomy of the Cerebellum.....	13
2.10.2. Development of the Cerebellum.....	14
2.10.3. Histology of the Cerebellum.....	16
2.10.4. Physiology of the Cerebellum.....	16
2.10.4.1 Neuronal Circuits of the Cerebellum.....	16
2.10.4.2 Afferent Pathways to the Cerebellum.....	17
2.10.4.3. Efferent Pathways from the Cerebellum.....	18
2.10.4.4. Cerebellum Functions.....	18
2.11. Antioxidants.....	20
2.11.1. Garlic.....	20
2.11.2. Chemical Composition of Garlic.....	20
2.11.3. Biological Properties of Garlic.....	21
2.11.4. <i>Momordica charantia</i>	23

2.11.5. Chemical Components of <i>Momordica charantia</i>	23
2.11.6. Biological Activities of <i>Momordica charantia</i>	24
3. MATERIAL AND METHODS	25
3.1. Experimental Animals.....	25
3.2. Formation of the Experimental Animal Groups	26
3.3. Experimental Animals and Electromagnetic Field Exposure	26
3.4. EMF Exposure System	29
3.5. Preparation of Tissue Samples.....	30
3.5.1. Perfusion	30
3.5.2. Routine Histological Tissue Processing	33
3.5.3. Sectioning Method.....	33
3.5.4. Staining Process.....	35
3.5.5. Tissue Preparation for Electron Microscopy.....	36
3.6. Stereological Analysis.....	37
3.6.1. The Numerical Density of the Purkinje Cells.....	38
3.6.2. The Volume of the Cerebellum.....	40
3.6.3. The Estimated Total Number of the Purkinje Cells.....	41
3.6.4. The Coefficient of Variance (CV) and the Coefficient of Error (CE)	41
3.7. Biochemical Analysis.....	44
3.7.1. Blood Sample Collection.....	44
3.7.2. Analysis of Superoxide Dismutase Enzyme Activity.....	44
3.7.3. Analysis of Catalase Enzyme Activity.....	45
3.8. Determination of Total Phenolic Content and Antioxidant Power.....	46
3.8.1. Preparation of Sample Extract.....	46
3.8.2. Method to Assess the Total Phenolic Content.....	47
3.8.3. Methods to Assess the Antioxidant power.....	47
3.8.3.1. Ferric ion Reduction Antioxidant Power (FRAP).....	47
3.8.3.2. Determination of DPPH Free-Radical Scavenging Effect.....	47
3.9. Statistical Analysis	48
4. RESULTS	49

4.1. Stereological Findings.....	49
4.1.1. The Numerical Density of Purkinje Cells in Cerebellum.....	49
4.1.2. The Total Volume of Cerebellum.....	52
4.1.3. The Total Number of Purkinje Cells in Cerebellum.....	54
4.2. Light and Electron Microscopic Findings.....	56
4.2.1. Light Microscopic Findings.....	56
4.2.2. Electron Microscopic Findings.....	62
4.3. Biochemical Findings.....	87
4.3.1. Mean SOD Enzyme Activity for the Groups.....	87
4.3.2. Mean CAT Enzyme Activity for the Groups.....	89
4.4. Findings of Total Phenolic Content and Antioxidant Power.....	91
5. DISCUSSION.....	92
5.1. Electromagnetic Field and Cerebellum.....	93
5.2. SOD and CAT activities.....	94
5.3 Garlic.....	96
5.4. <i>Momordica charantia</i>	97
6. CONCLUSION AND RECOMMENDATIONS	99
6.1. Conclusion	99
6.2. Recommendations.....	99
REFERENCES	100
APPENDICES.....	114
Ethical Committee Approval Certificate	114
CURRICULUM VITAE.....	115

1. INTRODUCTION

The extensive use and availability of mobile phones worldwide raises the concern about the effect of 900 MHz electromagnetic field (EMF) on the human body. Mobile phones emit electromagnetic radiations that may affect both animal and human tissue negatively and lead to alteration of the functions (Ragbetli et al., 2010; Maskey et al., 2010). Use of mobile phones for long period can be a risk for brain tumors (Hardell et al., 2006), hence there is raised concern about the biological effects of EMF on the body systems. Examples of sources of EMF other than mobile phones are microwave ovens, radar, Wi-Fi, local area networks, radio stations, cordless telephones and airport millimeter scanners (Moulder, 1998; Ahlbom et al., 1998; Rubtsova et al., 2015). The effects of EMF exposure on the central nervous system (CNS) are remarkable (Odaci et al., 2008; Sonmez et al., 2010; Odaci et al., 2016), because the mobile phones are used close to the brain and related organs (Mausset et al., 2001). EMF exposure can cause damage of the cortical, hippocampal, and basal ganglia neurons in the brain (Salford et al., 2003). The commonly used frequencies of EMF in wireless telecommunication systems are 900, 1800 and 2450 MHz (Rubtsova et al., 2015). In mobile phones, the most common frequency is 900 MHz according to the Global System for Mobile Communications (GSM). Exposure to EMF may trigger neurodegenerative diseases like Alzheimer's disease, Parkinson's disease, chronic fatigue and amyotrophic lateral sclerosis (Terzi et al., 2016). Mobile phone radiation has carcinogenic and genotoxic effects. In 2011, The International Agency for Research on Cancer (IARC) classified the electromagnetic radiation of mobile phone as "possibly human carcinogen" (Davis et al., 2013). Swedish study indicated that people who start using mobile phones regularly before the age of 20 have four times higher risk of ipsilateral glioma (Hardell and Carlberg, 2015), and a strong association was found between mobile phone use for more than 10 years and acoustic neuroma (Hardell et al., 2008).

Generally, the young people are the most common users of mobile phones (Heinrich et al., 2011), so they are more vulnerable to the side effects of EMF exposure. The response and the rate of absorption of radiofrequency EMF differs between children and adults. The child brain absorbs a higher amount of radiofrequency energy than the adult brain, because

the child skull bones has a reduced bone density and also there is a large amount of fluids in the child brain in comparison to the adult brain (Davis et al., 2013).

Many researchers have focused on the 900 MHz EMF impact on the hippocampus and the cerebellum of various experimental animals (Bas et al., 2009; Rağbetli et al., 2009; Tang et al., 2015; Erdem Koç et al., 2016; Aslan et al., 2017). It was found that exposure to EMF at a frequency of 900 MHz for long-term had reduced Purkinje cells number in the cerebellum of female rats (Sonmez et al., 2010). Beside of this result, it was found that prenatal exposure to EMF can also cause a significant reduction of Purkinje cells number in the developing rat cerebellum (Ragbetli et al., 2010). Another study also showed that exposure to mobile phone prenatally causes physiological changes in the Purkinje cells of rat cerebellum (Haghani et al., 2013). Exposure of pregnant rats to 900 MHz EMF causes Purkinje cell loss and persistent cellular pathological changes in the rat offspring cerebellum (Odaci et al., 2016). The effects of exposure to EMF of mobile phone during the adolescence period have been evaluated in male rats and it was found that EMF radiation caused a decrease in the Purkinje cells number and abnormal intensely stained cytoplasm (Aslan et al., 2017). Exposure to 3mT EMF caused many remarkable structural changes in the Purkinje cells of rat cerebellum, in addition to reduction of Purkinje cells number. These changes include condensed nuclei, broken or absent cristae of the mitochondria, dilated endoplasmic reticulum and appearance of many vacuoles in the cytoplasm (Ozra et al., 2010)

Biological effects of EMF exposure were studied by many scientists (Salford et al., 2003; Mausset-Bonnefont et al., 2004; Friedman et al., 2007; Manikonda et al., 2007; Hardell and Sage, 2008). The high energy radiofrequency exposure decreases cellular GABA content in the cerebellum (Mausset et al., 2001). Exposure to GSM 900 MHz microwaves leads to cellular and molecular changes in the rat brain; it induces glial reaction which indicates neuronal damage and also decreases the amount of postsynaptic NMDA receptors (Mausset-Bonnefont et al., 2004). Moreover, the extremely low frequency EMF (<300 MHz) makes changes on many neuronal activities in rat hippocampus; as extremely low frequency field (ELF) exposure results in alteration of calcium signaling pathways contributing to abnormal NMDA receptor activities (Manikonda et al., 2007). Also, exposure to 835 MHz EMF might impair calcium homeostasis by changing the calcium binding proteins expression and the

permeability of calcium across cell membranes in the mouse hippocampus (Maskey et al., 2010). It was observed that sub-chronic exposure to 900 MHz EMF induces reactive astrocytosis in rat brain which is indicated by increased level of GFAP in different regions of brain including the cortex, striatum and hippocampus. This reactive gliosis can lead to damage of neurons, synapses, axons, and myelin sheath (Ammari et al., 2010). In 2003, it was found that single exposure to GSM 900 MHz for 2 hours increased the permeability of the blood-brain barrier and albumin leakage in rat brain 50 days after the exposure (Salford et al., 2003). Other researchers confirmed these results; as they found that exposure to 900 MHz EMF radiation for 28 days significantly damaged the blood-brain barrier in rat hippocampus and cortex (Tang et al., 2015). It was detected that in acute term, mobile phone irradiation can generate reactive oxygen species (ROS) and this is mediated by NADH oxidase in the plasma membrane, and these ROS can stimulate the mitogen-activated protein kinase (MAPK) cascades through several steps (Friedman et al., 2007). Exposure to microwave radiation of variable range of frequencies from 900-2450 MHz for a long time resulted in cognitive impairment and damage of DNA in rat brains (Deshmukh et al., 2015). Moreover, an *in vitro* study confirmed the genotoxic effects of radiofrequency EMF; that exposure to 900 MHz EMFs even with low energy (1 or 2 W/Kg) could cause oxidative DNA base damage in Neuro-2a cells. This was attributed to increased production of ROS (Wang et al., 2015). It was found that exposure to EMF emitted from mobile phones at different frequencies (900, 1800 and 2100 MHz) for a period of six months resulted in oxidative stress, elevation of lipid peroxidation and induction of DNA damage in the tissue of the frontal lobe of the rat brain (Alkis et al., 2019).

The genotoxic effects of EMF radiation was explained by the level of generation of ROS (Kocaman et al., 2018). Exposure to EMF has been found to cause increased free radicals formation in the cells (Kivrak et al., 2017a). The reactive oxygen species can damage cellular molecules such as proteins, lipids and DNA (Cui et al., 2004). The cytotoxic effects of ROS are due to peroxidation of membrane phospholipids; this alters the membrane conductivity and leads to loss of membrane integrity (Halliwell, 2001). The living organisms have antioxidative enzymatic mechanisms, like glutathione (GSH), glutathione peroxidase (GPx), catalase (CAT), and superoxide dismutase (SOD), to remove the oxidative damage

caused by ROS and their by-products (Calcabrini et al., 2017). These antioxidant defense systems control free radicals formation and prevent their damaging effects on the biological systems (Goraca et al., 2010). The antioxidants work through their free radical scavenging activities (Halliwell, 1995) and we know that EMFs cause ROS overproduction that impairs the antioxidant defense system. Sometimes the level of free radicals in the tissues may be high, such situation suppresses the defense capacities of the antioxidants (Calcabrini et al., 2017), as seen in the EMF exposure.

Mobile phone EMF radiation results in a decreased level of GSH in brain tissue and blood (Meral et al., 2007). A decreasing of GSH due to the oxidative stress produced by EMF exposure may result in impairment of removal of the lipid peroxides (Aslan and Meral, 2007). Many scientists focused on the effect of 900 MHz on different organs and they found significant decrease in CAT, GPx and SOD activities in the EMF exposure group compared to the control group (Aydin and Akar, 2011; Sepehrimanesh et al., 2016), since EMF exposure increases ROS that cause oxidative stress by changing the CAT, GSH and SOD levels in tissues (Devrim et al., 2008; Martínez-Sámano et al., 2010). A study has concluded that exposure of the rat brain to ELF in acute term, had decreased CAT and SOD activity after exposure (Martínez-Sámano et al., 2012).

Generally, antioxidants have been classified into endogenous groups e.g. melatonin (MEL), SOD, GPx and CAT and exogenous groups e.g. vitamins C, A and E (Niki et al., 1995; Lobo et al., 2010; Goraca et al., 2010) and these compounds should be supplied in the diet. Antioxidants are either synthetic or natural foods that are used in traditional medicine. Many Indian medicinal plants provide antioxidants, such as *Allium sativum* (Garlic (GL)) and *Momordica charantia* (MC) (Bitter melon) (Lobo et al., 2010).

GL is known as a flavoring agent and a traditional remedy for various illnesses since old times (Sato et al., 2006; Park et al., 2009). It contains various antioxidant compounds, these include water-soluble and lipid-soluble organosulfur components and flavonoids such as allixin and selenium. GL's characteristic flavor and odor and most of its potent biological activity depends on its organosulfur compounds (Borek, 2001). S-allyl-L-cysteine is one of the organosulfur compounds that are obtained by extraction of GL cloves for a long time; more than 10 months. GL extracts has many beneficial effects on health e.g. antiviral,

antifungal, anti-protozoal, anti-inflammatory, neuroprotective, hepatoprotective, cardioprotective, anticarcinogenic, immunomodulatory, hypolipidemic, anti-hypertensive, anti-diabetic and antioxidant properties (Bisen and Emerald, 2016). The LD₅₀ (lethal dose, 50%) values of garlic extract given by oral, intraperitoneal and subcutaneous routes were found to be > 30 ml/kg respectively in male and female of both Wistar rats and ddY mice (Nakagawa et al., 1984). However, garlic has very low toxicity and is listed as “generally recognized as safe” (GRAS) by the U.S. Food and Drug Administration (Neltner et al., 2011).

An *in vitro* study concerning the antioxidant effects of GL in young and aged rat brain was conducted. This study found that GL could be effective in preventing oxidative brain damage in young animals, whereas the aging brain was resistant to the antioxidant effects of GL *in vitro* (Brunetti et al., 2009). Another study on GL showed the effects of black GL ethanol extract on the cerebellum of rats that exposed to monosodium glutamate (food flavor enhancer). The main finding was that the estimated total number of Purkinje cells of the rat cerebella treated with black GL and exposed to monosodium glutamate was significantly higher than that of rats exposed to monosodium glutamate only (Aminuddin et al., 2015).

MC is a member of the cucurbitaceae family. It has two most common names; bitter melon and bitter gourd, as every piece of it is bitter. It has a wide range of beneficial effects on health: anticancer, antiviral, anti-inflammatory, analgesic, hypolipidemic, and hypocholesterolemic effects. Bitter melon has long been famous as food and medicine in Asian and African countries. It contains vitamins, minerals, and flavonoids and it provides a rich supply of phenolic compounds like gallic acid. These phenolic compounds have a potent antioxidant activity. MC also contains other various bioactive compounds, especially saponins, peptides, and alkaloids (Tan et al., 2016). In a study conducted on Sprague Dawley rats, the MC was found safe to be given orally at a dose of ≤ 2000 mg/kg and that the LD₅₀ was considered to be > 2000 mg/kg (Husna et al., 2013).

A study was conducted to evaluate the effect of MC on oxidative stress-induced disturbances in brain monoamines and plasma corticosterone in Wistar albino rats. This study showed that MC significantly eliminated the oxidative stress and its subsequent changes. MC extract also exhibits attenuating effect on lipid peroxidation in brain indicating its protective effect against oxidative stress (Kavitha et al., 2011). It has been proven *in vitro* that

polysaccharide of MC protects rat brain from ischemic injury by attenuating the neural cell death that is caused by oxygen and glucose loss. The same study also showed that MC decreased the volume of infarction in ischemic brain at *in vivo* level. All of these functions have been done through its antioxidant scavenging property (Gong et al., 2015).

As it was mentioned above, the EMF exposure has noticeable side effects on the neurons of the CNS. These effects were studied mainly on the hippocampus and few studies were conducted on the cerebellum. A confirmation of the effect of EMF on the cerebellum is needed. In addition, the protection from these side effects would be beneficial. The protection of subjects from susceptibility to neurodegenerative diseases like Alzheimer's and Parkinson's diseases, it clearly needs more studies. It is mentioned that the EMF radiation may trigger them (Terzi et al., 2016). The possibility of the natural antioxidants such as GL and MC for protection of the neurons and glia from EMF exposure is an important issue, as stated above. A lot of antioxidants have been used for their role in protection of CNS especially hippocampus from the mobile phone radiation. To our knowledge, few studies have concerned about the protection of the cerebellum from the mobile phone radiation and whether the natural antioxidants have a role in protecting the cerebellum or not. Furthermore, specifically the GL and MC have not been used before to investigate whether they can protect the cerebellum from mobile phone radiation or not. Because of that, we conducted this study to make an idea about the possibility of protection of rat cerebellum especially Purkinje cells from the side effects of 900 MHz EMF exposure for a 28 days-period, using GL and MC. Histological and stereological techniques provide significant results on the morphology and the estimation of cells or particles number in tissues or organs, respectively.

2. GENERAL INFORMATION

2.1. Electromagnetic Field

The EMF is formed by presence of an electric field made by electric charges and a magnetic field made by the flow of these charges simultaneously. EMF can propagate over large distances. The radiofrequency antenna maximizes the transfer of electric energy into electromagnetic energy. The physical medium is not necessary for the electromagnetic waves to propagate. They can propagate in the vacuum, unlike mechanical waves (e.g. sound waves), which require a material medium (Staebler, 2017).

2.2. Electromagnetic Field Frequency

Frequency is used to describe periodical signals over a duration. It shows how many times an identical elementary event recurs per second. The static field has a zero frequency because it is constant in time. The unit of frequency in the international system (SI) is called hertz (Hz). It is often used as multiples: kilo, mega or gigahertz (kHz, MHz or GHz). Frequency is a fundamental parameter of an EMF. Frequency is a physical quantity used in telecommunications and spectral analysis. Wavelength is the distance traveled by the wave during one period and it is measured in meters (m). Both the frequency and the wavelength characterize EMF. The frequency and wavelength are inversely proportional: the higher the frequency, the smaller the wavelength (Staebler, 2017).

2.3. Sources of the Electromagnetic Field

The sources of EMF can be divided into natural and artificial sources. The natural EMFs are those found in the Earth and not made by human beings e.g. Sun light and ultraviolet rays. The artificial fields are those generated in the production, transport and consumption of electrical energy in addition to tele-communication applications. As the technology progresses the EMFs are used with a wide range of frequencies up to hundreds of GHz (Staebler, 2017). Man-made sources include cell phones, computers, microwave ovens, wireless networks and power lines (Rubtsova et al., 2015).

2.4. Propagation of the Electromagnetic Fields

The science of telecommunications aims to optimize the EMFs propagation to ensure service coverage in a certain area. The waves can propagate across large distances and there must be synchronous generation of an electric field and a magnetic field. The field remains restricted near to the source in case of the absence of one of these two components. During propagation of an electromagnetic wave in free space the energy is distributed across an increasingly large surface area; when the surface area increases the energy decreases. The electric and the magnetic fields are perpendicular to each other and to the direction of propagation opposite the source (**Figure 1**) (Staebler, 2017).

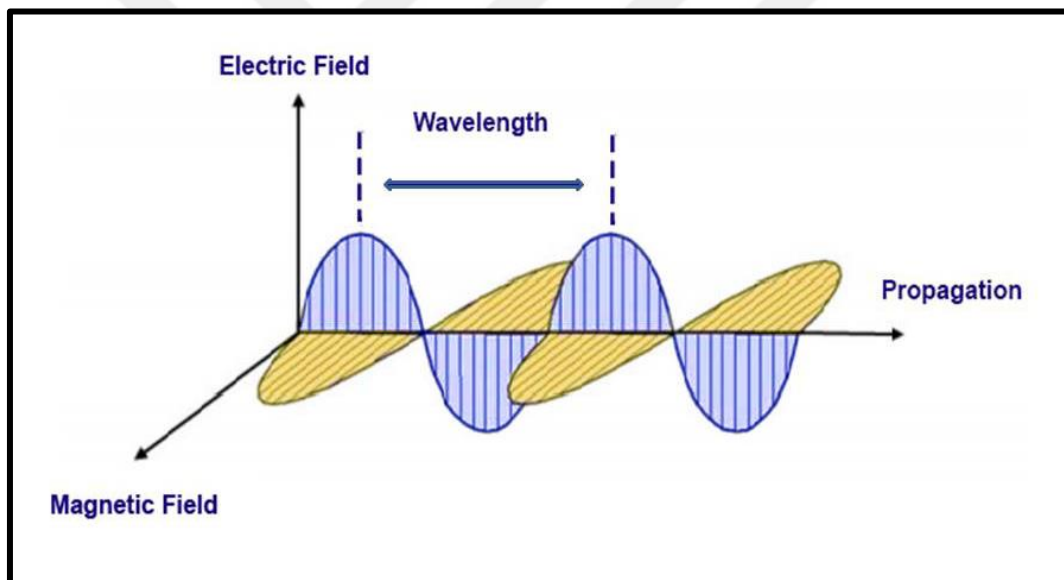


Figure 1. Propagation of the electromagnetic fields modified from Staebler, (Staebler, 2017)

2.5. Types of Electromagnetic Radiations

Electromagnetic radiations can be considered as waves radiations with wavelength and amplitude and this is called (the wave model), and it can be considered as emitted particles called photons and this is known as (the particle model). Each photon has energy. If these photons have high energy enough to break the ionic bonds between the atoms of the molecules or remove an electron from atom, then this type of radiation is called ionizing radiation. The ionizing radiations including X rays, γ rays and cosmic rays, have very high

frequencies and they result in detrimental effects on health. The other type of radiations is called the non-ionizing radiations; as they are unable to ionize the molecules. Non-ionizing radiations consist of: low frequency and extremely low frequency EMF, radiofrequency, microwaves and optical radiations i.e. infrared, visible light and UV radiation. Non-ionizing radiations also make changes in the tissues and affect the body (Staebler, 2017; Kocaman et al., 2018).

2.6. Electromagnetic Field Spectrum

The EMF spectrum is defined on the basis of frequencies and wavelengths as shown in (**Figure 2**). The International Telecommunication Union (ITU) has classified the EMF frequencies and their different uses. The term extremely low frequency (ELF) is used for radiations of 3-30 Hz. Very low frequency (VLF) is used for radiations from 3 to 30 kHz. Low frequency (LF) to very high frequency (VHF) are the frequencies from 30 kHz up to 300 MHz, while ultra high frequency (UHF) to extremely high frequency (EHF) ranges from 300 MHz to 300 GHz. Mobile phones, Wi-Fi, GPS and Bluetooth are classified as UHF (300 MHz to 3 GHz) (Staebler, 2017). The specific absorption rate (SAR) describes the rate of EMF energy penetration per unit of tissue, and it is expressed in units of watts per kilogram (W/kg) (Rubtsova et al., 2015).

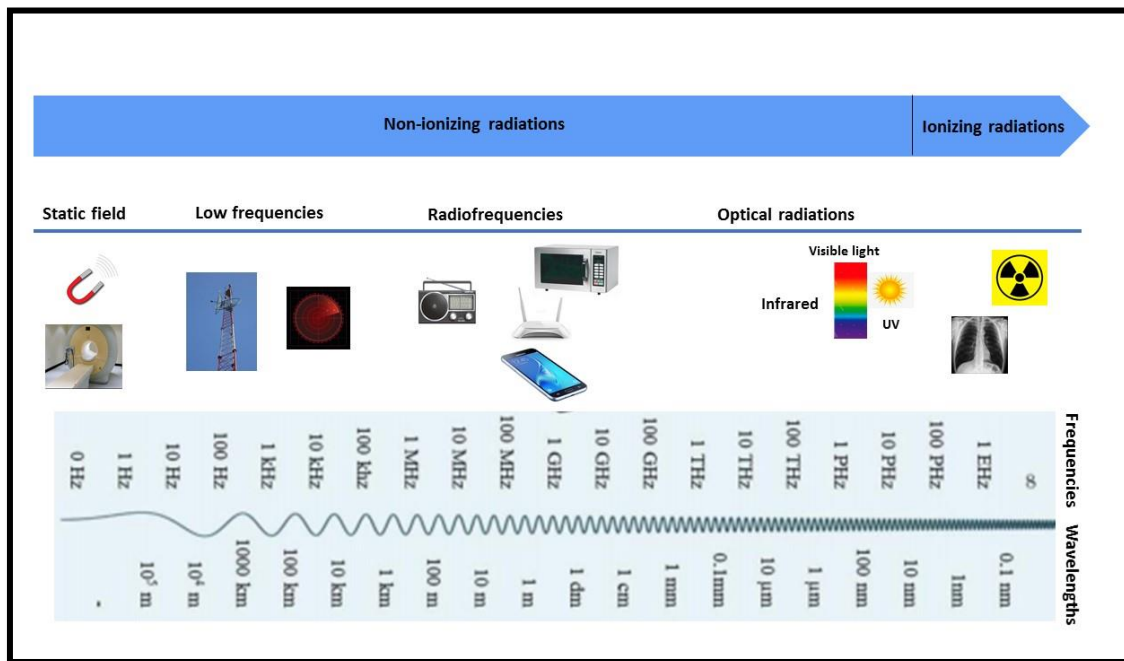


Figure 2. Electromagnetic field spectrum redrawn from Staebler, (Staebler, 2017)

2.7. Effects of Electromagnetic Fields on Human Health

Because the mobile phones are used close to the head and ears, many epidemiological studies have confirmed that 900 MHz exposure may have an influence on the brain and on the auditory and vestibular functions (Hardell et al., 2006; 2007; 2008; Lahkola et al., 2008, van Rongen et al., 2009, Dubey et al., 2010, Hardell and Carlberg, 2015). An association has been found between the mobile phone use and several brain tumors. The long term use of mobile phone for ≥ 10 years is associated with ipsilateral glioma and acoustic neuroma as confirmed by a meta-analysis of various case-control studies in Sweden (Hardell et al., 2008). Oxidative stress has a role in the pathophysiology of neurodegenerative diseases and EMF can cause severe oxidative stress, accordingly EMF may trigger neurodegenerative diseases e.g. Parkinson's and Alzheimer's disease, demyelinating disease, chronic fatigue and ALS (Terzi et al., 2016).

It has been suggested that ELF radiation is associated with childhood leukemia due to exposure during intrauterine or neonatal life. Studies have evidenced that ELF is considered one of the risk factors of human breast cancer. Experiments have been done to examine

human breast cancer cells when exposed to ELF; it has been found that the breast cancer cells grew faster after ELF exposure and that ELF can interfere with the protective anticancer effects of melatonin (Hardell and Sage, 2008). The International Agency for Research on Cancer (IARC) of the World Health Organization (WHO) has classified EMF radiation from mobile phones as a possible carcinogen in humans (Davis et al., 2013).

Some scientists have categorized the effects of EMF into thermal and non-thermal effects (Terzi et al., 2016). The EMFs have energy that is absorbed by the biological tissues and this energy can be converted into thermal energy. Talking on mobile phone for a long period results in severe exposure to EMF and leads to heating at the side of head (Preece, 1999). It has been suggested that initiation of the second and third messenger pathways can be a response of thermoreceptors in living cells to the heating effect of EMF (Glaser, 2005). Symptoms such as headache, dizziness, tinnitus and sleep disorders can result from exposure to EMF, and they are collectively given the term of EMF hypersensitivity. These symptoms were observed to be more prevalent in people living near mobile phone base stations (Khurana et al., 2010) and the EMF sensitivity can be a result of sensitive nervous system and immune activity (Terzi et al., 2016).

2.8. Biological Effects of Electromagnetic Fields

It was found that exposure to 900 MHz EMF radiation for 28 days significantly increased the blood-brain barrier permeability in hippocampus and cortex of rats and this was detected by the observation of albumin and heme oxygenase-1 extravasation. Also, cellular edema and degeneration of neuronal cell organelles was noticed in the brain of these rats (Tang et al., 2015). Exposure to 835 MHz EMF might change the calcium binding proteins (calbindin D28-k and calretinin) expression and the permeability of cell membranes for calcium in the mouse hippocampus; that indicate impairment of the calcium homeostasis (Maskey et al., 2010). Exposure to 900 MHz EMF induces reactive astrogliosis in rat brain which is indicated by increased level of GFAP in different brain regions. This reactive gliosis can lead to damage of neurons, synapses, axons, and myelin sheath (Ammari et al., 2010). It was detected that in acute term, mobile phone irradiation can generate reactive oxygen species (ROS) which can activate ERK1 and 2 cascades; these are mitogen-activated protein

kinase (MAPK) cascades. The MAPK cascades are signal transduction pathways that mediate the effects of various stimuli to regulate the following processes: proliferation, differentiation, metabolism and the stress response. ROS generation is mediated by NADH oxidase in the plasma membrane (Friedman et al., 2007). The reactive oxygen species can be produced as part of normal metabolism. When accumulation of ROS exceeds the normal physiological needed amounts, ROS will lead to oxidative damage of the cellular proteins, lipids and DNA (Cui et al., 2004). EMF exposure results in oxidative stress as it increases the generation of free radicals. The high level of free radicals consumes the antioxidant enzymes and results in impairment of the antioxidant defense system (Calcabrini et al., 2017). A significant decrease has been found in CAT, GPx and SOD enzymes' activities in rat lymphoid organs and polymorphonuclear leukocytes as a result of exposure to 900MHz EMF (Aydin and Akar, 2011). EMF can lead to oxidative stress in several organs such as heart, liver, kidney and ovaries in rats through alteration of the CAT, GSH and SOD levels (Devrim et al., 2008; Martínez-Sámano et al., 2010). In a study, acute exposure to EMF had decreased CAT and SOD enzyme activity in Wistar rats' brain (Martínez-Sámano et al., 2012). Researchers have investigated the effect of exposure to microwave radiation of three frequencies 900, 1800 and 2450 MHz for a long time (180 days) on the cognitive function, heat shock protein 70 level and DNA. This experiment was performed in male Fischer rats. Their results concluded that long term exposure to microwave radiation at low intensities with frequency range from 900-2450 MHz can impair cognitive function, increase heat shock protein 70 and cause DNA damage in rat brain (Deshmukh et al., 2015).

2.9. Impact of Mobile Phone Radiation on the Cerebellum

It was found that long-term exposure to 900 MHz EMF reduced Purkinje cells number in the cerebellum of female rats (Sonmez et al., 2010). Prenatal exposure to EMF can result in a significant decrease of Purkinje cells number in the developing cerebellum of rats (Ragbetli et al., 2010). A study showed that exposure to mobile phone prenatally causes physiological changes in the Purkinje cells of rat cerebellum (Haghani et al., 2013). Exposure of pregnant rats to 900 MHz EMF resulted in Purkinje cell loss and persistent cellular pathological changes in the rat offspring cerebellum (Odaci et al., 2016). The effects of

exposure to mobile phone EMFs during the adolescence period have been evaluated in adolescent male rats and it was observed that EMF caused a decrease in the Purkinje cells number and abnormal intensely stained cytoplasm (Aslan et al., 2017).

2.10. Cerebellum

The cerebellum is the part of the brain that lies in the posterior cranial fossa, separated from the occipital lobes of the cerebral hemispheres by the tentorium cerebelli. It is the largest part of the hindbrain (Gray and Standring, 2008). The cerebellum is formed of two lateral hemispheres and a midline vermis. The surface of the cerebellum consists of sulci and folia (Sinnatamby, 2011). The cerebellum has an outer cortex and a core of white matter. The cerebellar cortex consists of outer molecular layer, middle Purkinje cell layer and inner granule cell layer adjacent to the white matter. Among the identified neurons in the cerebellum, Purkinje cells are the biggest cells with a characteristic flask shape (Pawlina and Ross, 2016; Mescher, 2013). The cerebellum connects sensory to motor regions of the brain, and its function is to coordinate movement. Cerebellar damage causes incoordination of movement, disturbances of balance (Barrett et al., 2012; Hall, 2016). Because the anatomy, biochemistry, and physiology of the nervous system among mammals is generally similar; mice or rats can be considered as models of human CNS function and disease (Treuting et al., 2017).

2.10.1. Anatomy of the Cerebellum

The cerebellum in rats can be divided dorsally into two lateral hemispheres and a midline vermis. The cerebellum can be divided into the corpus, which coordinates muscle movements and tone, and the flocculonodular region, which controls equilibrium. Humans have well-developed limbs capable of extensive independent movement particularly of fingers and toes, as an adaptation to this the human cerebellum has expanded lateral hemispheres in comparison to rodents' cerebellum. The indentations on the surface of the cerebellum are called *sulci* and the folds between them are called *folia*. Cerebellar lobules in humans are much larger than those of rodents due to an increase in the length and number of their folia. The deep cerebellar nuclei in rodents are relatively less defined and smaller than

those of humans. Despite these quantitative distinctions in cerebellar structure, the quality of the basic functions is similar for both humans and rodents (Treuting et al., 2017). Fibers travel to and from the cerebellum via the cerebellar peduncles. The rostral peduncle consists mainly of efferent fibers from the deep cerebellar nuclei to higher brain regions, in addition it contains afferent fibers from the ventral spinocerebellar tract. The middle peduncle consists entirely of axons from the contralateral pontine nuclei, which are the relay center for impulses from the cerebral cortex ipsilateral to these nuclei. The caudal peduncle contains afferent fibers from the vestibular and olivary nuclei as well as the dorsal spinocerebellar tract, and it relays efferent fibers to the vestibular nuclei and reticular formation (Hagan et al., 2012).

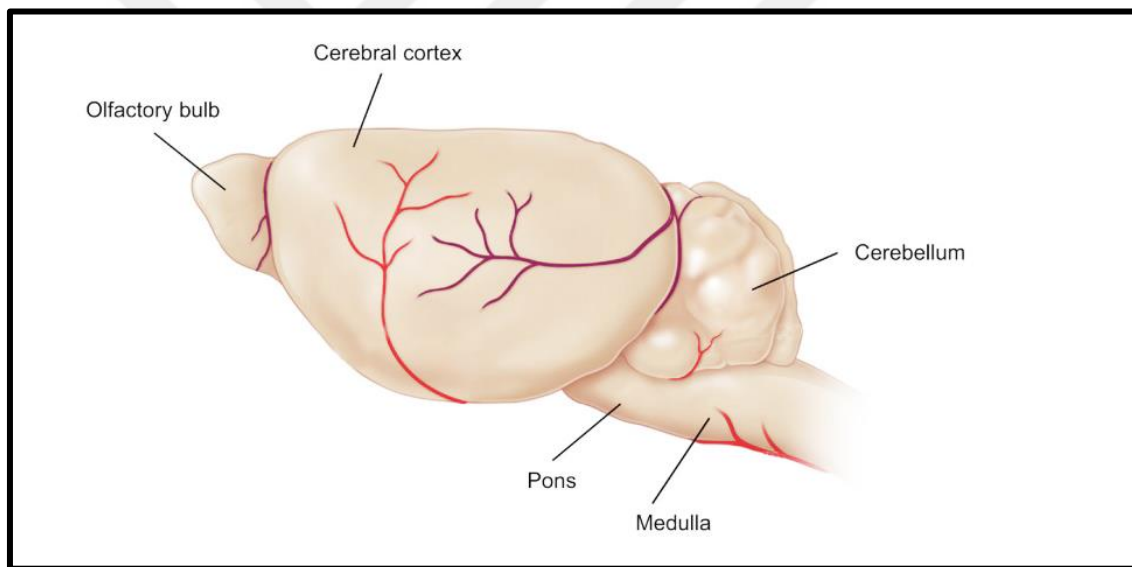


Figure 3. Lateral view of the rat brain modified from Treuting et al., (Treuting et al., 2017)

2.10.2. Development of the Cerebellum

The crescent shaped cerebellar anlage is demarcated by two ventricular landmarks, the anterior extension of the tela choroidea of the fourth ventricle and the embryonic cerebellar fissure. The cerebellar tela choroidea extends from the medullary fourth ventricle posteromedially to the lateral recess of the pontine fourth ventricle anterolaterally. The embryonic cerebellar fissure begins caudally as a single midline incision beneath the fused posterior cerebellar primordium, then splits to follow the unfused cerebellar halves, first separating each from the isthmus then from the pons. There are three divisions of the

cerebellar primordium: the lateral, the subisthmal and the postisthmal cerebellar primordia. Each of these primordia gives origin to different parts of the developing cerebellum. The nuclear transitory zone cells originate in the lateral cerebellar primordium close to the junction with the tela choroidea and migrate superficially and medially. Starting at day 16, the nuclear transitory zone splits into two groups of cells: transversely oriented cells and longitudinally oriented cells. The transversely oriented cells are the source of a decussating fiber tract, called the hook bundle of Russell. The longitudinally oriented cells give fibers to the ipsilateral superior cerebellar peduncle. The nuclear transitory zone cells translocate from superficial position to deep position in the cerebellum to form the deep nuclei, and the cortical transitory zone cells migrate in radial pattern to the surface to form the Purkinje cells layer (Altman and Bayer, 1985a).

The deep neurons descend in the direction of the inferior cerebellar peduncle fibers, and this occurs throughout the cerebellum on day 17. The Purkinje cells ascend in the direction of the external germinal layer, which starts to spread from caudal to rostral on day 17. By day 22 a small-celled and a large-celled subdivision is identifiable in each of the three deep nuclei; the dentate (laterally), interpositus, and fastigial (medially). These nuclei can be distinguished before their descent into the cerebellum depth. In the hemispheres the Purkinje cells have a rostral-to-caudal cytogenetic gradient while in the vermis they have a reverse gradient from caudal to rostral. In the hemispheres the Purkinje cells are generated earlier than those of the vermis. The Purkinje cells of the hemispheres originate from the lateral cerebellar primordium capping the lateral recess of the fourth ventricle anteriorly. The Purkinje cells of the anterior vermis originate from the subisthmal cerebellar primordium medially lining the isthmal canal. The Purkinje cells of the posterior vermis originate in the postisthmal cerebellar primordium overlying the tela choroidea caudally. The young Purkinje cells migrate from the neuroepithelium to the superficial part of the cerebellum in a caudal-to-rostral pattern, this goes parallel to the distribution of the external germinal layer superficially from posteroventral to anterodorsal. This pattern does not depend on the time of origin of Purkinje cells (Altman and Bayer, 1985b; 1985c).

2.10.3. Histology of the Cerebellum

The cerebellum consists of a cortex of gray matter and a medulla of white matter. The cerebellar cortex is composed of an outermost molecular layer, intermediate Purkinje cell layer and a granular layer adjacent to the white matter. At the junction between the molecular and granule cell layers are Purkinje cells whose cell bodies are flask-shaped and the largest among other cell bodies. Each Purkinje cell has many dendrites that arborize in the molecular layer. The Purkinje cell has a single axon which represents the outflow from the cerebellum. The outer molecular layer contains plenty neuropil network with fewer, scattered small neurons; the basket and stellate cells. Granule cell layer contains granule cells that send axons into the molecular layer, these axons branch in a T shape pattern and they synapse with the dendrites of Purkinje cells and basket cells. Golgi cells lie at the meeting area between the molecular and the granular layers (Mescher, 2013; Pawlina and Ross, 2016; Hagan et al., 2012).

2.10.4. Physiology of the Cerebellum

2.10.4.1. Neuronal Circuits of the Cerebellum

The stellate, basket, Golgi, and Purkinje cells release GABA neurotransmitter, whereas the neurotransmitter released by the granule cells is glutamate. Climbing fiber inputs strongly excite single Purkinje cells, whereas mossy fiber inputs lead to a weak excitation of many Purkinje cells via the granule cells. The parallel fibers of granule cells excite basket and stellate cells, which in turn inhibit the Purkinje cells. The mossy fiber collaterals and parallel fibers excite Golgi cells, and Golgi cells inhibit granule cells. The Purkinje cells inhibit the deep cerebellar nuclei. These nuclei are excited by collaterals from the climbing and mossy fibers (**Figure 4**). Although the deep cerebellar nuclei are inhibited by the Purkinje cells, they always excite the thalamus and the brainstem. At the end, the overall function of these neuronal circuits is to modulate or determine timing of the excitation of the deep cerebellar nuclei to the brainstem and thalamus (Barrett et al., 2012).

2.10.4.2 Afferent Pathways to the Cerebellum

The afferent fibers from other regions of the brain and from the periphery join together to form the climbing fiber or mossy fiber input to the cerebellum. The corticopontocerebellar pathway begins in the cerebral motor and premotor cortices and also in the cerebral somatosensory cortex. It passes via the pontine nuclei and pontocerebellar tracts to the lateral divisions of the cerebellar hemispheres on the contralateral side of the brain. The vestibulocerebellar tract transmits impulses from the labyrinths and from the vestibular nuclei. The tectocerebellar tract transmits auditory and visual impulses from the superior and inferior colliculi. The olivocerebellar tract transmits proprioception from the whole body through a relay in the olivary nuclei. Proprioceptive impulses from the head and neck are transmitted via cuneocerebellar tract. Dorsal and ventral spinocerebellar tracts transmit proprioceptive and exteroceptive impulses from the body. The olivocerebellar tract projects to the cerebellum via climbing fibers while the other remaining tracts project via mossy fibers (Barrett et al., 2012; Hall, 2016).

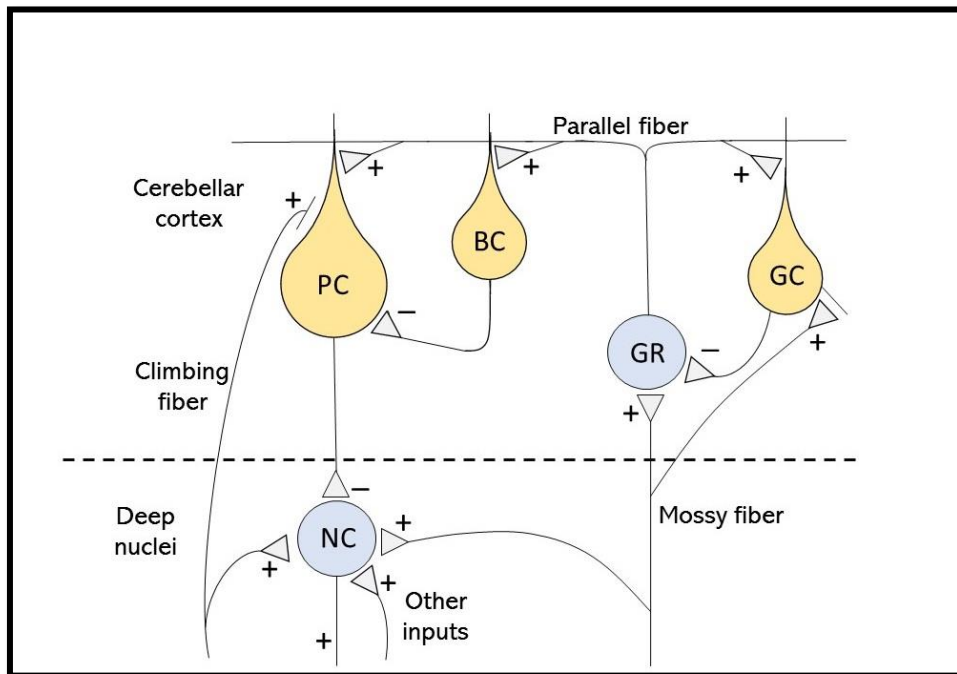


Figure 4. Diagram of the neuronal circuits in the cerebellum redrawn from Barrett et al., (Barrett et al., 2012).
Purkinje cell (PC); Basket cell (BC); Granule cell (GR); Golgi cell (GC); Nuclear cell (NC)

2.10.4.3. Efferent Pathways from the Cerebellum

From the deep cerebellar nuclei (dentate, interposed and fastigial nuclei), efferent fibers leave the cerebellum and are directed to other parts of the brain. A pathway starts in the vermis and then passes through the medulla and pons. This pathway function is to control the equilibrium and the posture of the body. A second pathway from the intermediate zone of the cerebellar hemisphere passes through the interposed nucleus to the ventrolateral and ventroanterior nuclei of the thalamus and then to the cerebral cortex, to several midline structures of the thalamus and then to the basal ganglia and the red nucleus and reticular formation of the upper part of the brain stem. This pathway coordinates the reciprocal contraction of the agonist and antagonist muscles of the peripheral parts of the limbs. A third pathway originates in the cerebellar cortex of the lateral zone of the cerebellar hemispheres and passes to the dentate nucleus, then to the ventrolateral and ventroanterior nuclei of the thalamus and finally to the cerebral cortex. This pathway has a vital role in helping coordinate of sequential motor activities started by the cerebrum (Hall, 2016).

2.10.4.4. Cerebellum Functions

The cerebellum coordinates motor control via three functional divisions (**Figure 5**):

- 1) The vestibulocerebellum: this division consists of the flocculonodular lobe and adjacent part of the vermis. Its function is coordination of the body equilibrium.
- 2) The spinocerebellum: this division consists of the intermediate zones of the cerebellar hemispheres and most of the vermis. Its function is coordinating the movement of the distal parts of the limbs.
- 3) The cerebrocerebellum: this division consists of the lateral zones of the cerebellar hemispheres. Inputs to this division come from the cerebral motor cortex, premotor and somatosensory cortices of the cerebrum. Outputs are directed upward back to the brain. The cerebrocerebellum works together with the cerebral sensorimotor system to plan the sequential voluntary movements of body and limbs. It performs this in a feedback way (Hall, 2016).

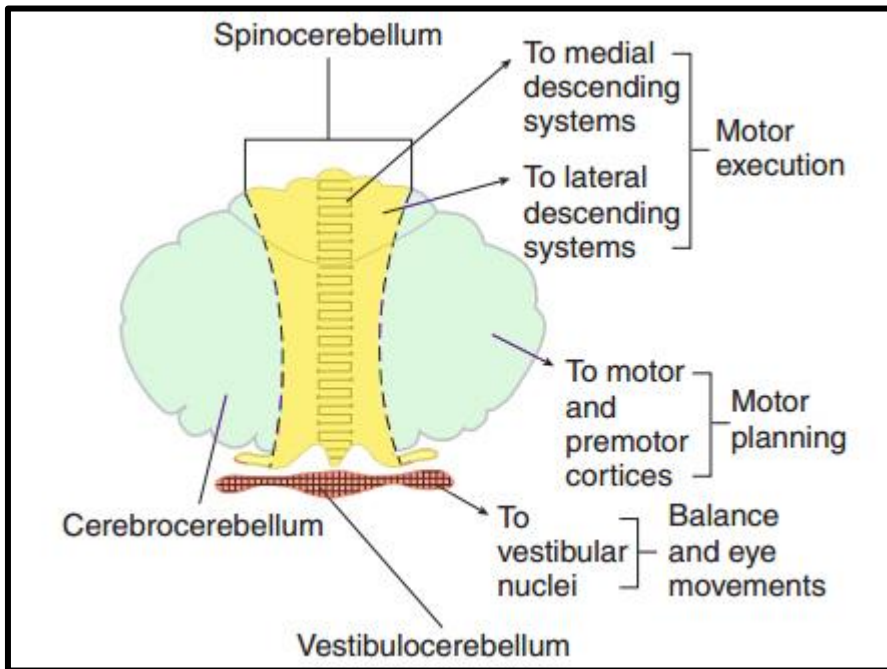


Figure 5. Functional divisions of the cerebellum modified from Barrett et al., (Barrett et al., 2012)

2.11. Antioxidants

The antioxidants are molecules that has the ability to neutralize the reactive oxygen species. As the free radicals are normally produced by the body through certain physiological processes, the body has its own antioxidant defense system. The antioxidants can be endogenous or exogenous. The endogenous ones involve the antioxidant enzymes and other non-enzymatic substances. The exogenous antioxidants involve natural substances in diet and synthetic substances (Lobo et al., 2010; Goraca et al., 2010). Antioxidants may be also divided into enzymatic and non-enzymatic groups (Capasso, 2013).

2.11.1. Garlic

GL is one of the most important vegetables worldwide. It has long been used since the ancient times in food as flavoring substance and also as a medicine for many diseases due to its biological activities (Borek, 2001; Park et al., 2009; Martins et al., 2016) (**Figure 6**).

2.11.2. Chemical Composition of Garlic

GL contains various antioxidant compounds, these include water-soluble and lipid-soluble organosulfur components and flavonoids such as allixin and selenium. GL's characteristic flavor and odor and most of its potent biological activity are due to these organosulfur compounds (Borek, 2001). The major constituents responsible for that flavour are mostly non-volatile, sulfur-containing compounds called thiosulfinates. Thiosulfinates include alliin or S-allyl-cysteine sulfoxide that represents the most predominant precursor of GL flavour (Block et al., 1993; Horníčková et al., 2010). GL contains volatile sulfur-containing compounds with powerful bioactive properties such as ajoenes and several compounds other than alliin, such as allicin, 1,2-vinyldithiin, allixin and S-allyl-cysteine (Jabbes et al., 2012; Kopec et al., 2013) and sulfides, such as methyl allyl-, diallyl-, and dipropyl-sulfides, which are produced from the decomposition of thiosulfinates (Lanzotti et al., 2014). The most characteristic volatile and odorous organosulfur compounds of GL are released after the disruption of the cell membrane, causing the removal of alliin and other sulfoxides from the cytoplasm, by the enzyme alliinase (Bloem et al., 2010). However, GL is also rich in vitamins (vitamin C and vitamins of B complex), antioxidants, flavonoids and

minerals particularly Zn, Mg, Fe, Cu and Se (Rekowska and Skupień, 2009). It also contains plenty of other non-volatile phytonutrients, with beneficial medicinal properties, especially flavonoids, saponins and saponinins, nitrogen oxides, phenolic compounds, amides and proteins. Additionally, GL has been also considered as one of the richest sources of total phenolic compounds among the commonly consumed vegetables (Lanzotti et al., 2014).



Figure 6. Garlic (obtained from Samsun, Turkey)

2.11.3. Biological Properties of Garlic

GL has many beneficial effects on health as it is antimicrobial, anti-inflammatory, neuroprotective, hepatoprotective, cardioprotective, anticarcinogenic, immune promoting, hypolipidemic, anti-hypertensive, anti-diabetic and antioxidant properties (Bisen and Emerald, 2016; Borlinghaus et al., 2014; Capasso, 2013; Kopec et al., 2013; Rahman, 2007). The healthy properties of GL are mainly due to its strong antioxidant activity (Kopec et al., 2013). Allicin as a bioactive component of GL, has a biological antioxidant potential via certain mechanisms that include free radicals trapping, interaction with thiol containing proteins, scavenging of hydroxyl radicals, inhibition of superoxide and NO production and modification of SH-dependent activities (Rabinkov et al., 1998; Rahman, 2007; Borlinghaus et al., 2014; Capasso, 2013; Kopec et al., 2013). Raw and aged GL contains large amounts of total phenolic compounds and has high antigenotoxic effect. GL has significant antioxidant

activity and protective effects against DNA damage induced by H₂O₂ and lipid peroxidation products (Park et al., 2009). It was observed that aged GL extract and S-allyl-cysteine (most abundant molecule in the aged GL extract) significantly protect neuronal cells from ROS (H₂O₂)-mediated insults. Aged GL extract was also found to preserve the pre-synaptic synaptosomal associated protein from ROS-mediated damage (Ray et al., 2011). The protective activity of aged GL extract and S-allyl-cysteine can involve different antioxidant mechanisms: scavenging of free radicals and prooxidant species, activation of Nrf2 factor, inhibition of prooxidant enzymes, induction of antioxidant enzymes and chelating effects (Colin-Gonzalez et al., 2012). A study has been conducted to evaluate the antioxidant effects of a GL extract in young and aged rat brain in vitro. The 8-iso-prostaglandin F_{2α} was used as an index of cellular oxidative damage. It was observed that GL could prevent oxidative damage in young rat brain, but the aging brain was unresponsive to the antioxidant activity of GL in vitro (Brunetti et al., 2009). Another study showed the effects of black GL ethanol extract on the cerebellum of rats treated with monosodium glutamate (food flavor enhancer). It was found that the estimated total number of Purkinje cells of the cerebella of rats treated with black GL and exposed to monosodium glutamate was significantly higher than that of rats exposed to monosodium glutamate only (Aminuddin et al., 2015). Monosodium glutamate has damaging effects on the hippocampus and it was found that the administration of black GL extract protected the rat brain and reversed the deleterious effects of monosodium glutamate on the spatial memory (Hermawati et al., 2015). Diallyl trisulfide - organosulfur compound in GL- has antioxidative and neuroprotective effects; diallyl trisulfide protects B35 neural cells against oxygen glucose deprivation-induced cellular injury by suppressing ROS formation. Diallyl trisulfide can be developed as a medicine in cerebral ischemic injuries such as stroke (Xu et al., 2015). Natural antioxidants like GL and ascorbic acid protect the rat developing hippocampus from lead toxicity which causes neuron apoptosis (Ebrahimzadeh-Bideskan et al., 2016). In another study, it was found that diallyl sulfide protected rat brain from iminodipropionitrile neurotoxicity, and this was due to the antioxidant, free radical scavenging and anti-inflammatory activities of diallyl sulfide (Zhang et al., 2016). Administration of GL could be an effective treatment for lead-induced oxidative insult in rat brain, kidney and liver via alleviating oxidative stress (Manoj Kumar et al., 2017).

The β -amyloid ($A\beta$) deposits in the brain can trigger neuroinflammation which finally leads to Alzheimer's disease (AD). Researchers had observed that aged GL extract may improve the short-term recognition memory and relieve the neuroinflammation in β -amyloid -induced rats (Nillert et al., 2017). A study has shown that monosodium glutamate deteriorates the working memory of rats and that the fermented ethanolic GL extract was found to be able to prevent this monosodium glutamate-induced disruption of working memory (Nurmasitoh et al., 2018). It was concluded that the administration of GL powder to adult rats could reduce the deteriorating effect of high fat diet on long term potentiation in the granular cells of the hippocampal dentate gyrus (Salehi et al., 2018). S-allyl-cysteine, a compound in GL, had been found to prevent anxiety-like behavior and depression caused by chronic restraint stress in rats and it attenuated the biochemical and morphological changes in brain, this was attributed to its antioxidant activities (Becerril-Chávez et al., 2017). S-allyl-cysteine also has a potent neuroprotective effect as explained by an experiment in rat model of multiple sclerosis disease (Escribano et al., 2018).

2.11.4. *Momordica charantia* (Bitter melon)

MC is a member of the cucurbitaceae family (Habicht et al., 2011). It has two most common names; bitter melon and bitter gourd because every piece of it is bitter (Tan et al., 2016). It is commonly used in traditional medicine in developing countries particularly in Asia, Africa (Basch et al., 2003; Singh et al., 2011; Tan et al., 2013).

2.11.5. Chemical Components of *Momordica charantia*

MC contains vitamins, minerals, and flavonoids (Lucas et al., 2010). It provides a good supply of phenolic compounds including gallic and gentistic acids. These phenolic compounds have a potent antioxidant activity (Horax et al., 2005). MC also contains other various bioactive compounds such as saponins, sapogenins, proteins, polypeptide-p, and alkaloids (Tan et al., 2016). The most common flavonoids in MC are catechin and epicatechin (Budrat and Shotipruk, 2008). It contains phenylpropanoids that include caffeic acid and chlorogenic acid (Horax et al., 2005; Kubola and Siriamornpun, 2008).

2.11.6. Biological Activities of *Momordica charantia*

Many studies have revealed that bitter melon has many therapeutic properties: hypoglycemic, hypolipidemic, hypocholesterolemic, antimicrobial, anti-inflammatory, analgesic, and anticancer effects (Fernandes et al., 2007; Nerurkar et al., 2008; Fuangchan et al., 2011; Abalaka et al., 2011; Fang et al., 2012a; 2012b). In addition, the bitter melon has a beneficial role in wound healing (Prasad et al., 2006). MC may be used in the prevention and treatment of diseases whose pathogenesis is related to oxidants or free radicals and it can be applied in medicinal drugs (Santos et al., 2010). It has been found that bitter melon might improve obesity-associated peripheral inflammation and neuroinflammation in mice fed high-fat diet (Nerurkar et al., 2011). The antioxidant activity of MC was investigated and confirmed in previous studies by using many in vitro assays such as the DPPH radical-scavenging activity, hydroxyl radical-scavenging activity, β -carotene–linoleate bleaching assay, FRAP assay and total antioxidant capacity (Kubola and Siriamornpun, 2008; Santos et al., 2010; Ozusaglam and Karakoca, 2013; Tan et al., 2013). A research was performed to assess the antioxidant potential of MC fruit extract in ammonium chloride-induced hyperammonemia in adult Wistar male rats. The findings indicated that MC provided protection against hyperammonemia by exerting antioxidant potentials and maintaining the hepatic tissue integrity (Thenmozhi and Subramanian, 2011). In a study, the treatment of male Wistar rats with MC fruit extract had increased the antioxidant hepatic enzymes CAT, SOD and GPx and protected the liver from carbon tetrachloride intoxication (Semiz and Sen, 2007). In case of intra-cerebral hemorrhage injury, treatment with MC polysaccharide could scavenge ROS, significantly inhibiting the thrombin-induced neuronal death in primary hippocampal neurons and it could also inhibit caspase 3 and JNK 3 signaling pathway. This means MC polysaccharide has neuroprotective and antioxidant effects (Duan et al., 2015). A study was conducted to evaluate the effect of MC on oxidative stress-induced disturbances in brain monoamines and plasma corticosterone in Wistar albino rats. This study showed that MC significantly removed the oxidative stress and its subsequent changes. The MC extract also attenuated lipid peroxidation in brain indicating its protective effect against oxidative stress (Kavitha et al., 2011).

3. MATERIAL AND METHODS

3.1. Experimental Animals

Fifty-six Wistar albino male rats, 12-week-old and with weights of 280 ± 30 g, were used for this experiment. The animals were obtained from the Experimental Animal Research Center and Surgical applications of Ondokuz Mayıs University, Samsun, Turkey. The study was initiated after the approval of the Local Ethical Committee for Experimental Animals at Ondokuz Mayıs University, Samsun, Turkey (date 31.03.2017 and No: 2017/11). All experimental procedures were carried out according to the protocol guidelines. The experimental parts of the study including histological and stereological analysis were done in the Department of Histology and Embryology at Faculty of Medicine, Ondokuz Mayıs University, Samsun, Turkey. The rats were kept in stainless-steel cages. During the whole period of the experiment, the rats were maintained under 12h light/12h dark cycle in room temperature (22 ± 2 °C) with humidity of 40-50 % in the laboratory. The rats were free to obtain the food and water (**Figure 7**).



Figure 7. Wistar albino rats of the current study

3.2. Formation of the Experimental Animal Groups

In the present study the rats were randomly divided into eight groups; each group consisted of seven male rats as follows:

Group 1: Pure control group (Cont) (n=7)

Group 2: Sham group (n=7)

Group 3: Electromagnetic field (EMF) group (n=7)

Group 4: EMF+garlic (GL) group (n=7)

Group 5: EMF+*Momordica charantia* (MC) group (n=7)

Group 6: EMF+GL+MC group (n=7)

Group 7: GL group (n=7)

Group 8: MC group (n=7)

3.3. Experimental Animals and Electromagnetic Field Exposure

Before starting the experiment, the rats were weighed 280 ± 30 g and were kept in the separate cages and all EMF groups subjected to 900 MHz EMF except Cont, sham, GL and MC groups. Exposure time is between 09:30 A.M. to 12:30 P.M. for 60 minutes every day for 28 days. After 28 days, all animals were undergoing cardiac perfusion under anesthesia (100 mg/kg ketamine + 15 mg/kg xylazine) and brains were taken from the cranium. Detailed information about the processes have been given in (Table 1).

Group 1: Pure control group

This group of animals was kept in room away from the EMF exposure system therefore; this group was not exposed to EMF. Diet restriction was not performed in this group of rats and they lived in their cages for 28 days during the experiment.

Group 2: Sham group

The animals in this group were put into the round plastic cage that was used to EMF exposure. Animals of this group were not exposed to EMF. They were placed into the circular plastic cage between 11:30 A.M. -12:30 P.M. every day for one hour per day for 28 days without being subjected to the EMF.

Group 3: EMF group

In order to do EMF exposure, a round plastic cage was designed to accommodate a maximum of 16 rats with a radius of 25 cm and a height of 20 cm as shown in the (Figure 8). They were exposed to EMF with a frequency of 900 MHz at equal distances from the monopole antenna for one hour per day for a period of 28 days (between 09:30-10:30 A.M. every day). EMF generator (Microwave Test Transmitter, Set Electronics Ltd, Isparta, Turkey) with an output of 1 to 2 Watts operating at 900-1800 MHz was used as a source of EMF (Figure 9). Rats were exposed to EMF with a 900-MHz half-wave monopole antenna. The antenna used was equivalent to mobile phone antenna with circular polarization and direction.



Figure 8. Round plastic cage containing rats exposed to EMF

Group 4: EMF+GL group

Each rat in this group was given GL (360 mg/kg/day) (Aminuddin et al., 2015) via oral gavage and after 30 minutes, the rats were exposed to EMF with a frequency of 900 MHz at equal distances from the monopole antenna for one hour per day for 28 days. In addition, care was taken to expose the rats of this group to the EMF between 09:30-10:30

A.M. every day. The round plastic cage composed of 16 compartments, with a radius of 25 cm and a height of 20 cm was used to subject all rats to the EMF. The outer coats of the GL were removed and then GL was grinded and dissolved in the distilled water before given to the rats via oral gavage. GL was purchased from the local market in Samsun-Turkey.

Group 5: EMF+MC group

This group was given MC (200 mg/kg/day) (Kavitha et al., 2011) via oral gavage and after 30 minutes, the rats were exposed to EMF frequency of 900 MHz inside a round plastic cage for one hour per day for 28 days. The rats were equidistant from the monopole antenna. Each rat was exposed to the EMF at the same time every day from 10:30-11:30 A.M. The round plastic cage composed of 16 compartments, with a radius of 25 cm and a height of 20 cm was used to subject all rats to the EMF. For MC extract, mature MC fruits are purchased from an orchard in Çarşamba district of Samsun province and the fruit species is identified to the department of Botany at Faculty of Sciences. After that, a certain amount of fruit was added to a certain amount of olive oil and kept for 30 days. At the end of 30 days MC fruits were completely dissolved in olive oil. The resulting solution was centrifuged by filtration through a thin sieve, and after the centrifugation the oil part was separated and ready for use (Pişkin et al., 2014).

Group 6: EMF+GL+MC group

This group was given GL (360 mg/kg/day) (Aminuddin et al., 2015) and MC (200 mg/kg/day) (Kavitha et al., 2011) via oral gavage and after 30 minutes, the rats were subjected to EMF frequency of 900 MHz inside a round plastic cage for 28 days for one hour a day. The rats were equally distant from the monopole antenna. All rats have been exposed to the EMF from 10:30-11:30 A.M. each day. The round plastic cage consisting of 16 compartments with a radius of 25 cm and a height of 20 cm was used to subject all rats to the EMF.

Group 7: GL group

Animals in this group were given GL (360 mg/kg/day) (Aminuddin et al., 2015) via oral gavage every day for 28 days between 09:00-10:00 A.M.

Group 8: MC group

Animals in this group were given MC (200 mg/kg/day) (Kavitha et al., 2011) via oral gavage every day for 28 days between 09:00-10:00 A.M.

3.4. EMF Exposure System

EMF generator (Microwave Test Transmitter, Set Electronics Ltd, Isparta, Turkey) with an output of 1 to 2 Watts operating at 900-1800 MHz was used as a source of EMF (**Figure 9**). Rats were exposed to EMF with a 900-MHz half-wave monopole antenna. The antenna used was equivalent to mobile phone antenna with circular polarization and direction. The exposure system consisted of round plastic cage with 16 separate compartments with a radius of 25 cm and a height of 20 cm, monopole antenna of the exposure system and EMF meter (**Figure 10**). The rats positioned in the round plastic cage were kept at equal distances from the monopole antenna. The heads of rats were positioned in the direction of the antenna to ensure equal distribution of the EMF. To reduce the stress on these rats during exposure, several air holes were made in the plastic cover of the round plastic cage. The EMF generator power was adjusted to be 2 watts during exposure.

Table 1. Information on the experimental groups

Group 1:	Wistar albino rats (7)	Pure control group was not exposed to EMF
Group 2:	Wistar albino rats (7)	Sham group placed inside the round plastic cage without being exposed to the 900 MHz EMF
Group 3:	Wistar albino rats (7)	EMF group exposed to the 900 MHz EMF
Group 4:	Wistar albino rats (7)	EMF+GL group received (360 mg/kg/day) GL and exposed to the 900 MHz EMF
Group 5:	Wistar albino rats (7)	EMF+MC group received (200 mg/kg/day) MC and exposed to the 900 MHz EMF
Group 6:	Wistar albino rats (7)	EMF+GL+MC group received (360 mg/kg/day) GL and (200 mg/kg/day) MC and exposed to the 900 MHz EMF
Group 7:	Wistar albino rats (7)	GL group received (360 mg/kg/day) GL without EMF exposure
Group 8:	Wistar albino rats (7)	MC group received (200 mg/kg/day) MC without EMF exposure



Figure 9. EMF generator (Microwave Test Transmitter, Set Electronics Ltd, Turkey)

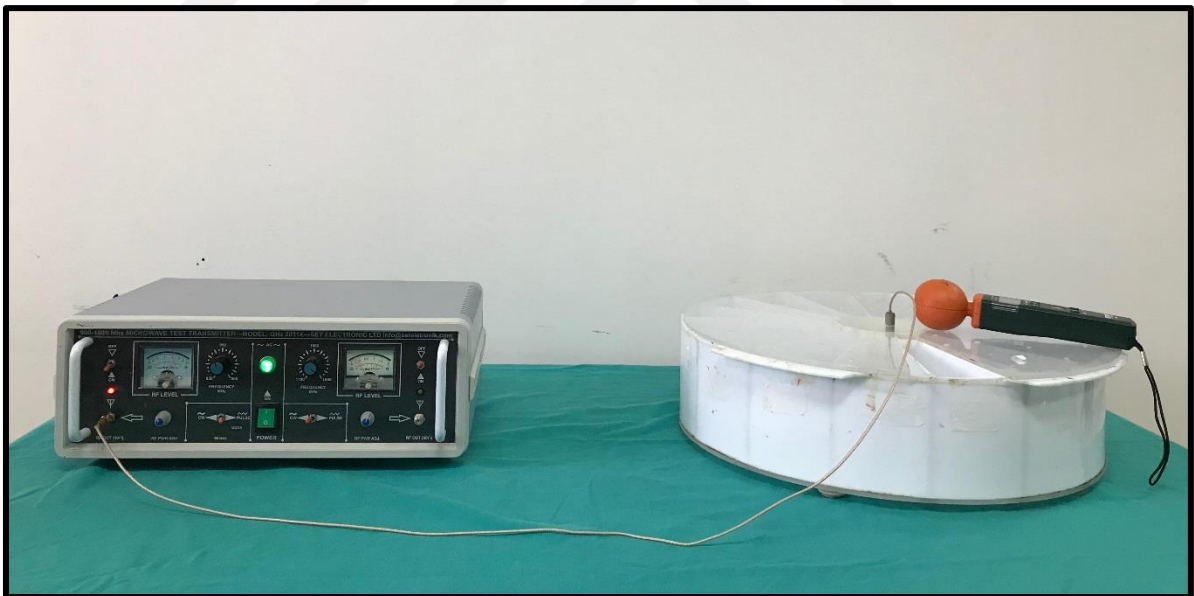


Figure 10. EMF exposure system

3.5. Preparation of Tissue Samples

3.5.1. Perfusion

Animals were weighed before perfusion. The average weight of the rats is about 280 ± 30 g. At the end of the experimental period, all rats were received intraperitoneal 100

mg/kg ketamine (Ketalar®, Eczacibasi, Istanbul, Turkey) and 15 mg/kg xylazine (XYLAZINBIO 2%, Bayer, Istanbul, Turkey) for general anesthesia (**Figure 11**). After general anesthesia, cardiac perfusion was carried out first using saline solution and then 10% formalin solution. Craniotomy was performed and the whole brain was removed. All used solutions and materials required for perfusion was prepared one day before the operation, the solutions were kept at room temperature.

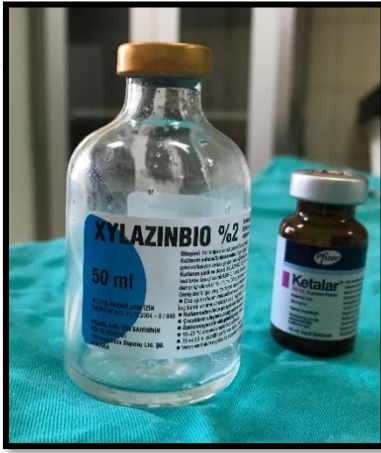


Figure 11. Anesthetic solutions for pre-perfusion anesthesia

The deep anesthetized rats were placed on the operating table with its back down, and then the chest was opened with the help of a pair of scissors and scalpel from the bottom of the diaphragm to the top of the chest to reveal the heart. When the heart was in operation, the tissue perfusion performed by inserting a plastic cannula in the apex of the left ventricle. Simultaneously with this procedure, a small incision was made in the right atrium with the aid of scalpel to make sure solution is flowing freely. Throughout the perfusion process tetanic contractions were observed in the rat extremities, which are a sign of formalin fixation. Perfusion is almost completed when spontaneous movement during the perfusion is observed. All the rats used in our study showed irregular contractions (formalin dance) during the perfusion process. Skull bones were carefully broken via bone scissors to remove the brain.

When the brain was completely removed (along with the cerebellum and other brain regions) (**Figure 12**), it was entirely placed in plastic tissue container containing 10%

formalin and was left in the fixation solution for two weeks at room temperature. During fixation period, the fixative solution has been changed every three days for the quality of fixation. Whole brain was left in the same fixative for two weeks and then the cerebellum was separated and taken for histological follow-up (**Table 2**). In this study, the whole cerebellum was used. The purpose of the perfusion technique was to minimize the artifacts during fixation.



Figure 12. Rat brain

Table 2. Chemical solutions and duration of follow-up of cerebellum tissues

Chemical Solution	Duration
70% Alcohol (Ethyl Alcohol-Tekkim Chemicals -Turkey)	1 hour
80% Alcohol	1 night
96% Alcohol	1 hour
96% Alcohol	1 hour
Absolute alcohol	2 hours
Absolute alcohol	2 hours
Xylene (Sigma-Aldrich)	2 hours
Xylene	2 hours
Paraplast (Tekkim Chemicals -Turkey)	1 hour
Paraplast	2 hours

3.5.2. Routine Histological Tissue Processing

The cerebellum of each animal was taken from the 10% formalin fixative solution and washed in the running water for one night. Following the washing process, the tissue follow-up procedures shown in (Table 2) were performed. Tissue tracking was done on the Thermo Scientific TM Citadel 2000 Tissue Processor (Fisher Scientific UK Ltd Bishop Meadow Road Loughborough LE11 5RG) brand tissue-tracking device (Figure 13). Cerebella of the rats were embedded into the paraplast at 60° C. After routine histological follow-up, the impregnation process was completed by putting the cerebella within the 'L' shape stainless metal mold containing embedding paraffin wax to prepare tissue blocks for cutting process.

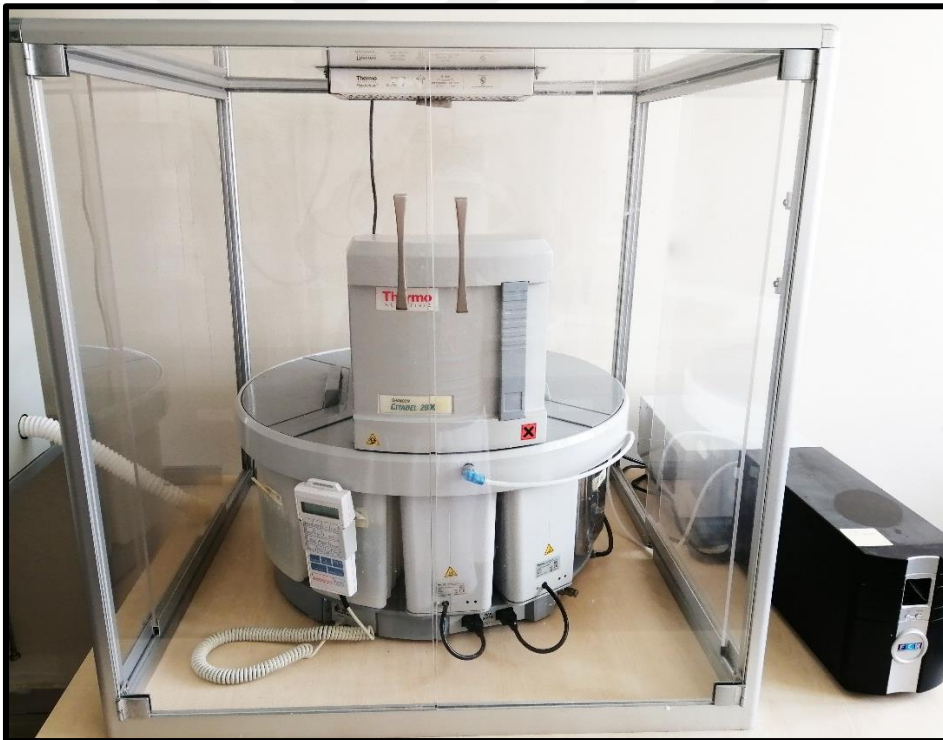


Figure 13. Tissue tracking device (Thermo Scientific TM Citadel 2000 Tissue Processor)

3.5.3. Sectioning Method

The strategy of the cerebellum tissue sectioning was determined by conducting a pilot study using a single cerebellum tissue block before obtaining the coronal sections of cerebellum tissues for this study. After random selection of the first section, systematic

random sampling (SRS) was applied to the next sampled sections for stereological analysis using the physical disector counting technique. Paraffin sections were taken from the cerebellum tissue blocks using disposable metal microtome blades (Type N35, Feather company, Osaka, Japan) and rotary microtome (Leica RM2125RT, Nussloch, Germany) (**Figure 14**) was used to obtain 10 μm -thick serial sections in coronal plane from the cerebellum tissue blocks with section interval 1/20. Tissue sections of 5 μm thickness were also taken for histopathological examination. 5% of powdered gelatin (in the form of dissolving 5 g of gelatin in 100 ml of distilled water) was added to the distilled water heated to 45°C in the flotation bath (MH8517 Paraffin Section Flotation Baths) (**Figure 15**) before the sectioning was started. As a result, the sections stick firmly to the slide and do not slip from the slide during staining process. The slides with sections were saved in the laboratory drying oven at 58 °C for one night (**Figure 16**) before the staining process was started. As a result of SRS, an average of 13 pairs of sections were obtained from each animal and these sections were stained with cresyl violet.



Figure 14. A rotary microtome (Leica RM2125RT)



Figure 15. A flotation bath (MH8517 Paraffin Section Flotation Baths)



Figure 16. A laboratory drying oven

3.5.4. Staining Process

The tissue sections were stained with cresyl violet (**Figure 17**). Cresyl violet staining solution was prepared by dissolving 0.1g cresyl violet into 100 ml distilled water. The dyes and solutions used during the staining of the cerebellum sections are shown in (**Table 3**). The

duration of penetration of the dye into the cerebellum section was determined by a pilot study applied in a single section. Then the same process was implemented to all cerebellum sections based on the pilot study. Before the staining process, the cresyl violet solution was heated in the oven at about 55°C to get better penetration of the dye into the tissues and to enhance staining. The following procedures were carried out for the staining of the sections (**Table 3**). The light microscope (Olympus, BX51, Japan) was used to investigate the quality of the cresyl violet-stained sections.



Figure 17. Cerebellum sections were stained with cresyl violet

Table 3. Chemicals and duration used for staining of the cerebellum sections

Chemicals	Duration
Xylene (x4) (Sigma-Aldrich)	2 hours
Absolute alcohol (x2)	10 minutes
96% alcohol	10 minutes
80% Alcohol (Ethyl Alcohol-Tekkim Chemicals -Turkey)	10 minutes
70% alcohol	10 minutes
Distilled water	5 minutes
Cresyl violet (Sigma C5042-10G)	3 minutes
Distilled water	15 seconds
96% alcohol	5 seconds
Absolute alcohol	10 minutes
Xylene (x2)	1 hour
Entellan (Merck KGaA Darmstadt Germany)	For mounting

3.5.5. Tissue Preparation for Electron Microscopy

One cerebellum from each group was fixed in glutaraldehyde solution. After fixation in glutaraldehyde, the cerebella were dissected into small pieces using binocular dissecting microscope. Then the sampled tissues were processed according to the protocol in (Table 4) and embedded in resin. The resin-embedded tissue blocks were sectioned by an ultramicrotome (Leica Ultracut UCT, Leica Microsystems GmbH, Germany) using diamond blade. Thin sections of 70-80 nm thickness have been taken for histopathological examination by scanning transmission electron microscope (STEM) (JEOL, JSM-7001F, Tokyo, Japan).

Table 4. Chemicals and duration in tissue processing for electron microscopic examination

Chemicals	Duration
4% Glutaraldehyde	1 hour
0.1 M Phosphate buffer for washing	4 x15 minutes
1% Osmium tetroxide	1.5 hour (dark)
0.1 M Phosphate buffer for washing	4 x15 minutes
50%Aceton	15 minutes
70% Aceton	15 minutes
95% Aceton	15 minutes
100% Aceton	15 minutes
100% Aceton	15 minutes
Propyleneoxide	20 minutes
Propyleneoxide	20 minutes
50% Propyleneoxide + 50% Araldite mixture	1 hour
100% Araldite	1 hour

3.6. Stereological Analysis

The estimation of the total Purkinje cell number was performed using the physical disector method, which is an unbiased stereological method of counting (Sterio, 1984). A pilot study was done to determine the suitable sectioning interval and the number of sampled sections. The sectioning interval ratio for our study was 1/20. Serial two consecutive sections 10 µm thick were taken from each tissue block to obtain 10-18 coupled sections for each rat.

3.6.1. The Numerical Density of the Purkinje Cells

Only nine sections pairs from each rat were determined by the pilot study to estimate the numerical density of Purkinje cells. A number of coupled images at a magnification of x20 from the two consecutive sections were taken using a light microscope (Olympus BX43F, Tokyo, Japan) coupled with a microscope camera (Olympus SC50, Olympus Soft Imaging Solutions GmbH, Münster, Germany) connected to a personal computer (**Figure 18**). The imaging software used was Olympus cellSens Entry 1.14.

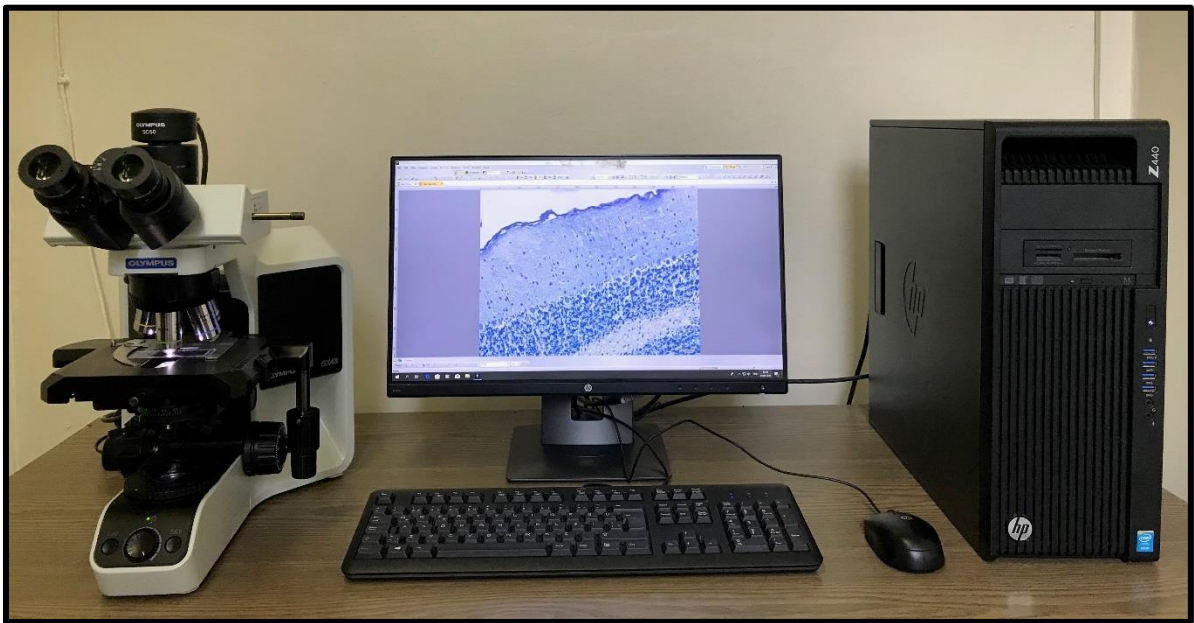


Figure 18. It shows the microscopy imaging system that was used for capturing the images of the cerebellum and measuring the cerebellum section area

The images are used as *reference* and *look up* for counting the particles number using an unbiased counting frame (Gundersen, 1977) (**Figure 19**). The Purkinje cells profiles found completely within the counting frame and not intersecting with any forbidden line of the frame were counted. The Purkinje cells profiles superimposing the inclusion line (green) were counted; while Purkinje cells profiles contacting the exclusion (red) border or its extensions were excluded from counting. The *reference* and *look up* images are shown and compared in ImageJ program (**Figure 20**). Each Purkinje cell profile fulfilling all the unbiased counting frame rules and found in the *reference* section but not in the *look up* section

was counted, while others were excluded. The counting was also performed after reversing the *reference* and the *look up* images; the *reference* used as *look up* and the *look up* as *reference*. The disector particles number, the counting frame area and the section thickness were used in certain formula to estimate the numerical density that is given below for each rat (Gundersen et al., 1988a).

$$N_v = \frac{\sum Q^-}{A \cdot t}$$

N_v : numerical density of Purkinje cells; $\sum Q^-$: total number of disector Purkinje cells; A : total area of counting frames used during the counting; t : mean section thickness.

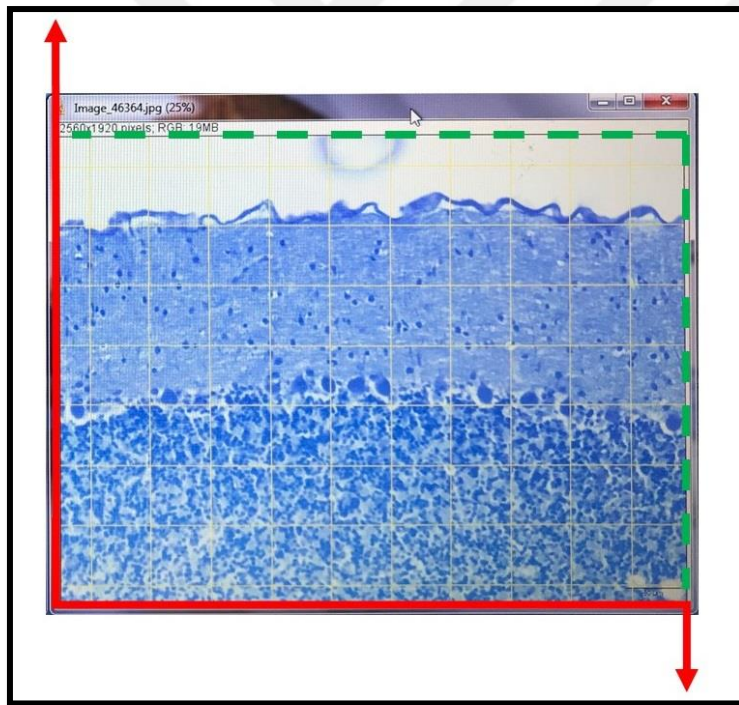


Figure 19. Unbiased counting frame

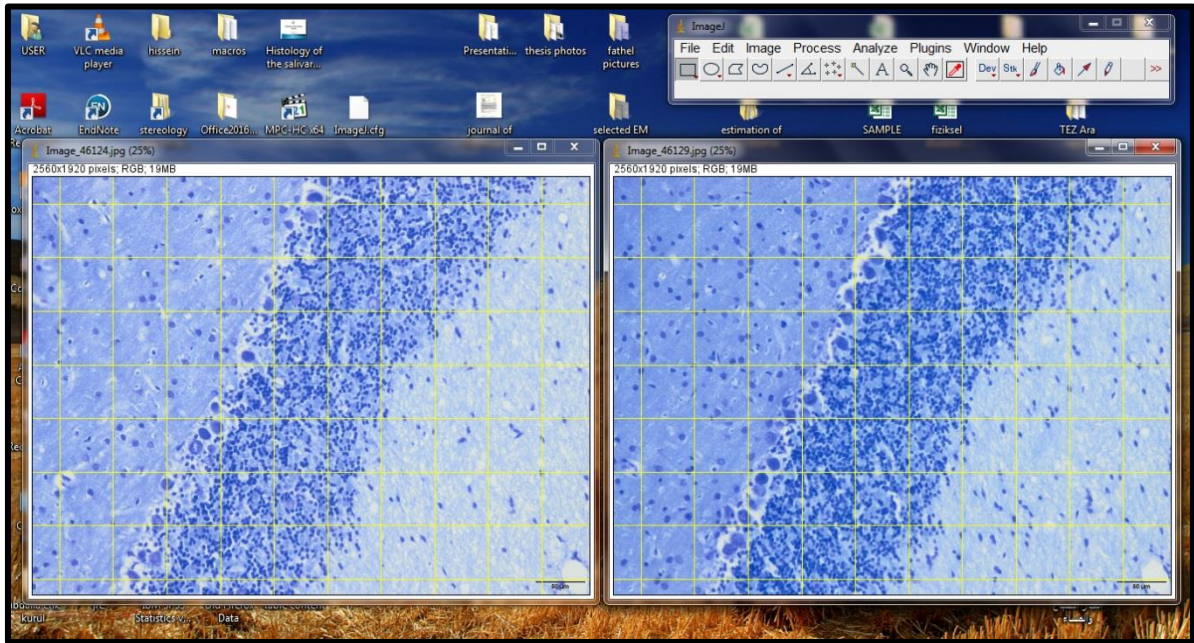


Figure 20. It shows *reference* and *look up* images of cerebellum in ImageJ program for counting the disector particles

3.6.2. The Volume of the Cerebellum

The reference volume of the cerebellum of each rat was estimated by using Cavalieri's principle (Gundersen and Jensen, 1987; Gundersen et al., 1988a; 1988b; Kristiansen and Nyengaard, 2012). To estimate the reference volume using point-counting grid, it is necessary to determine a fixed point in or on the unbiased counting frame used in particle counting. All points hitting the profiles of the tissue of interest (in this case, the cerebellum) must be counted through all sampled sections. This process is equal to throw an equally spaced point grid onto the sectional profiles with an interval equal to the step size. As a result, if we multiply the total number of points ($\sum P$) across all sections from an individual by the stepping size (point-associated area; $[a(p)]$), we can estimate the total profile area of the cerebellum visualized from the sampled sections. In our study, we estimated the total area of the cerebellum from the sampled sections for each rat by using the (closed polygon measurement) option in the software in the same system (**Figure 18**), which enables us to measure the cerebellum section area in (μm^2) directly (**Figure 21**). Multiplying the total area of the sampled sections ($\sum A$) with the distance between these sections' areas

(**T**) gives us an unbiased estimate of the reference volume (**V_{ref}**) of the cerebellum. The distance (**T**) is equal to the sectioning interval multiplied by the section thickness.

$$V_{\text{ref}} = \sum A \cdot T$$

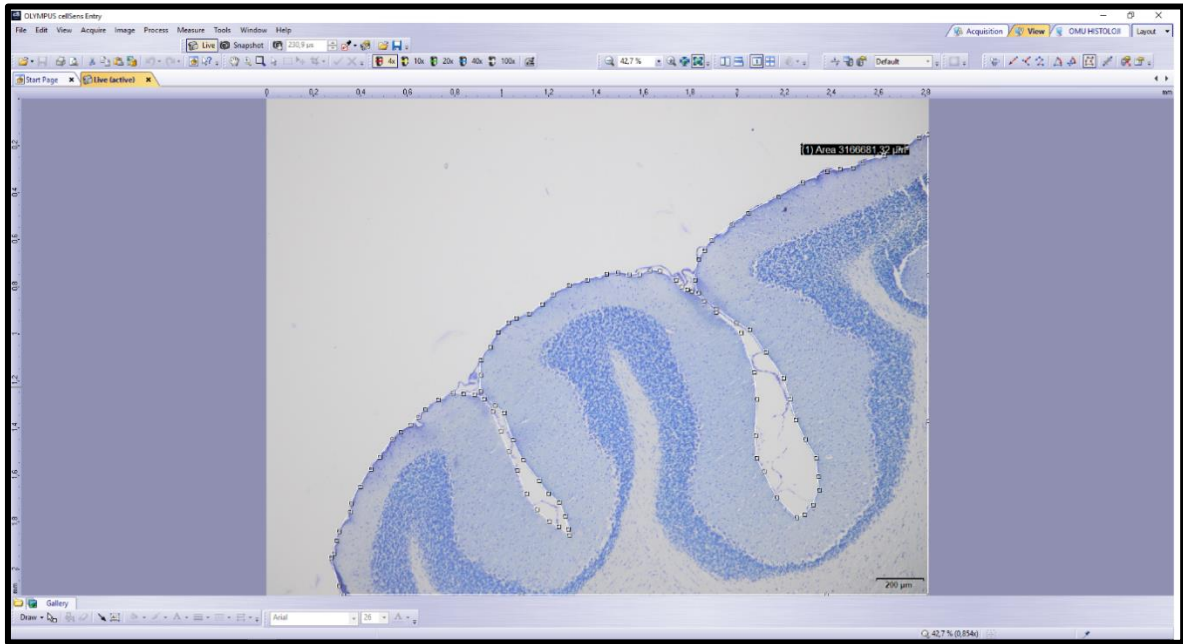


Figure 21. It shows measurement of the cerebellum section area

3.6.3. The Estimated Total Number of the Purkinje Cells

The total number of the Purkinje cells (**N**) in the cerebellum of each rat was estimated by multiplying the numerical density of the Purkinje cells (**N_v**) with the total reference volume of the cerebellum (**V_{ref}**) in the following equation (Gundersen et al., 1988a; Idrus and Napper, 2012).

$$N = N_v \cdot V_{\text{ref}}$$

3.6.4. The Coefficient of Variance (CV) and the Coefficient of Error (CE)

We estimated CV and CE values to ensure that our study has sufficient precision of a typical stereological design. CV is a measure of the group variability whereas CE is a measure

of the amount of error in the stereological estimation. The equations that we used in the calculations of CV and CE are shown below (Gundersen and Jensen, 1987; West et al., 1991; Gundersen et al., 1999).

$$CV = \frac{\text{standard deviation}}{\text{mean}} = \frac{\sqrt{\frac{\sum(x - \bar{x})^2}{n - 1}}}{\bar{x}}$$

x : the number of Purkinje cells in individual animal; \bar{x} : the mean number of Purkinje cells in each animal group; n : the number of animals in each group.

$CE_{(Nv)}$ for the estimate of the Purkinje cells' numerical density was calculated as follows:

$$A = \sum Q_i \cdot Q_i$$

$$B = \sum Q_i \cdot Q_{i+1}$$

$$C = \sum Q_i \cdot Q_{i+2}$$

$$\text{Noise} = \sum Q$$

$$\text{Var}_{(srs)} = (3(A - \text{Noise}) - 4B + C) / 240$$

$$\text{Total Var} = \text{Noise} + \text{Var}_{(srs)}$$

$$CE_{(Nv)} = \frac{\sqrt{\text{Total Var}}}{\sum Q}$$

$\sum Q$: the total number of disector Purkinje cells counted in all sampled sections of each rat; $Q_i \cdot Q_i$: the square of the disector Purkinje cells in each section; $Q_i \cdot Q_{i+1}$: the number of disector Purkinje cells from each section (i) multiplied by the number of the disector Purkinje cells from the next section (i+1) in the sequence; $Q_i \cdot Q_{i+2}$: the number of disector Purkinje

cells from each section (i) multiplied by the number of the disector Purkinje cells from the second next section (i+2) in the sequence.

$CE_{(V)}$ for the estimate of the total volume of the cerebellum was calculated as follows:

$$A = \sum A_i \cdot A_i$$

$$B = \sum A_i \cdot A_{i+1}$$

$$C = \sum A_i \cdot A_{i+2}$$

$$\text{Noise} = \sum 0.0724 \times 8 \times \sqrt{\sum A}$$

$$\text{Var}_{(srs)} = (3(A-\text{Noise}) - 4B + C)/240$$

$$\text{Total Var} = \text{Noise} + \text{Var}_{(srs)}$$

$$CE_{(V)} = \frac{\sqrt{\text{Total Var}}}{\sum A}$$

$\sum A$: the total area of all sampled cerebellum sections of each rat; $A_i \cdot A_i$: the square of the area of each cerebellum section; $A_i \cdot A_{i+1}$: the area of each cerebellum section (i) multiplied by the area of the next cerebellum section (i+1) in the sequence; $A_i \cdot A_{i+2}$: the area of each cerebellum section (i) multiplied by the area of the second next section (i+2) in the sequence.

$CE_{(N)}$ for the estimate of the total number of the Purkinje cells in the cerebellum was calculated using the following formula (Noorafshan et al., 2015; Rafati et al., 2017; 2018):

$$CE_{(N)} = \sqrt{CE^2_{(Nv)} + CE^2_{(V)}}$$

The upper limit for CE and CV is considered to be 0.05 and 0.10, respectively. Values below these limits indicate that the stereological design is sufficiently precise.

3.7. Biochemical Analysis

3.7.1. Blood Sample Collection

During the perfusion process and after access of the heart, 3 ml of intracardiac blood was collected from the heart of the rat into blood collection tubes. The blood was taken before passage of perfusion solutions through the circulatory system of the rats and centrifuged at 4 °C on (HettichEB 20 centrifuge, Hettich, Tuttlingen, Germany) for 15 min at 2000 rpm (**Figure 22**). The obtained serum samples were stored at -80 °C until biochemical analysis was done. The catalase (CAT) and superoxide dismutase (SOD) enzyme activities in the serum samples were analyzed by measuring absorbance values at the biochemistry department.



Figure 22. Centrifuge device

3.7.2. Analysis of Superoxide Dismutase Enzyme Activity

Highly reactive radicals produced by enzymes, such as xanthine oxidase and mitochondrial electron chain, appear in different pathologies with accumulation of superoxide anions (O_2^-) in cells and tissues (Viggiano et al., 2003). Accumulation of these molecules and other oxidant radicals should be avoided in order to resist the toxic effects of oxygen in aerobic organisms. When oxygen toxicity occurs in living tissues, an enzymatic defense mechanism initiated by SOD catalyzes the dismutation of oxygen and a

metalloenzymes (Peltola et al., 1992; Assady et al., 2011). In our study for assessing oxidative stress, SOD enzyme activity was measured using the SOD assay kit (Cayman Chemical Company, USA). The basic principle of the SOD assay kit used is based on the principle that xanthine-xanthine oxidase reaction results in the reaction with tetrazolium compound and purple reaction by removing superoxide radicals. The SOD in the sample removes the superoxide radicals from the medium and inhibits the reaction of the tetrazolium compound with oxygen. The absorbance values of the purple-colored solutions obtained after the experiment were measured using a microplate absorbance reader (Sunrise™, Tecan Trading AG, Männedorf, Switzerland) (**Figure 23**) at a wavelength of 450 nm (Ukeda et al., 1999).



Figure 23. A microplate absorbance reader (Sunrise™, TECAN)

3.7.3. Analysis of Catalase Enzyme Activity

Catalase (CAT) is antioxidant enzyme involved in the detoxification of hydrogen peroxide (H₂O₂) which is a toxic product of normal aerobic metabolism. The H₂O₂ at a low level stimulates the expression of stress-associated proteins and antioxidant enzymes, thus providing a response against oxidants. The conversion of the H₂O₂ molecule into oxygen and water occurs by the CAT enzyme. CAT demonstrates peroxidatic activity, in which low

molecular weight alcohols can serve as electron donors (Madeo et al., 1999; Martins and English, 2014). To determine the oxidative effect, Cayman's Catalase Assay Kit (Cayman Chemical Company, USA) utilized for determination of enzyme activity in the serum. The basic principle in the method is based on the CAT enzyme reaction with methanol in the presence of H_2O_2 . In this reaction, formaldehyde acts as a chromogen, causing a pink color in the reaction. After the relevant reactions, the absorbance of the samples was measured at a wavelength of 540 nm using a multi-mode microplate reader (BioTek Synergy 4, BioTek Instruments Inc., Vermont, USA) (**Figure 24**).



Figure 24. A microplate absorbance reader (BioTek Synergy 4)

3.8. Determination of Total Phenolic Content and Antioxidant Power

3.8.1. Preparation of Sample Extract

In this study extraction was made by ultrasound-assisted extraction with 80% methyl alcohol. For this, 2.5 g of the sample was added to 50 mL of 80% methyl alcohol at 20 °C for 30 minutes in ultrasonic water bath, then at room temperature for 2 hours. It was put in

centrifuge for 15 minutes at 3000 rpm to remove turbidity. The pre-analysis samples were filtered through a 0.45 Teflon filter.

3.8.2. Method to Assess the Total Phenolic Content

Singleton and Rossi (1965) 's method of determining the total phenolic content was modified. 2.5 ml of Folin-Ciocalteu was added onto 0.5 ml of sample diluted with the appropriate amount of methyl alcohol and left for 5 hours in a dark place to add 7.5% sodium carbonate solution. At the end of the period, the total phenolic content was calculated by means of the standard calibration curve, which was read against the witness at 760 nm wavelength and plotted with pure gallic acid.

3.8.3. Methods to Assess the Antioxidant power

3.8.3.1. Ferric ion Reduction Antioxidant Power (FRAP)

Samples extracted with methyl alcohol were diluted in an appropriate proportion; 10: 1: 1 (v: v: v) 300 mM acetate buffer: mixed with 20 mM FeCl₃: 10 mM 2,4,6-tripyridyl-s-triazine (TPTZ) solution (dissolved in 40 mM HCl), the absorbance at 593 nm was determined on the spectrophotometer. Calibration curve was drawn by using Trolox prepared solutions and the result was calculated (Gao et al., 2000).

3.8.3.2. Determination of DPPH Free-Radical Scavenging Effect

The method described by Tural and Koca (2008) was used to determine the reduction effect of DPPH radical (2,2-diphenyl-1-picrylhydrazyl). 50 L of the methyl alcohol-containing extract was mixed with 1 ml of DPPH solution and kept at room temperature in the dark until the reaction was completed and the absorbance at 517 nm was determined. In addition, the same procedure was carried out by preparing the control sample with methyl alcohol and the effect of removing the DPPH radical was calculated by the following formula. Calibration curve was drawn with Trolox prepared solutions and the result was calculated.

Absorbance of control sample -For example absorbance % DPPH inhibition = x100
absorbance of control sample

3.9. Statistical Analysis

The numerical data obtained from this study were evaluated by the SPSS software program (version 22.0). First, normality test was performed for the numerical density, the cerebellum volume and the total Purkinje cells' number, and this test results showed normal distribution of data. One-way ANOVA test was used to detect significant differences among the groups. Thereafter, Tukey's test was applied to compare the differences among the groups. According to normality test results, the data of the cerebellum volume and the total Purkinje cells' number had abnormal distribution. Therefore, Tamhane's T2 test was performed to compare each of the cerebellum volume and the total Purkinje cells' number among the groups. Each p value less than 0.05 was considered significant.

4. RESULTS

The present study was conducted to investigate the possible effects of GL and MC on the rat cerebellum which was exposed to 900 MHz EMF, using the physical disector technique. The cerebellar tissue sections were also examined by means of the light microscope and a microplate absorbance reader was used for biochemical analysis of the rat serum samples.

4.1. Stereological Findings

The numerical density of Purkinje cells was calculated in the entire cerebellum by the physical disector technique. The total volume of the cerebellum was estimated using Cavalieri's principle. Accordingly, the total number of Purkinje cells was calculated using certain equations. These estimations were done for the Cont group that was not exposed to 900 MHz EMF, sham group that was put in EMF exposure system while the system was turned off, EMF group that was exposed to 900 MHz EMF, EMF+GL group that was given GL and exposed to 900 MHz EMF, EMF+MC group that was given MC and exposed to 900 MHz EMF, EMF+GL+MC group that was given GL plus MC and exposed to 900 MHz EMF, GL group that was given GL, MC group that was given MC.

4.1.1. The Numerical Density of Purkinje Cells in Cerebellum

The mean numerical density of Purkinje cell in the cerebellum and the coefficient of error (CE) for it are shown in the following table and figure (**Table 5; Figure 25**).

Table 5. The mean numerical density of Purkinje cell (cell/mm³), (Mean±SD) and CE values for the estimate of the numerical density

Groups	The numerical density of Purkinje cell	CE
Cont	8273±318	0.035
Sham	5048±436	0.044
EMF	4725±337	0.046
EMF+GL	5747±731	0.042
EMF+MC	6482±611	0.041
EMF+GL+MC	7151±243	0.037
GL	7298±762	0.038
MC	7034±777	0.038

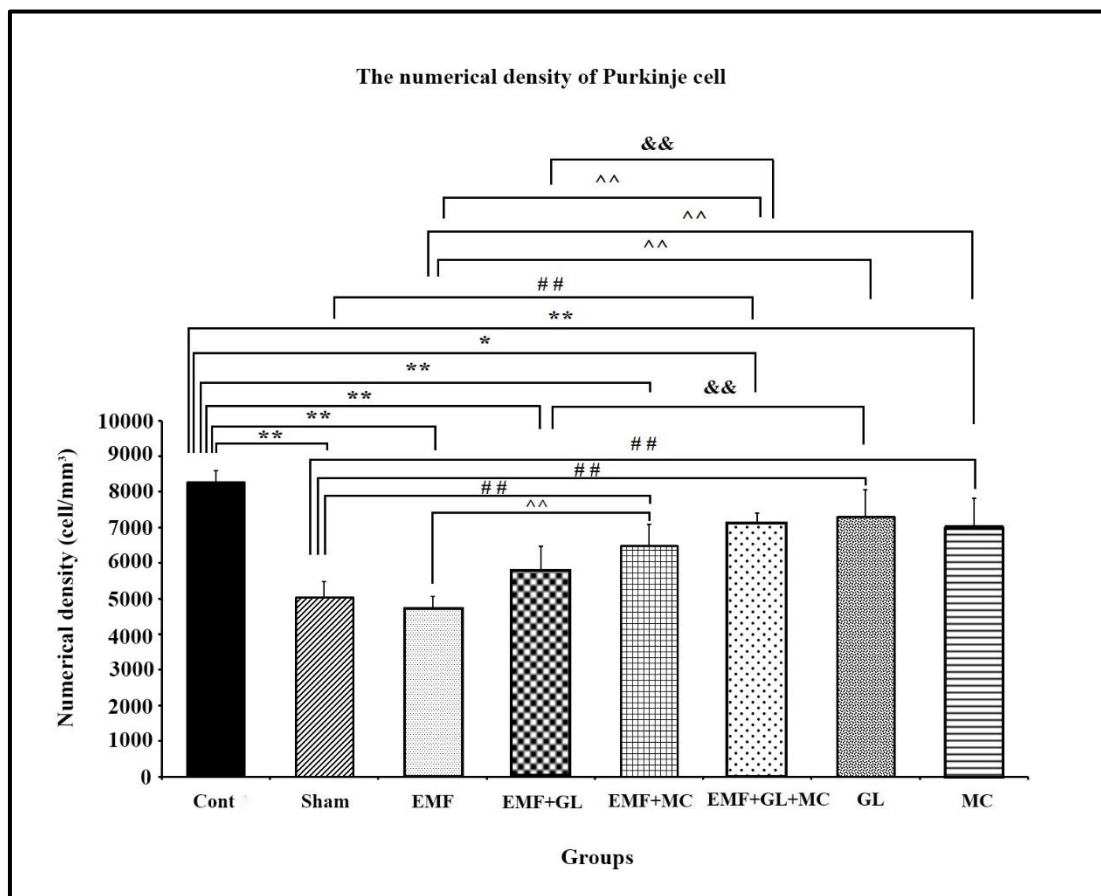


Figure 25. It shows differences in the numerical density of Purkinje cells in the cerebellum after exposure to EMF for 1 hour. Statistically significant differences at $p < 0.05$ are indicated by “*”, while significant differences at $p < 0.01$ are indicated by “**”, “##”, “^^” and “&&” (Mean \pm SD)

As a result of the statistical analysis of the data, it was found that the mean numerical density of Purkinje cells in the EMF and sham groups decreased significantly compared to the Cont group ($p < 0.01$). The mean numerical density of Purkinje cells in the EMF+GL and EMF+MC groups was significantly lower than that in the Cont group ($p < 0.01$). The EMF+GL+MC group showed significantly lower mean numerical density than Cont group ($p < 0.05$). The mean numerical density of Purkinje cells in the EMF+MC and EMF+GL+MC groups was significantly higher than that in the EMF and sham groups ($p < 0.01$). The mean numerical density of Purkinje cells in the EMF and sham groups was significantly lower than that in the GL and MC groups ($p < 0.01$) (**Table 6**).

Table 6. It shows the degree of significance among groups for the numerical density of Purkinje cells

Comparison between groups	Significance
EMF with Cont group	0.000
EMF with Sham group	0.974
Cont with Sham group	0.000
EMF+GL with EMF group	0.059
EMF+MC with EMF group	0.000
EMF+GL+MC with EMF group	0.000
GL with EMF	0.000
MC with EMF	0.000
Cont with GL group	0.082
Cont with MC group	0.010

4.1.2. The Total Volume of Cerebellum

The mean total volume of the cerebellum and the coefficient of error (CE) for it are shown in the following table and figure (**Table 7; Figure 26**).

Table 7. The mean total volume of the cerebellum (mm³), (Mean±SD) and CE values for each group

Groups	The total volume of cerebellum	CE
Cont	46.96±9.06	0.012
Sham	51.44±8.52	0.014
EMF	64.64±9.80	0.008
EMF+GL	66.37±7.77	0.012
EMF+MC	64.35±8.73	0.015
EMF+GL+MC	62.46±6.04	0.014
GL	64.81±5.08	0.014
MC	54.18±6.40	0.016

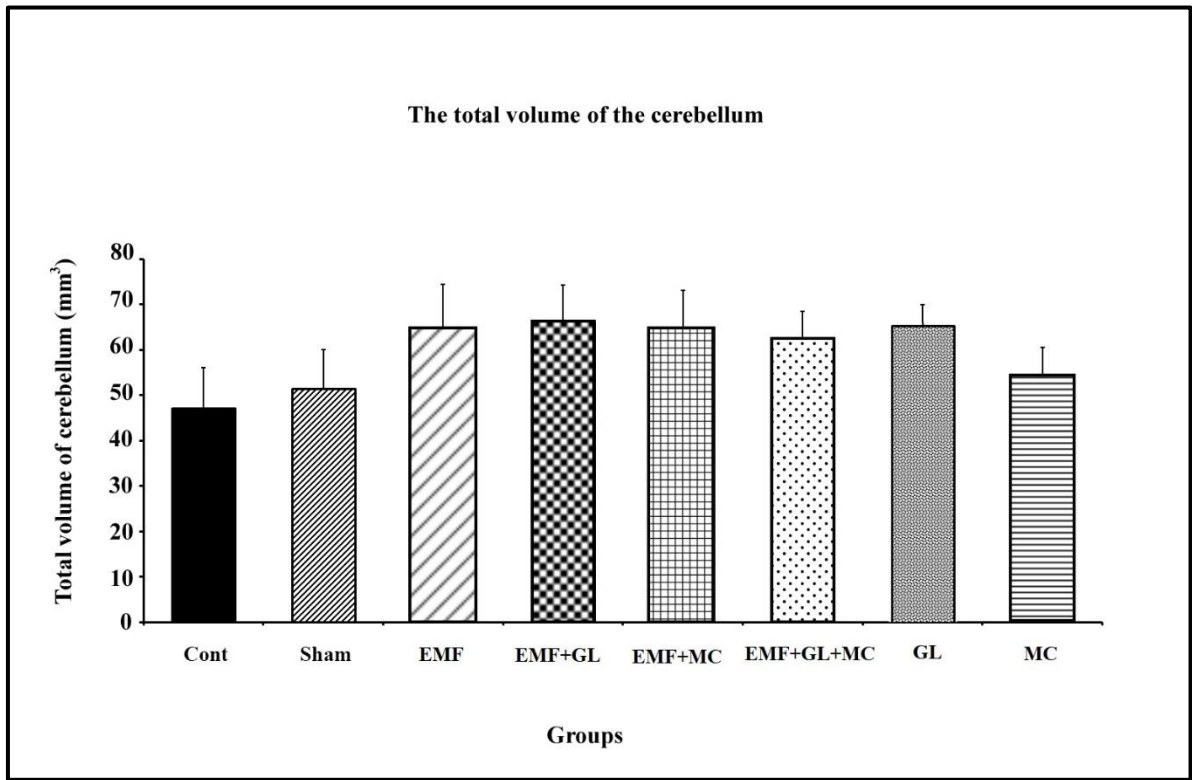


Figure 26. It shows the total volume of cerebellum for each group. No significant differences were observed among groups ($p > 0.05$) (Mean \pm SD)

As a result of the statistical analysis of the cerebellum volume, it was observed that there were no significant differences in the mean total volume of the cerebellum between all animal groups ($p > 0.05$) (**Table 8**).

Table 8. It shows the degree of significance among groups for the cerebellum volume

Comparison between groups	Significance
EMF with Cont group	0.220
EMF with Sham group	0.603
Cont with Sham group	1.000
EMF+GL with EMF group	1.000
EMF+MC with EMF group	1.000
EMF+GL+MC with EMF group	1.000
GL with EMF	1.000
MC with EMF	0.810
Cont with GL group	0.082
Cont with MC group	0.988

4.1.3. The Total Number of Purkinje Cells in Cerebellum

The mean number of Purkinje cells in the cerebellum, coefficient of error (CE) and coefficient of variance (CV) are shown in the following table and figure (**Table 9; Figure 27**).

Table 9. The mean number of Purkinje cells in the cerebellum (Mean± SD), CE and CV values for each group

Groups	Number of Purkinje cells	CE	CV
Cont	388914±80072	0.037	0.188
Sham	257216±29953	0.047	0.106
EMF	304539± 43477	0.046	0.130
EMF+GL	380549±60699	0.043	0.146
EMF+MC	414112±45258	0.044	0.100
EMF+GL+MC	447597±55265	0.040	0.113
GL	471283±42287	0.040	0.082
MC	377988±30202	0.041	0.073

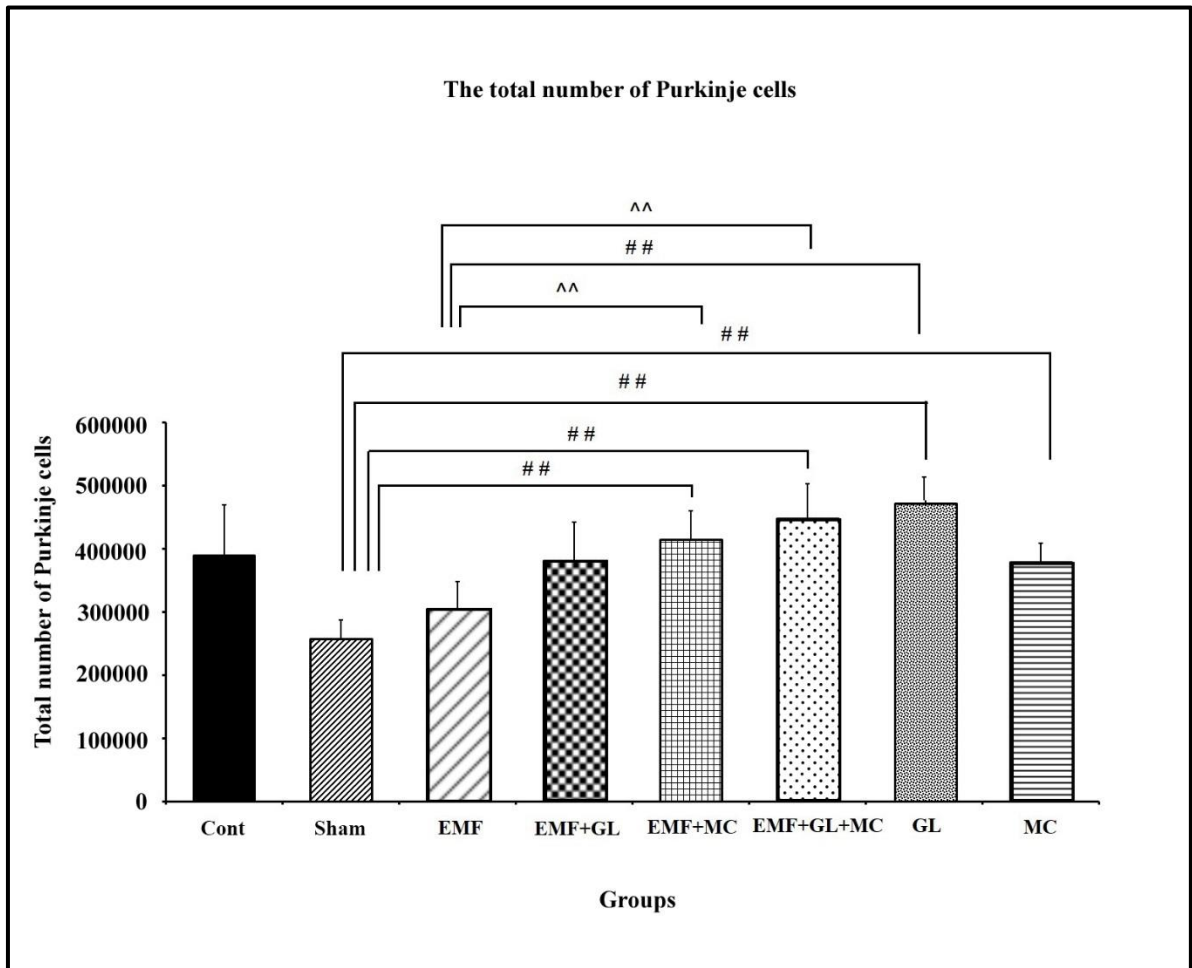


Figure 27. It shows the differences in the total number of Purkinje cells in the cerebellum after exposure to EMF for 1 hour. Significant differences at $p < 0.05$ are indicated by “^” while significant differences at $p < 0.01$ are indicated by “^” (Mean±SD)

As a result of the statistical analysis of the data, it was observed that the total number of Purkinje cells increased significantly in the EMF+MC and EMF+GL+MC groups compared to the EMF group ($p < 0.05$). The total number of Purkinje cells in the EMF group was lower than that in the Cont group but this was not statistically significant ($p > 0.05$). Also, the sham group had less Purkinje cells when compared to the Cont group but there was no statistical significance between them ($p > 0.05$). The GL group had significantly higher number of Purkinje cells than the EMF and the sham groups ($p < 0.01$). The total number of Purkinje cells in the MC group was significantly higher than the sham group ($p < 0.01$). In

addition, the total number of Purkinje cells in the EMF+MC and EMF+GL+MC groups was significantly higher than in the sham group ($p < 0.01$) (**Table 10**).

Table 10. It shows the degree of significance among groups for the total number of Purkinje cells

Comparison between groups	Significance
EMF with Cont group	0.790
EMF with Sham group	0.802
Cont with Sham group	0.208
EMF+GL with EMF group	0.621
EMF+MC with EMF group	0.045
EMF+GL+MC with EMF group	0.018
GL with EMF	0.001
MC with EMF	0.201
Cont with GL group	0.814
Cont with MC group	1.000

4.2. Light and Electron Microscopic Findings

4.2.1. Light Microscopic Findings

Tissue sections were taken from the cerebellum of all experimental animals. These sections were stained with cresyl violet stain and the cerebellar layers; molecular, Purkinje and granular layers were examined by the light microscope.

It was found that the numbers of normal Purkinje cells in the Cont group were more than in the EMF group (**Figure 28, 30**). In addition, the numbers of normal Purkinje cells in the EMF+MC and EMF+GL+MC were greater than in the EMF group (**Figure 30, 32, 33**). In the Cont group, the general structure of cerebellar layers appeared normal; well-preserved capillaries and Purkinje cells were observed (**Figure 28**). In the EMF group, the general structure of cerebellum was not only heavily affected but also the Purkinje and granular cells were heavily damaged, since they had condensed cell bodies and also there was no clear cell border (**Figure 30**). In the EMF+GL group, the histological structure of cerebellum was heavily destroyed, and the GL did not protect these cells from EMF exposure; the border of Purkinje cells nuclei is not smooth as many of the indentations were seen on it. Furthermore,

the cytoplasm of Purkinje cells was darkly stained (**Figure 31**). As seen in the LM images, the histological structure of cerebellar layers of the EMF+MC group was well protected by means of MC administration (**Figure 32**). In EMF+GL+MC group, the general structure of cerebellum appeared normal. Side effect of EMF exposure on the cerebellum has been decreased by means of GL and MC administration, since border of Purkinje cells and granular cells was seen clearly. And the density of Purkinje cell cytoplasm was normal, some of heavily impaired Purkinje cells were also seen (**Figure 33**). In GL and MC groups, the general structure of cerebellum, distribution of the Purkinje and granular cells looked normal. The border of Purkinje cells and their nuclei was also clearly observed (**Figure 34, 35**).

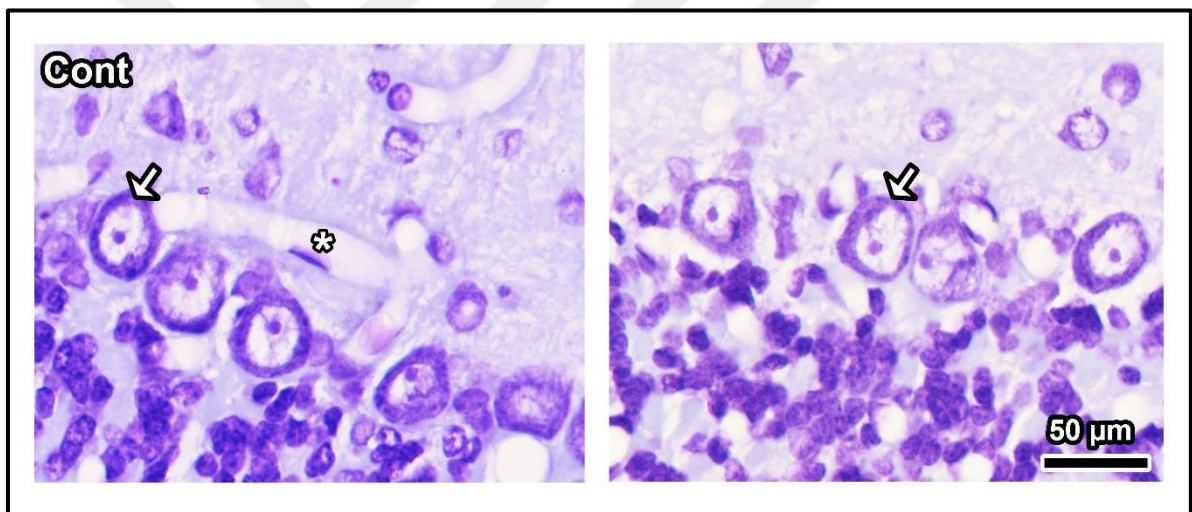


Figure 28. Histological images of the cerebellar layers stained with cresyl violet are seen. General structure of cerebellum is fine. Well preserved capillaries are seen in the molecular layer (*). The arrows indicate healthy Purkinje cells. Original magnification: X100

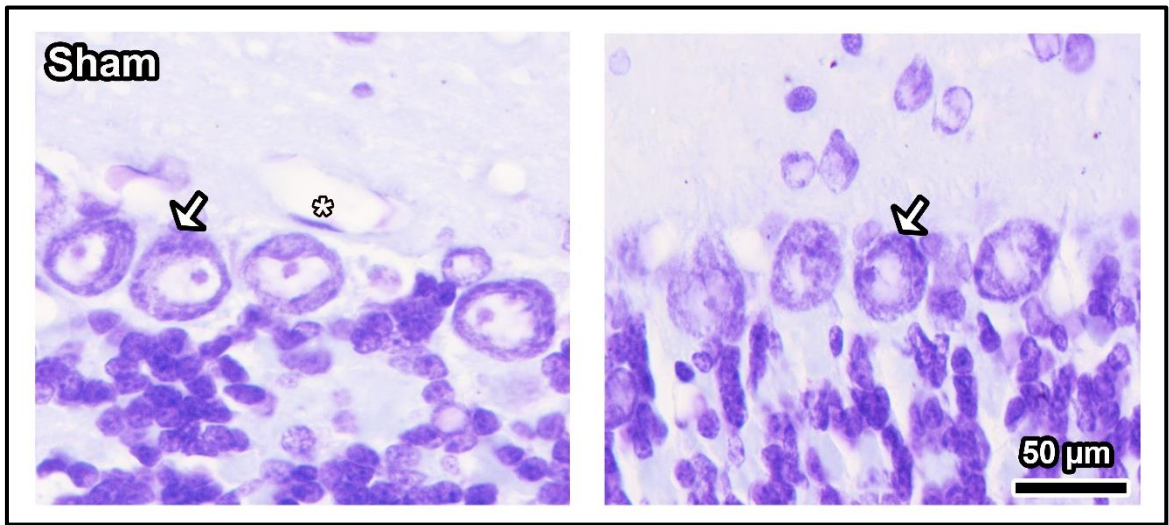


Figure 29. Histological images of the cerebellar layers stained with cresyl violet are seen. General structure of cerebellar layers is fine. A capillary lumen lined by endothelial cell is seen (*). The arrows indicate healthy Purkinje cells. Original magnification: X100

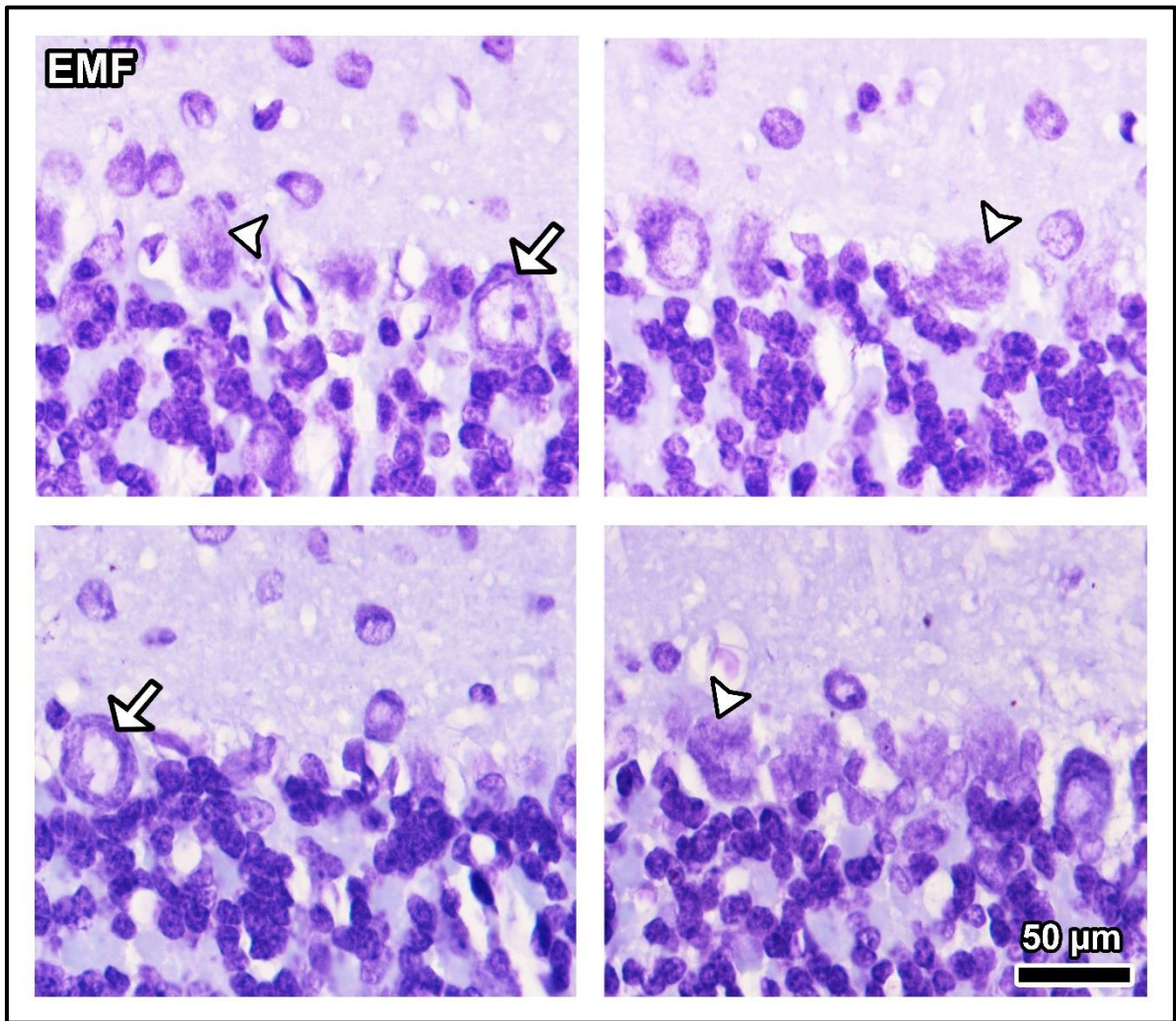


Figure 30. Histological images of the cerebellar layers stained with cresyl violet are seen. General structure of cerebellum as seen was heavily impaired, especially both types of neurons, Purkinje and granular cells, were heavily damaged since they have condensed cell bodies and there is no clear delineation of cells. The arrowheads indicate degenerated Purkinje cells, while arrows show healthy Purkinje cells. Original magnification: X100

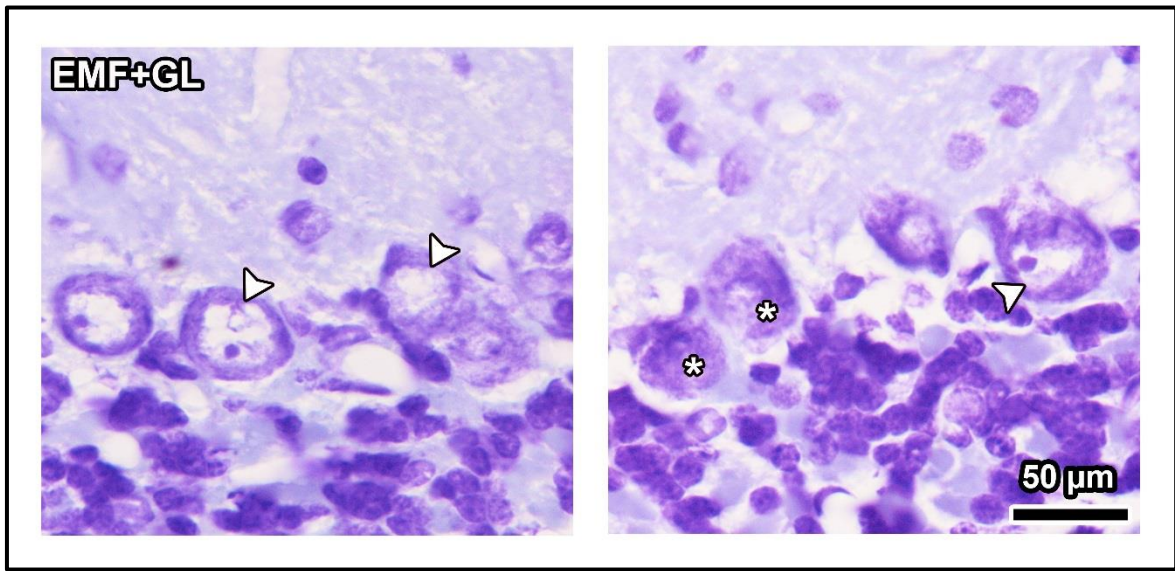


Figure 31. Histological images of the cerebellar layers stained with cresyl violet are seen. Histological structure of cerebellum as seen is heavily impaired, and no protection of the GL against EMF exposure. The border of Purkinje cells nuclei is not smooth, since many of the indentations can be seen on it. The cytoplasm of Purkinje cells is darkly stained. The arrowheads indicate indentations on nucleus. Degenerated Purkinje cells are shown by (*). Original magnification: X100

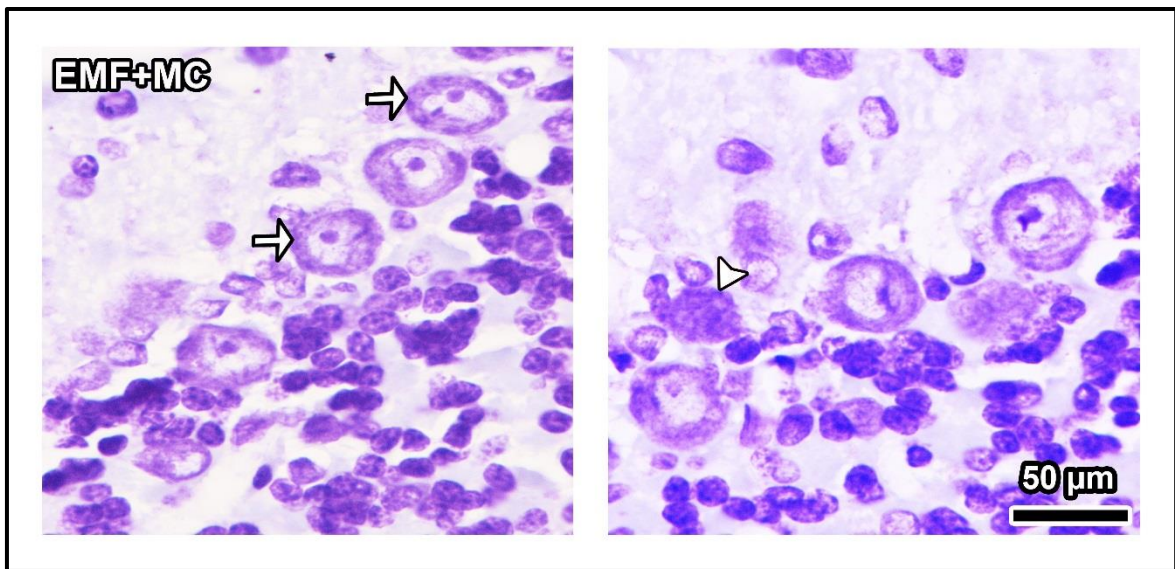


Figure 32. Histological images of the cerebellar layers stained with cresyl violet are seen. A well protected histological structure of cerebellar layers by means of MC administration is seen after EMF exposure. The arrows indicate healthy Purkinje cells, while the arrowhead shows degenerated cell. Original magnification: X100

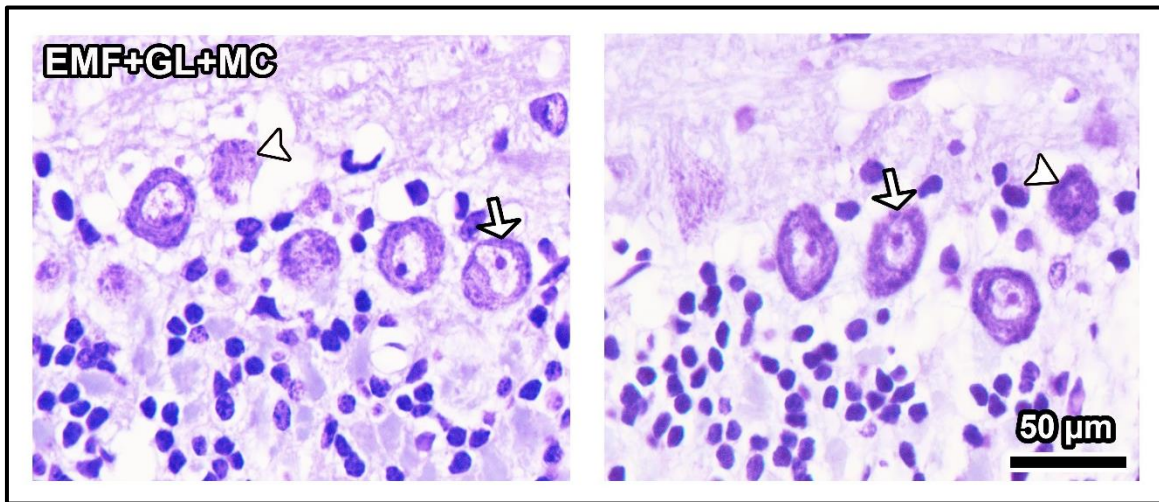


Figure 33. Histological images of the cerebellar layers stained with cresyl violet are seen. General structure of cerebellum looks fine. Side effect of EMF exposure on the cerebellum has been decreased by means of GL and MC administration, since border of Purkinje cells and granular cells is seen clearly (arrow). And the density of Purkinje cell cytoplasm is observed as normal, some of heavily impaired Purkinje cells are also seen (arrowheads). Original magnification: X100

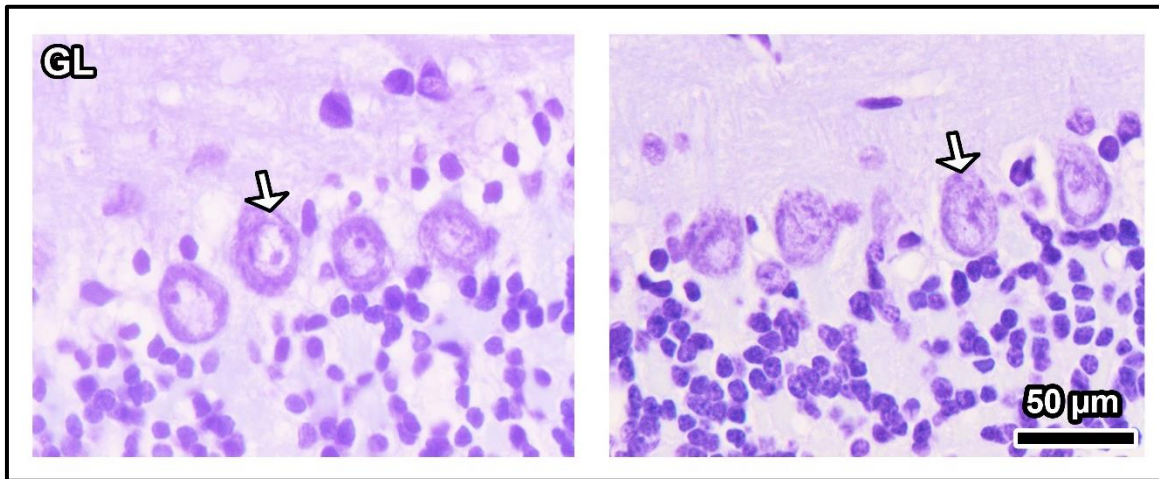


Figure 34. Histological images of the cerebellar layers stained with cresyl violet are seen. General structure of cerebellum, distribution of the Purkinje and granular cells looks fine. The border of Purkinje cells and their nuclei are also clearly seen. The arrows indicate healthy Purkinje cells. Original magnification: X100

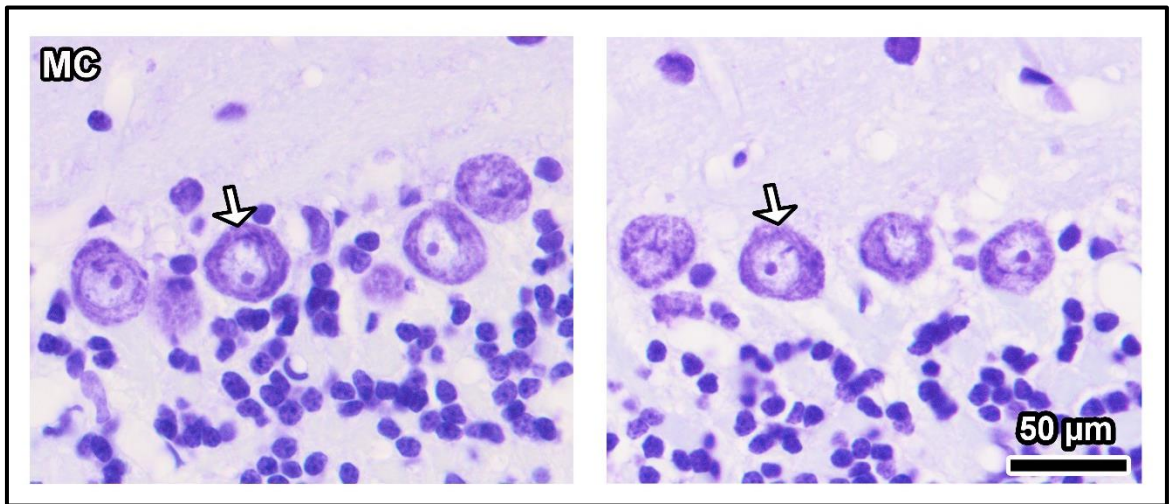


Figure 35. Histological images of the cerebellar layers stained with cresyl violet are seen. General structure of cerebellum, distribution of the Purkinje and granular cells looks fine. The border of Purkinje cells as well as their nuclei are also clearly seen. The arrows indicate healthy Purkinje cells. Original magnification: X100

4.2.2. Electron Microscopic Findings

The ultrastructure of the cerebellum in the Cont group was normal. The border of granular and Purkinje cells was seen clearly. Euchromatic nucleus and dense nucleolus were observed in the granular cell. The capillaries, myelinated nerve fibres and the surrounding tissue were in normal appearance (**Figure 36, 37**) while in the sham group heavily impaired myelin sheaths were observed (**Figure 38**). The ultrastructure of the cerebellum in the EMF group was affected and many of darkly stained cells were found. A side effect of EMF exposure on the granular cells of the cerebellum was obviously observed, the density of granular cells decreased and their integrity was impaired. A similar effect of EMF exposure on the myelinated axons was seen (**Figure 39, 40, 41, 42**). In the EMF+GL group, as a result of EMF exposure the size of granular cells nuclei was substantially decreased and also the shape of them was impaired, because many indentations were seen on the nucleus. An apoptotic granular cell surrounded by healthy granular cells was found and some myelinated axons were heavily impaired (**Figure 43, 44**). In the EMF+MC group, the ultrastructure of the granular cells in the cerebellum even after EMF exposure was protected by means of MC treatment. Well-preserved cells and nuclei borders were seen in this group. Most of the

capillaries and myelinated axons were protected (**Figure 45, 46, 47**). A damaged neuron as a result of EMF exposure was observed in EMF+MC images. This impaired neuron maybe it has been removed by means of apoptotic process (**Figure 47**). Regarding the EMF+GL+MC group, the ultrastructure of the granular cells in the cerebellum even after EMF exposure was protected by means of GL and MC (**Figure 48, 51**). However, the side effects of EMF exposure on cells and axons were also observed (**Figure 49, 50**). In the GL group, the ultrastructure and density of granular cells were also normal. Well-preserved myelinated axons, cell and nuclei borders were clearly observed (**Figure 52, 53, 54**). The general structure of cerebellar cortex in the MC group was fine, the density and structure of granular cells were normal. In addition, although some cells were shrunken and darkly stained that might be apoptotic cells but well-preserved capillaries can be seen (**Figure 55, 56, 57, 58**).

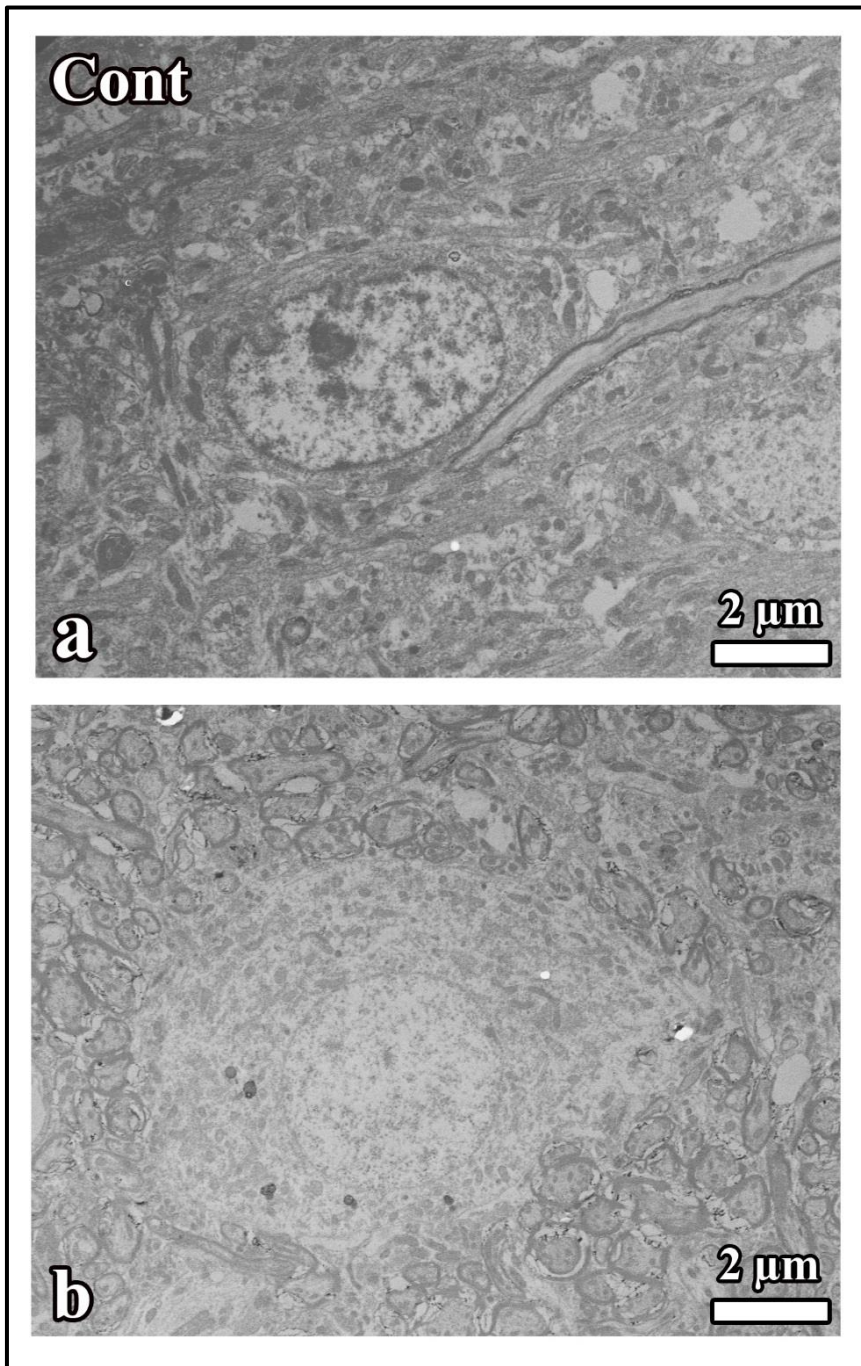


Figure 36. Electron microscopic images of the cerebellar cortex that belong to the control group are shown. The ultrastructure of the cerebellum is seen normal. The border of granular and Purkinje cells is seen clearly. Euchromatic nucleus and dense nucleolus are observed in the granular cell. A longitudinal section of myelinated axon and surrounding tissue looks fine (a). A normal structure of Purkinje cell is seen (b), the border of nucleus and cytoplasm are clear

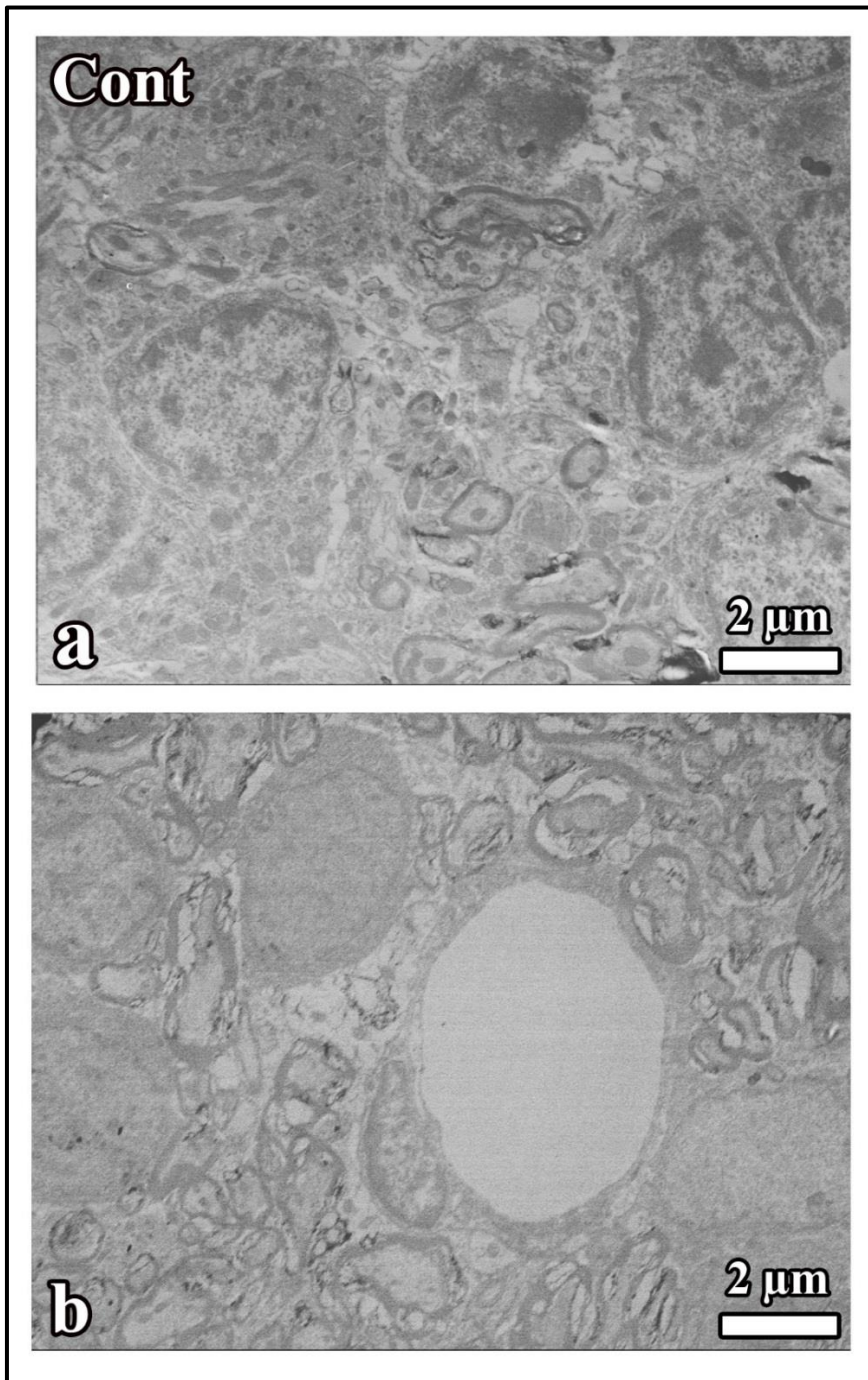


Figure 37. Electron microscopic images of the cerebellar cortex that belong to the control group are shown. The ultrastructure of granular cells in the cerebellum is normal (a). A capillary that is lined by endothelial cell and surrounding myelinated nerve fibres are seen (b)

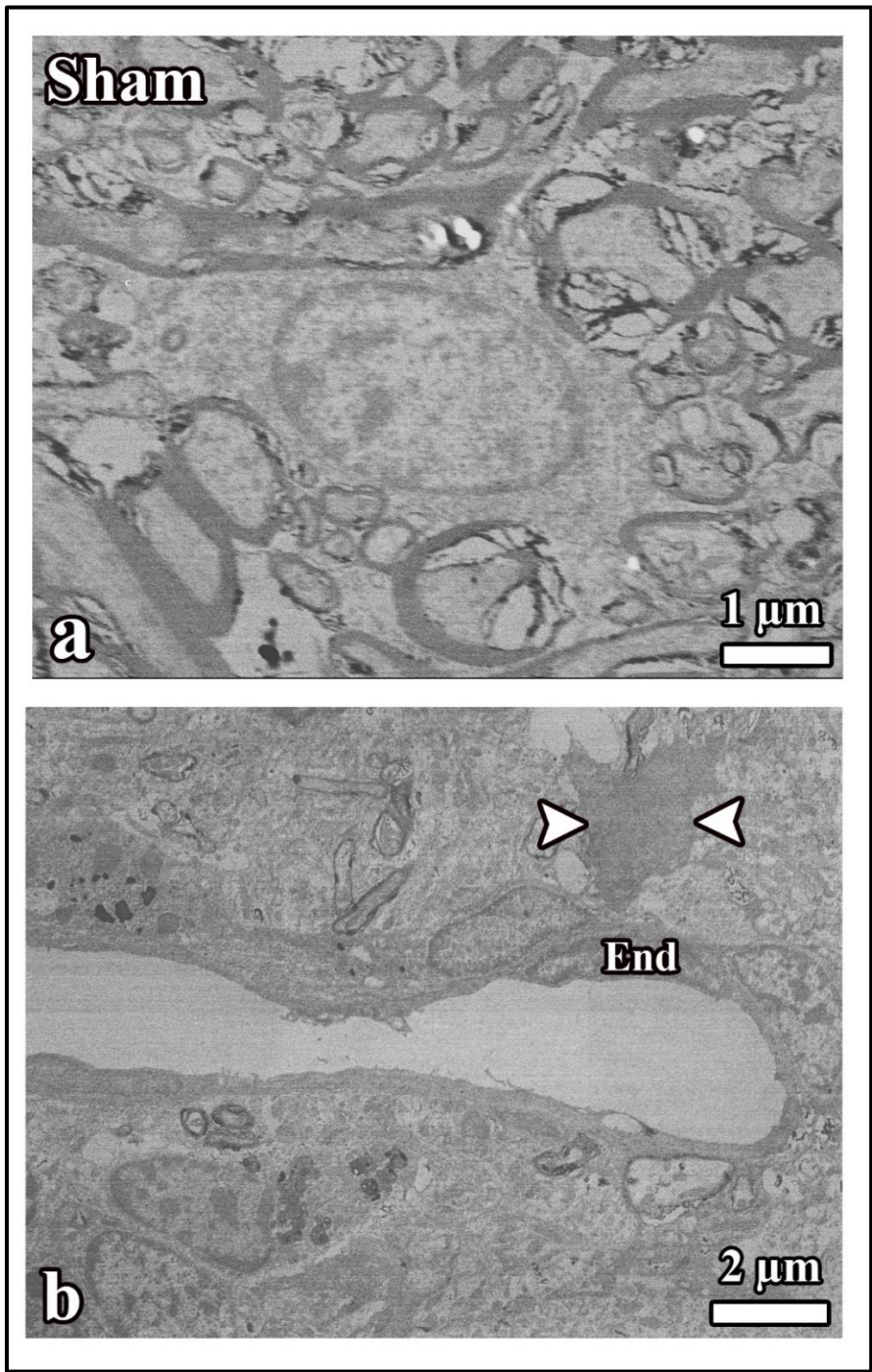


Figure 38. Electron microscopic images of the cerebellar cortex that belong to the sham group are shown. A heavily impaired myelinated axon sheaths are seen (a). A capillary is observed at the centre of picture, even structure of the capillary is found normal but some of darkly stained cell remnant can be seen around it (arrowheads) (b). Endothelial cell (End)

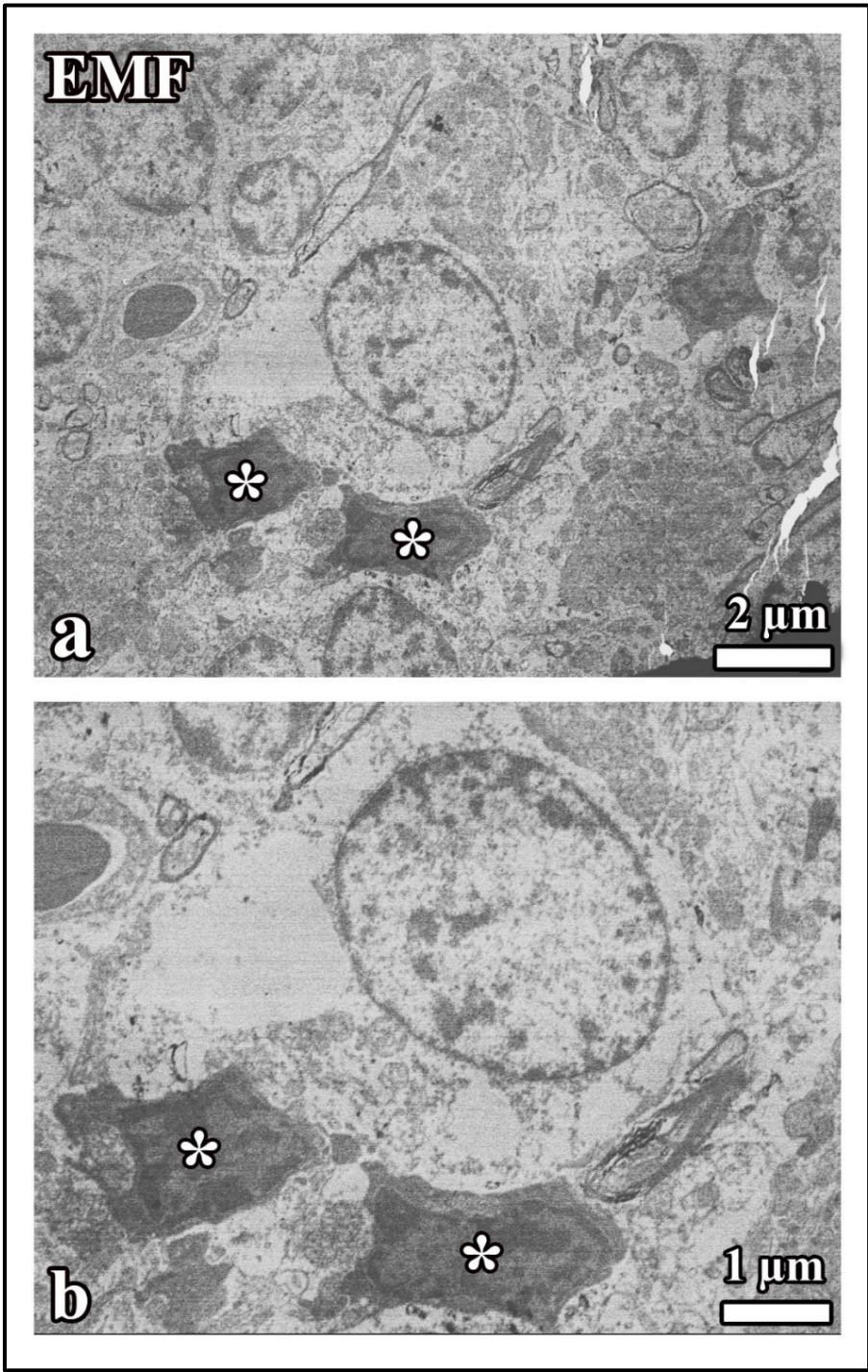


Figure 39. Electron microscopic images of the cerebellar cortex that belong to the EMF group are shown. The ultrastructure of the cerebellum is affected by EMF exposure, since many of darkly stained cells are seen in this group (*)

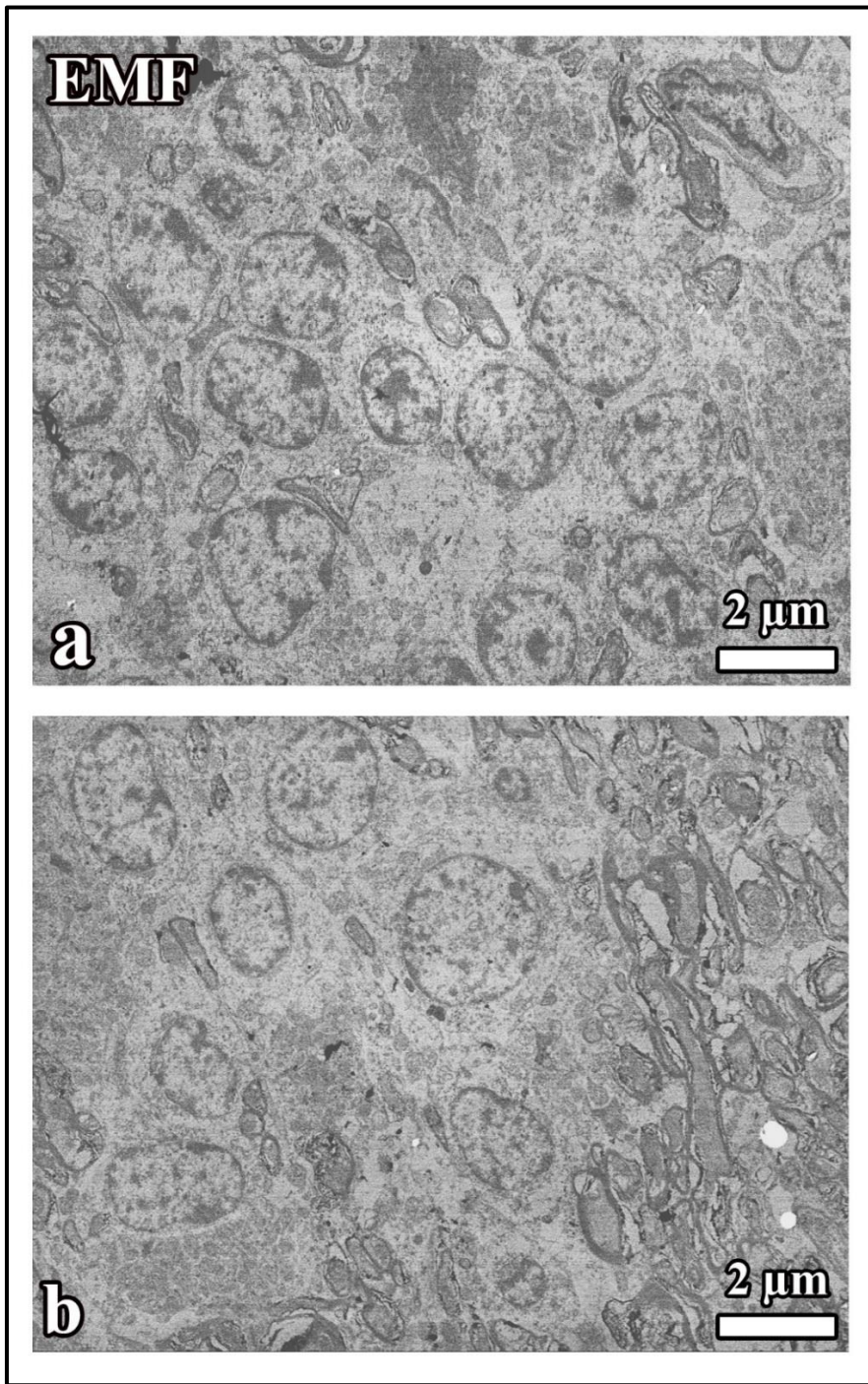


Figure 40. Electron microscopic images of the cerebellar cortex that belong to the EMF group are shown. A side effect of EMF exposure on the granular cells of the cerebellum is seen obviously. Since a decreased density of granular cells and impaired integrity of them are seen (a). A similar effect on the myelinated axons is also observed (b)

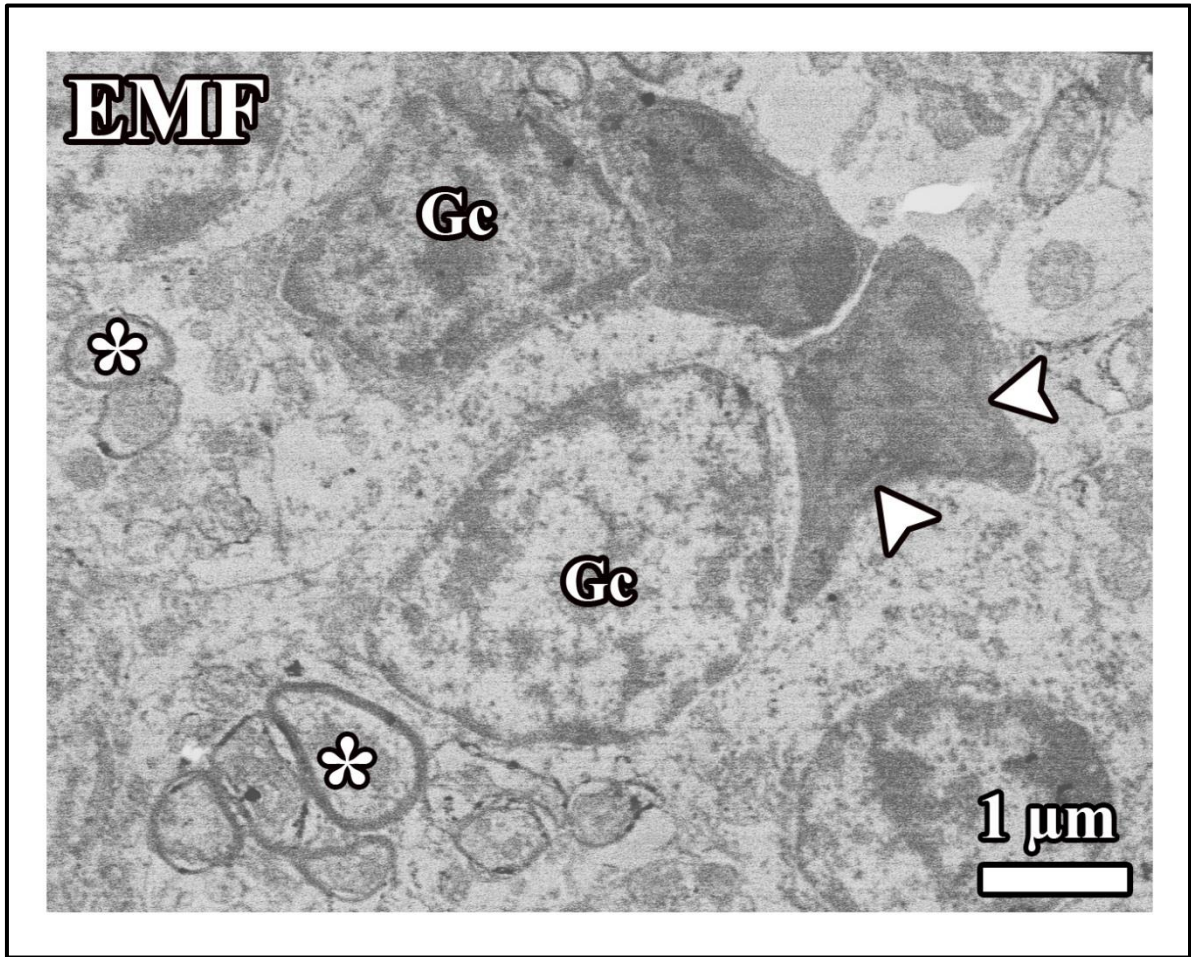


Figure 41. Electron microscopic image of the cerebellar cortex that belong to the EMF group is seen. A pronounced side effect of EMF exposure on the granular cells is seen since granular cells heavily shrunk (arrowheads). A decreased density of granular cells as well as impaired integrity of them are observed. A similar effect on the myelinated axons is also seen since most of axons are sheathed by thin myelin sheath (*). Granular cell (Gc)

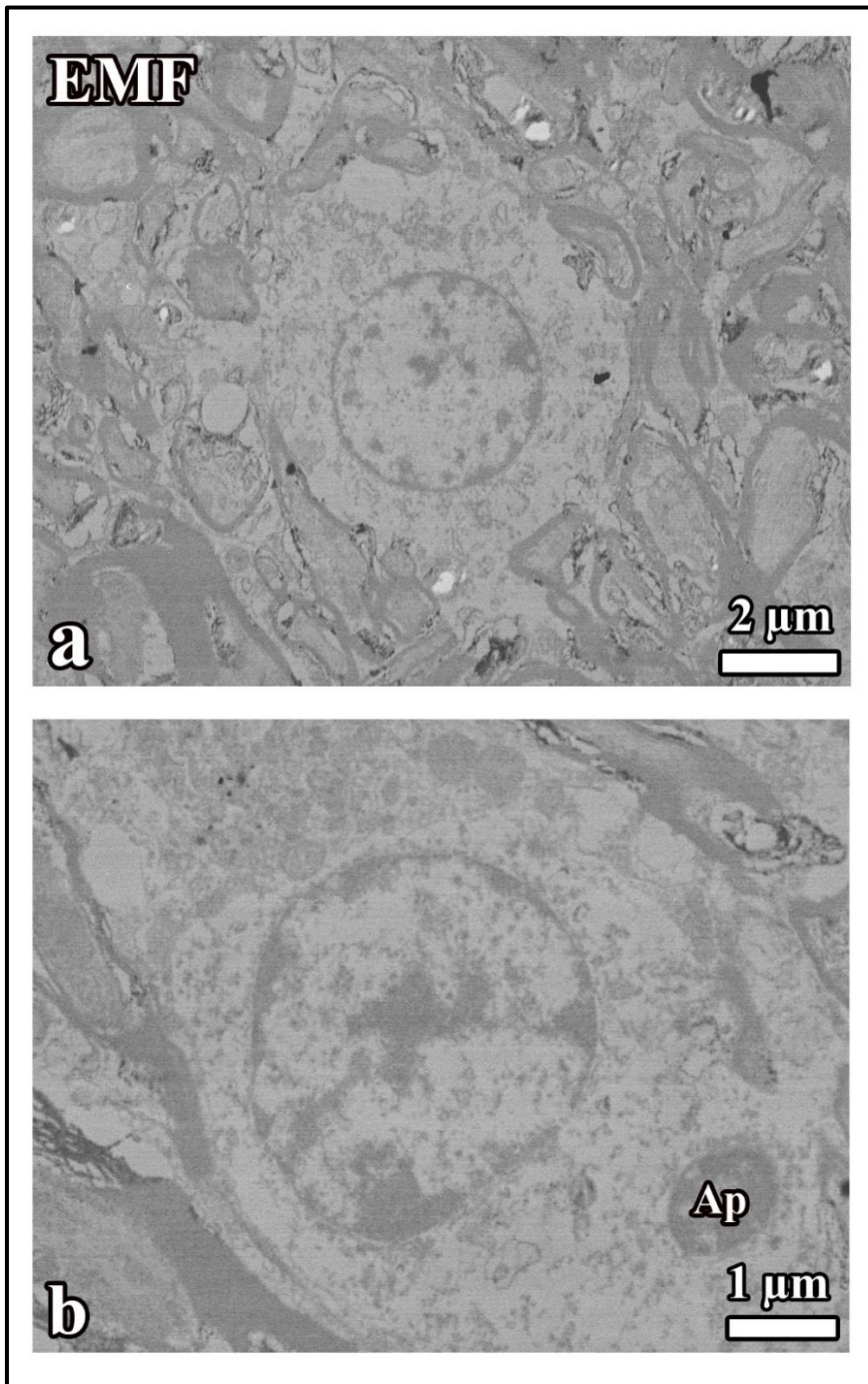


Figure 42. Electron microscopic images of the cerebellar cortex that belong to the EMF group are shown. A cell that might be neuroglial cell has a normal structure, double unit membrane around the nucleus is well preserved and chromatin distribution in the nucleus is also normal (a). A cell in the cerebellum is seen. The structure of cell is generally preserved but an apoptotic body-like structure is seen in the cytoplasm of cell (b). Apoptotic body (ap)

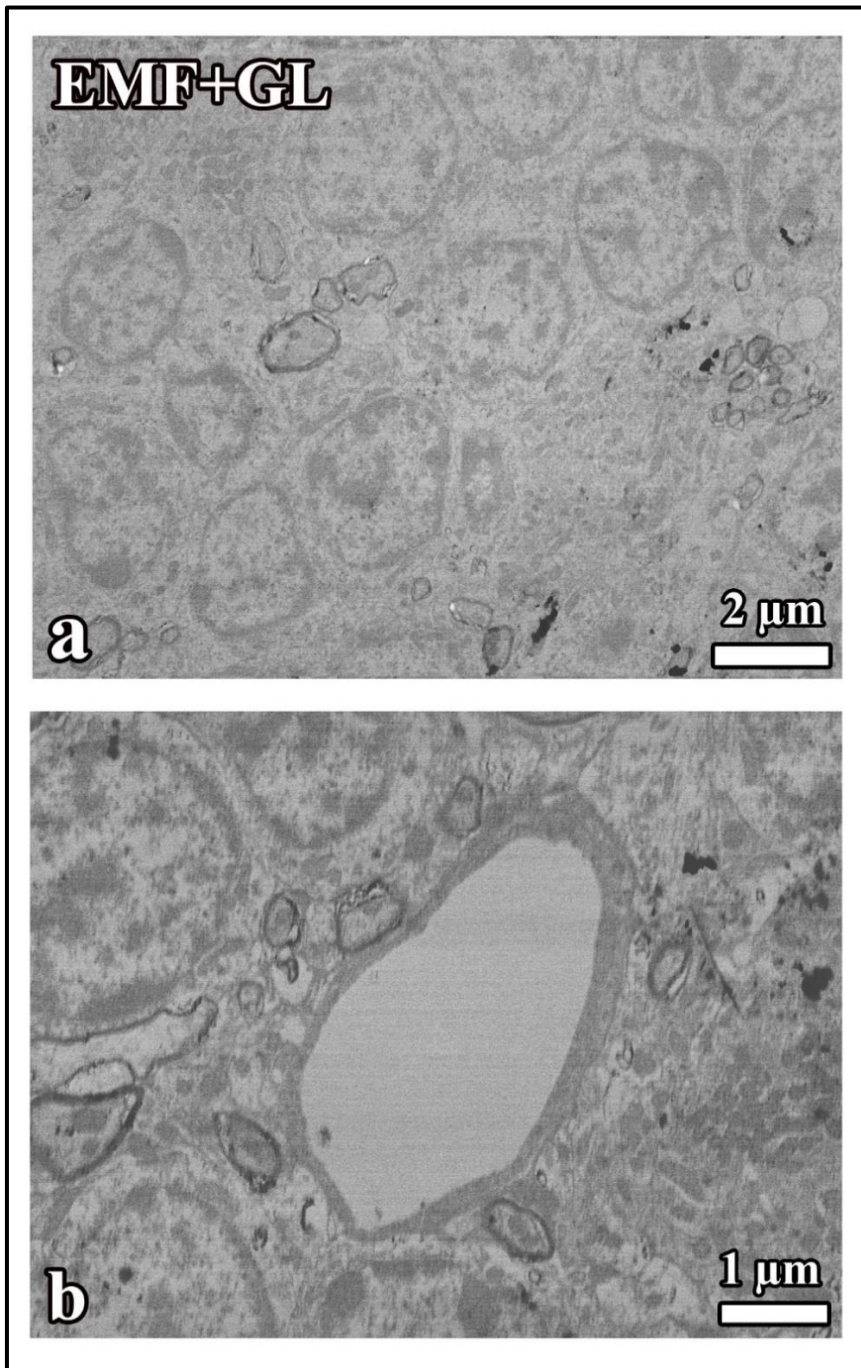


Figure 43. Electron microscopic images of the cerebellar cortex that belong to the EMF+GL group are shown. Granular cells in the cerebellar cortex are seen, as a result of EMF exposure the size of nuclei was substantially decreased and also the shape of them was impaired, because many indentations are seen on the nucleus (a). A well-preserved capillary and granular cells are observed in the cortex of cerebellum. The border of granular cells and capillary are clearly seen (b)

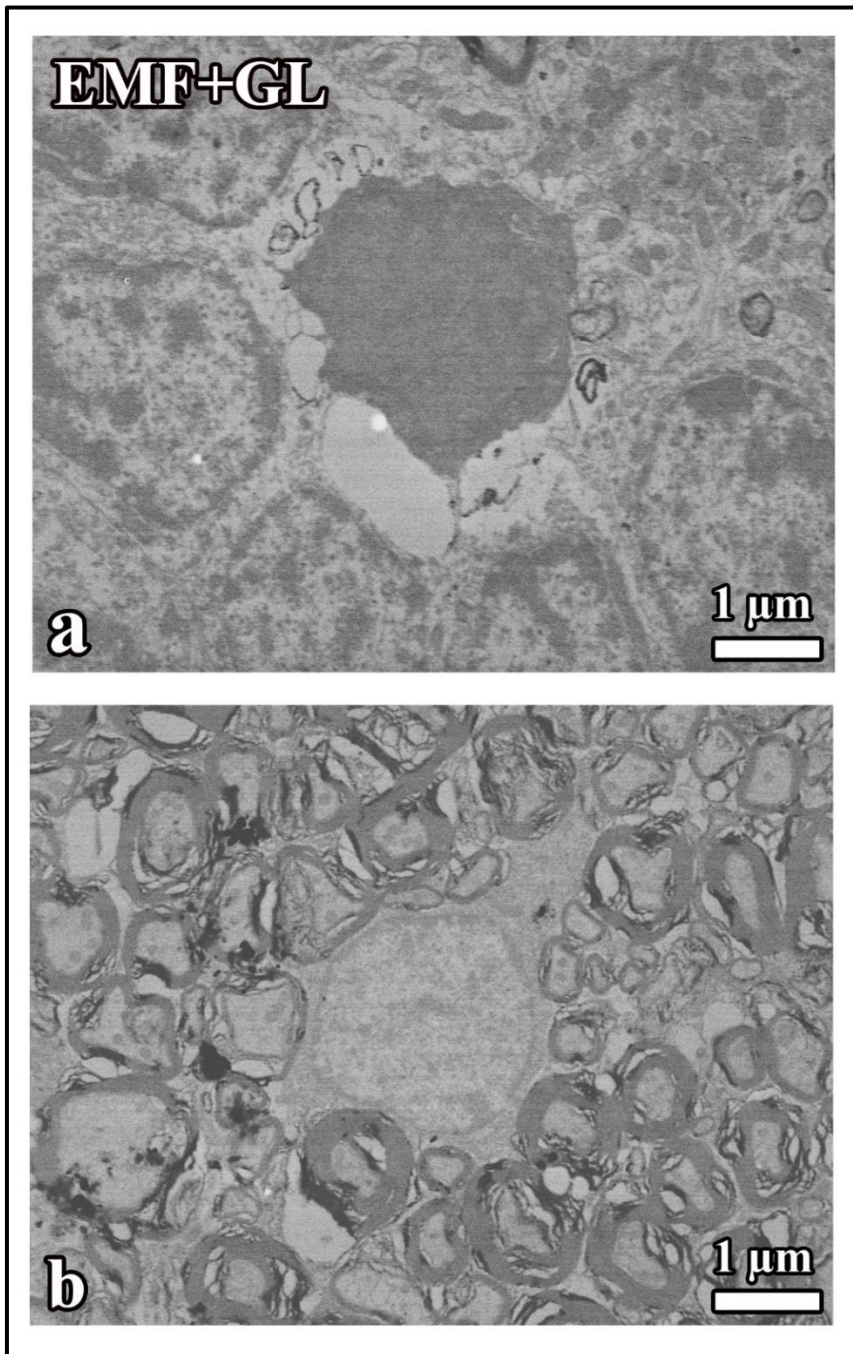


Figure 44. Electron microscopic images of the cerebellar cortex that belong to the EMF+GL group are shown.

Although the ultrastructure of the granular cells in the cerebellum is protected, side effect of EMF exposure is seen. An apoptotic granular cell surrounded by healthy granular cells is observed (a). An oligodendroglia is surrounded by many myelinated axons that some of them are normal but some are heavily impaired (b)

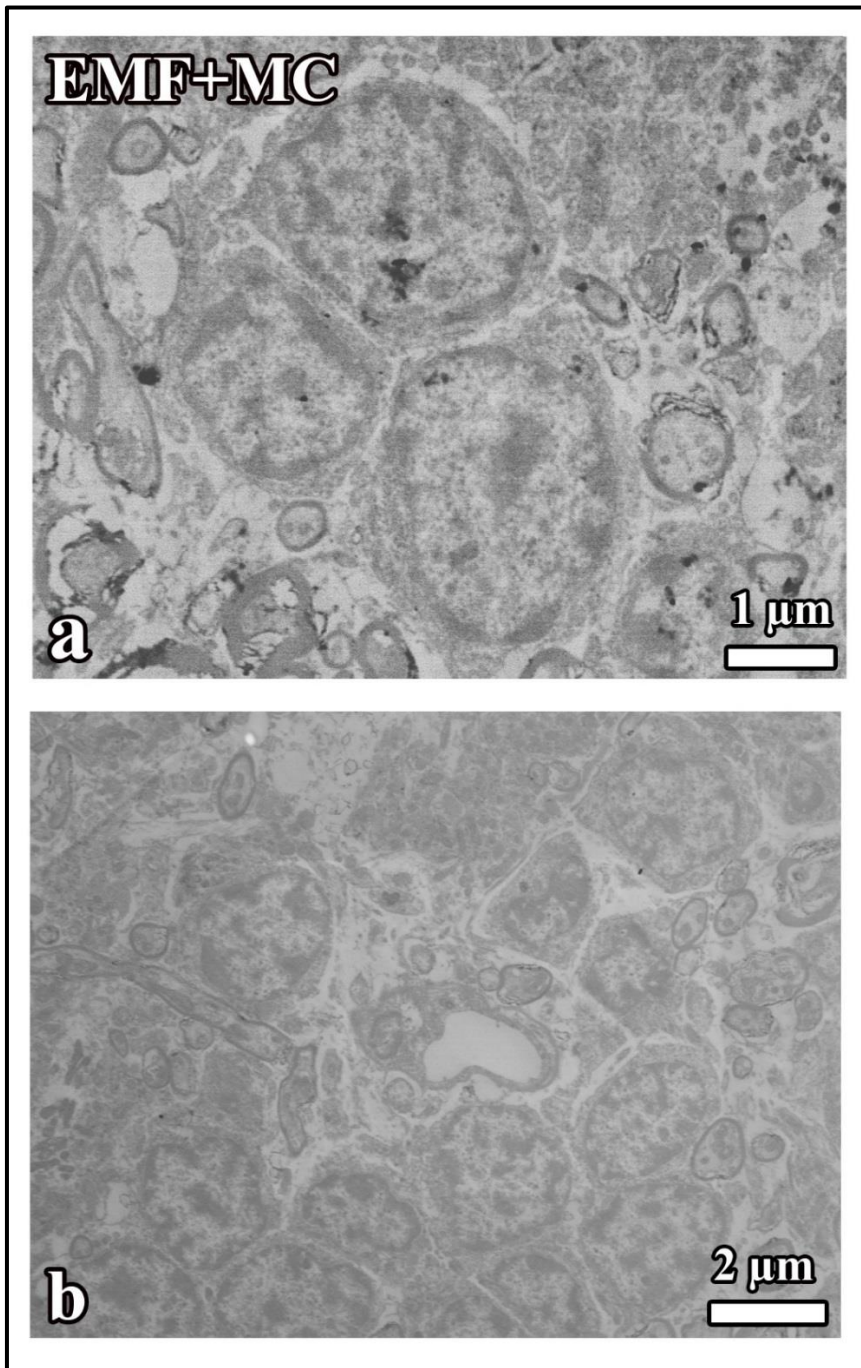


Figure 45. Electron microscopic images of the cerebellar cortex that belong to the EMF+MC group are shown.

The ultrastructure of the granular cells in the cerebellum even after EMF exposure was protected by means of MC. Well-preserved cell and nuclei borders are observed (a and b). A capillary that is lined by endothelial cell and many myelinated axons are seen, all of them have a protected structure (b)

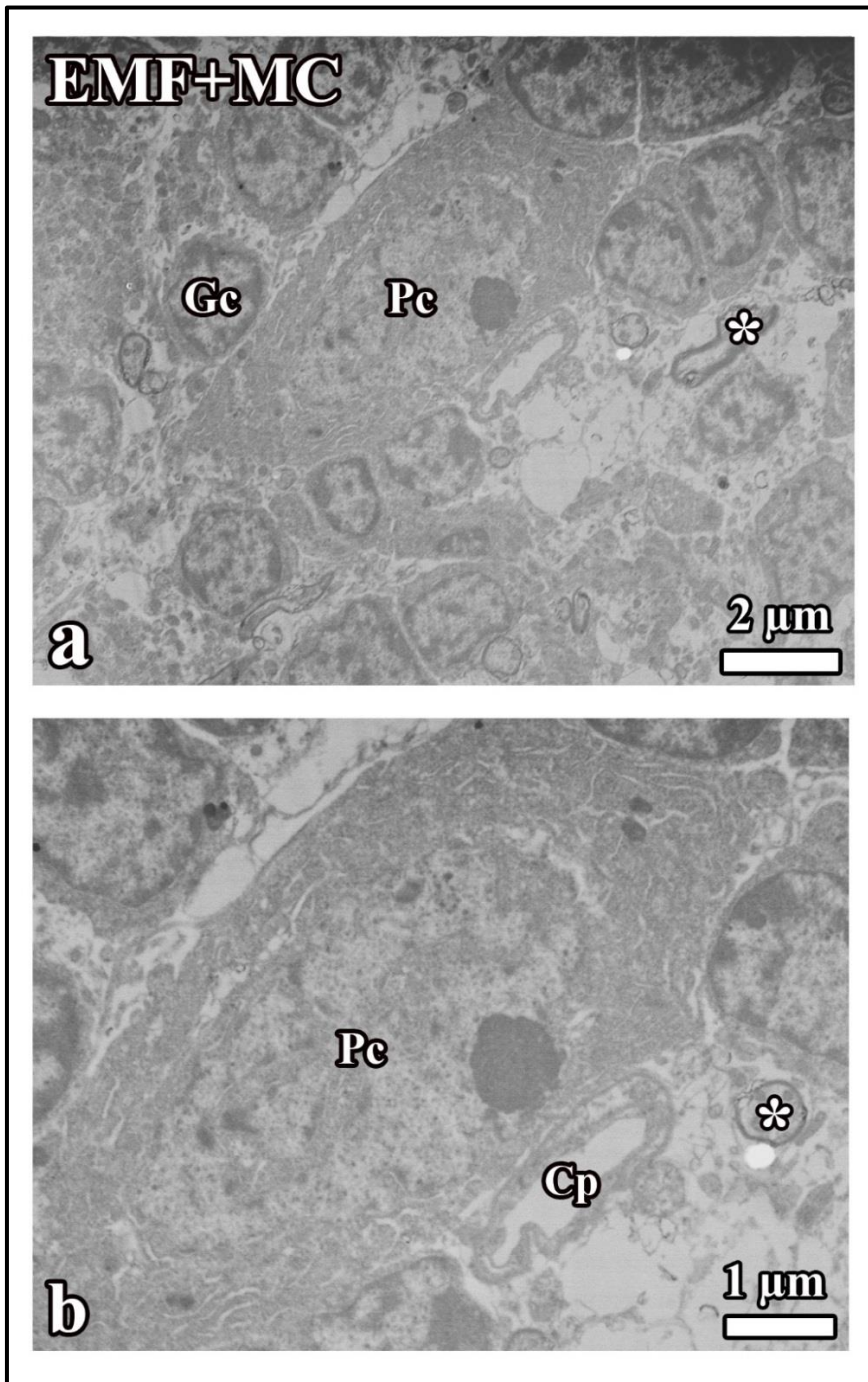


Figure 46. Electron microscopic images of the cerebellar cortex that belong to the EMF+MC group are shown.

As seen in both pictures, well-preserved structures of granular cells and a Purkinje cell were observed. The border of granular cells and Purkinje cell are clearly seen. The cytoplasm of Purkinje cell is filled by a stock of granular endoplasmic reticulum and conspicuous nucleus and nucleolus (a and b). Purkinje cell (Pc); Granular cell (Gc); axon (*); Capillary (Cp)

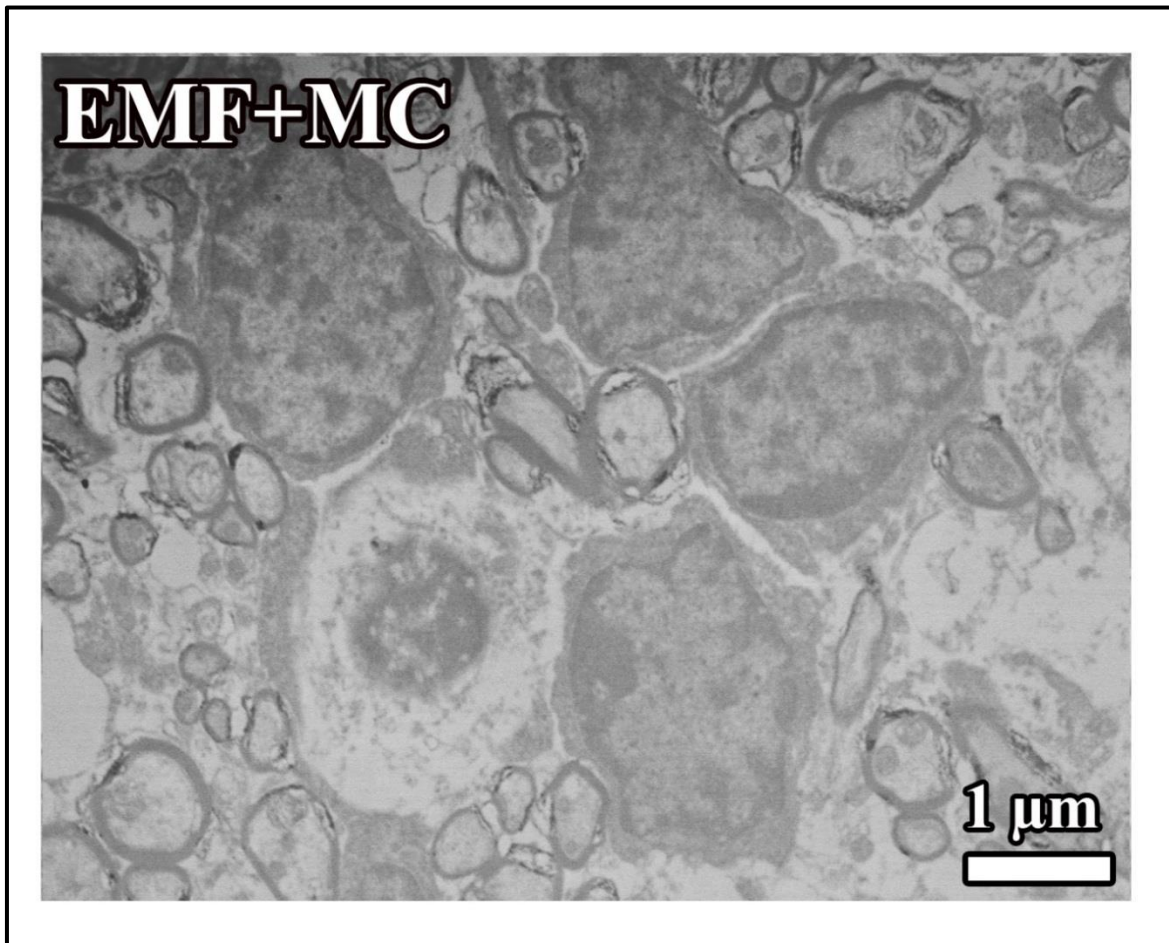


Figure 47. Electron microscopic image of the cerebellar cortex that belong to the EMF+MC group is shown. Generally, granular cells in the cortex are well protected but a damaged neuron as a result of EMF exposure is observed in the centre of the picture. It looks that the impaired neuron has been removed by means of apoptotic process since the nucleus of cell is very condensed, like apoptotic body. Most of axons in the image are in normal structure, some of them are covered by thin others by thick myelin sheath

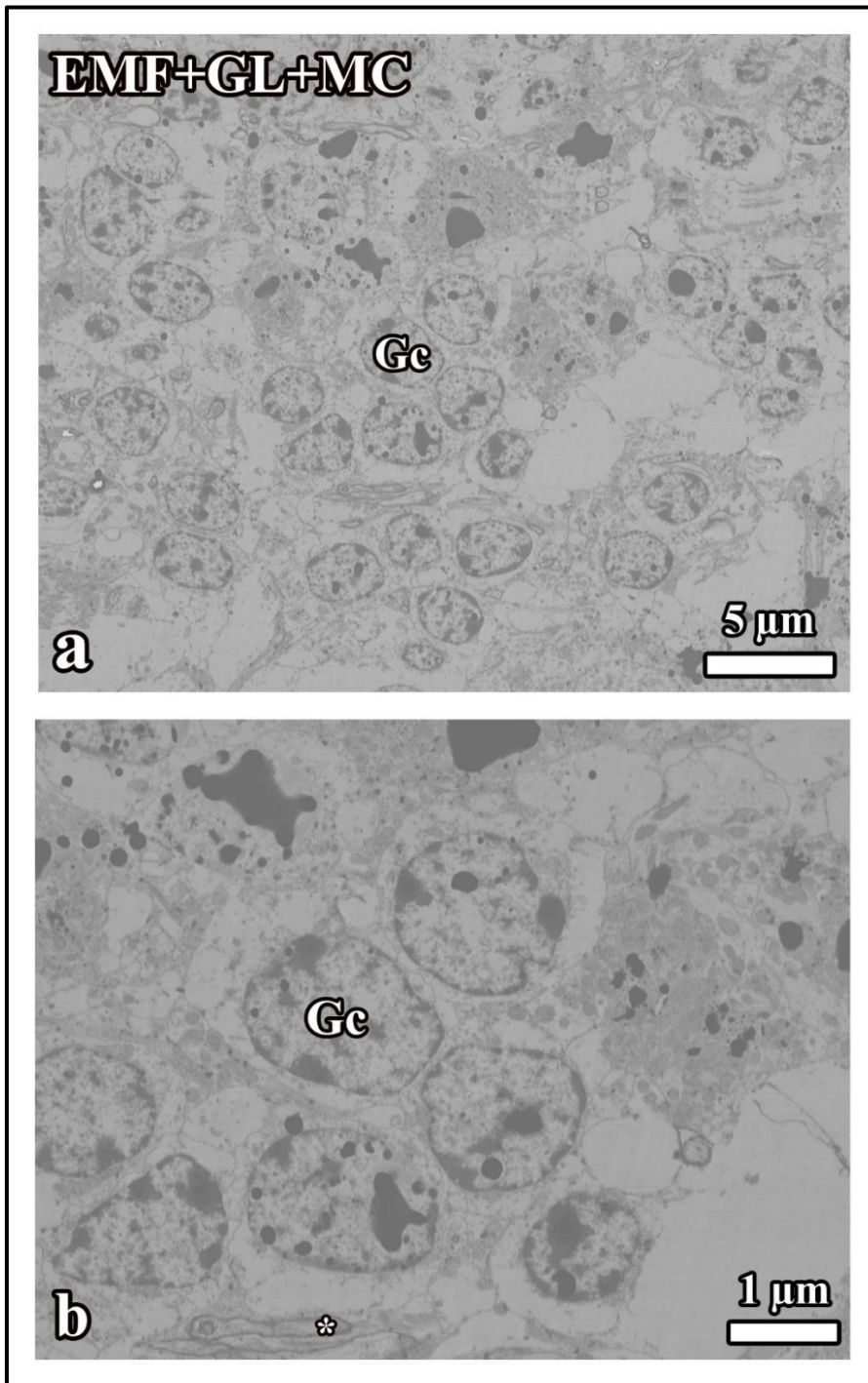


Figure 48. (a and b) Electron microscopic images of the cerebellar cortex that belong to the EMF+GL+MC group are shown. The ultrastructure of the granular cells in the cerebellum even after EMF exposure was protected by means of GL and MC. Well-preserved cell and nuclei borders can be observed. Some of black dots that are formed during staining process are seen at the upper part of images. Granular cell (Gc); Axon (*)

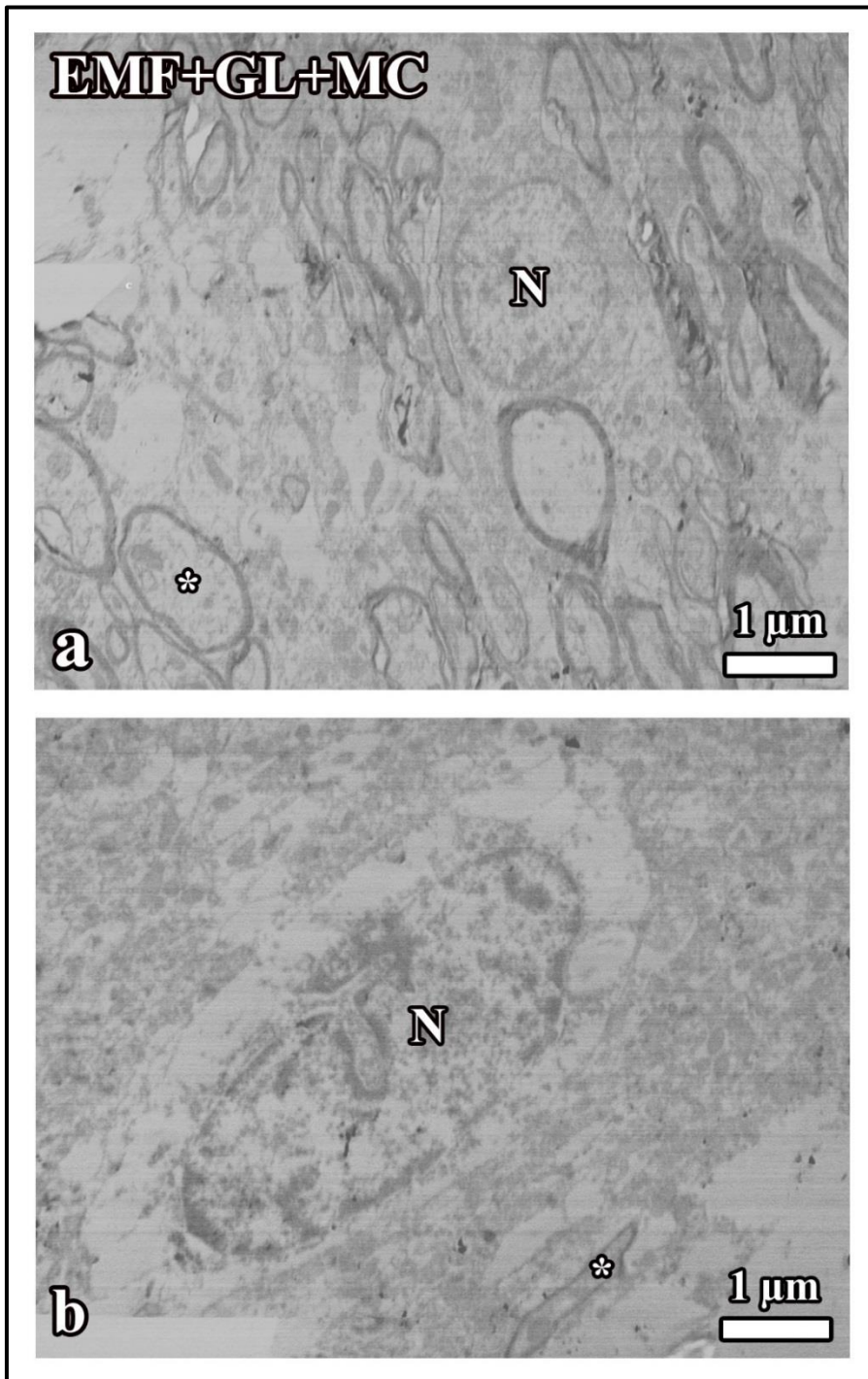


Figure 49. Electron microscopic images of the cerebellar cortex that belong to the EMF+GL+MC group are shown. A well-preserved nucleus of a glial cell as well as axons are seen (a). An invagination of nuclear envelope of a cell that might belong to a glial cell is observed (b). Nucleus (N); Axon (*)

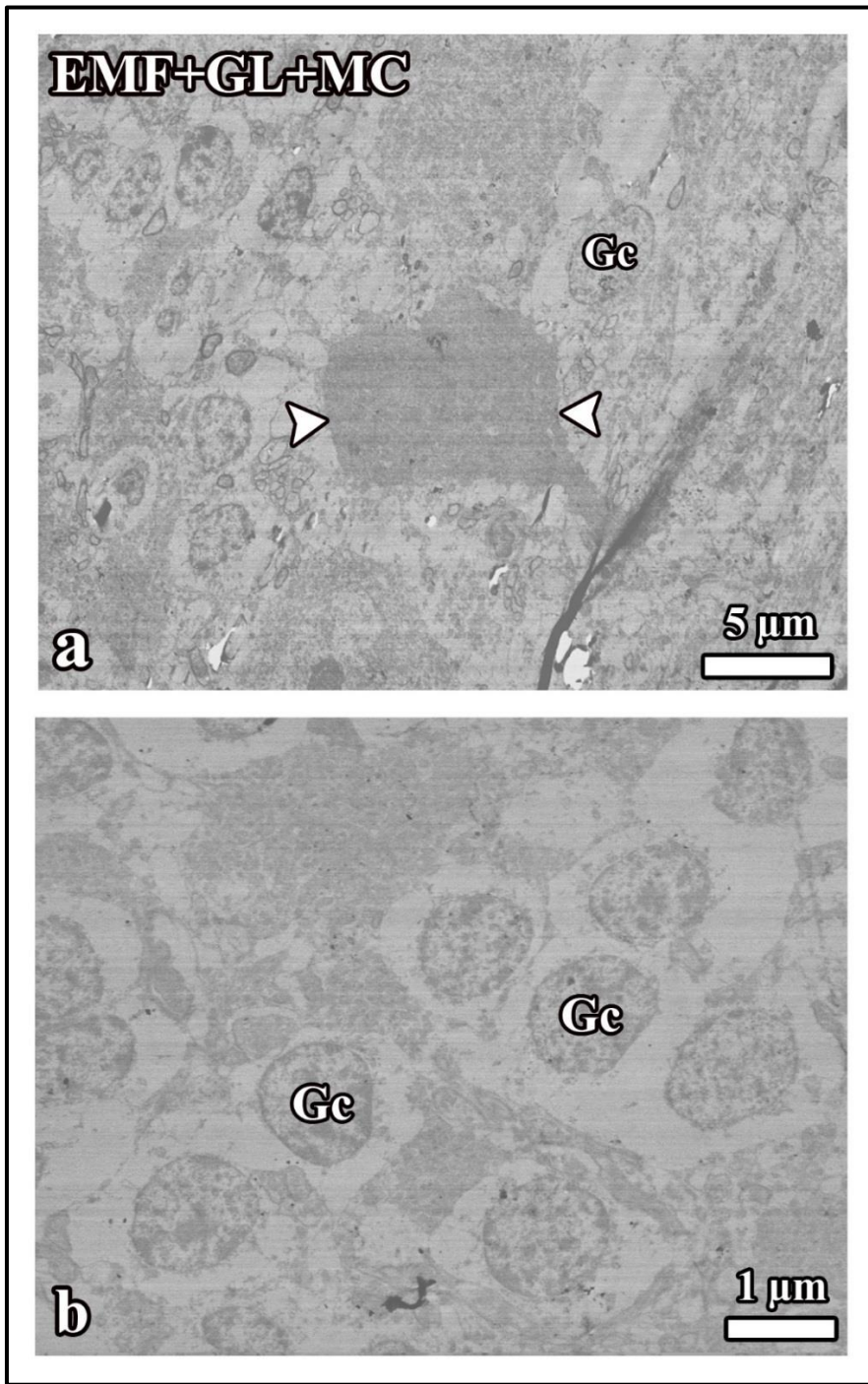


Figure 50. (a, b) Electron microscopic images of the cerebellar cortex that belong to the EMF+GL+MC group are shown. Although the most of ultrastructure of the granular cells in the cerebellum is protected, but some side effects of EMF exposure are seen. A dark cell is observed, this looks degenerated cell in the cerebellum (arrowheads). The density of granular cells is impaired since the distance between cells are increased (b). Granular cells (Gc)

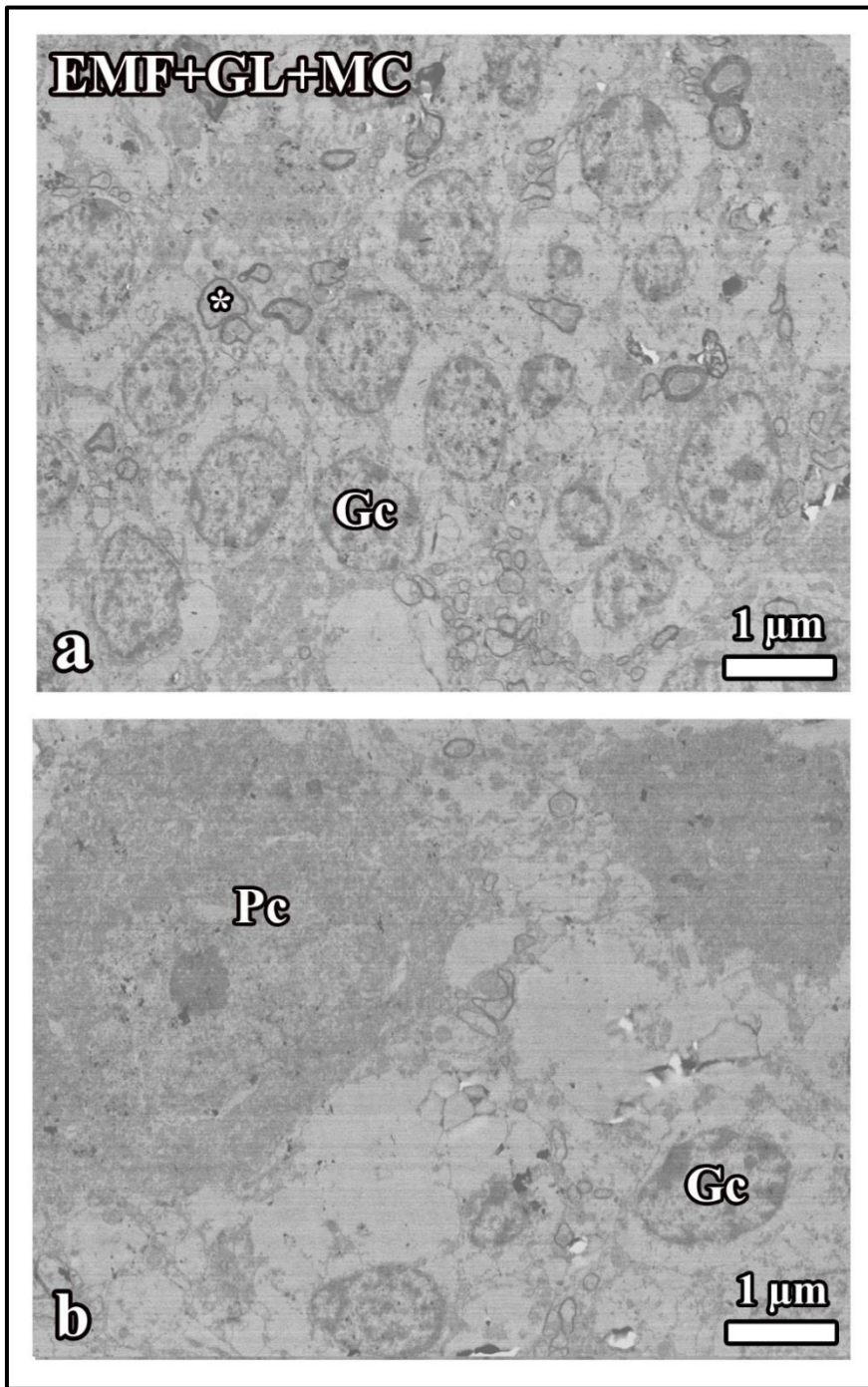


Figure 51. (a, b) Electron microscopic images of the cerebellar cortex that belong to the EMF+GL+MC group are shown. (a) Well-preserved structures of granular cells and myelinated axons were observed. (b) The border of granular cells and Purkinje cell are clearly seen. The cytoplasm of Purkinje cell is stained darkly, this might be resulted from EMF exposure. Purkinje cell (Pc); Granular cell (Gc); Axon (*)

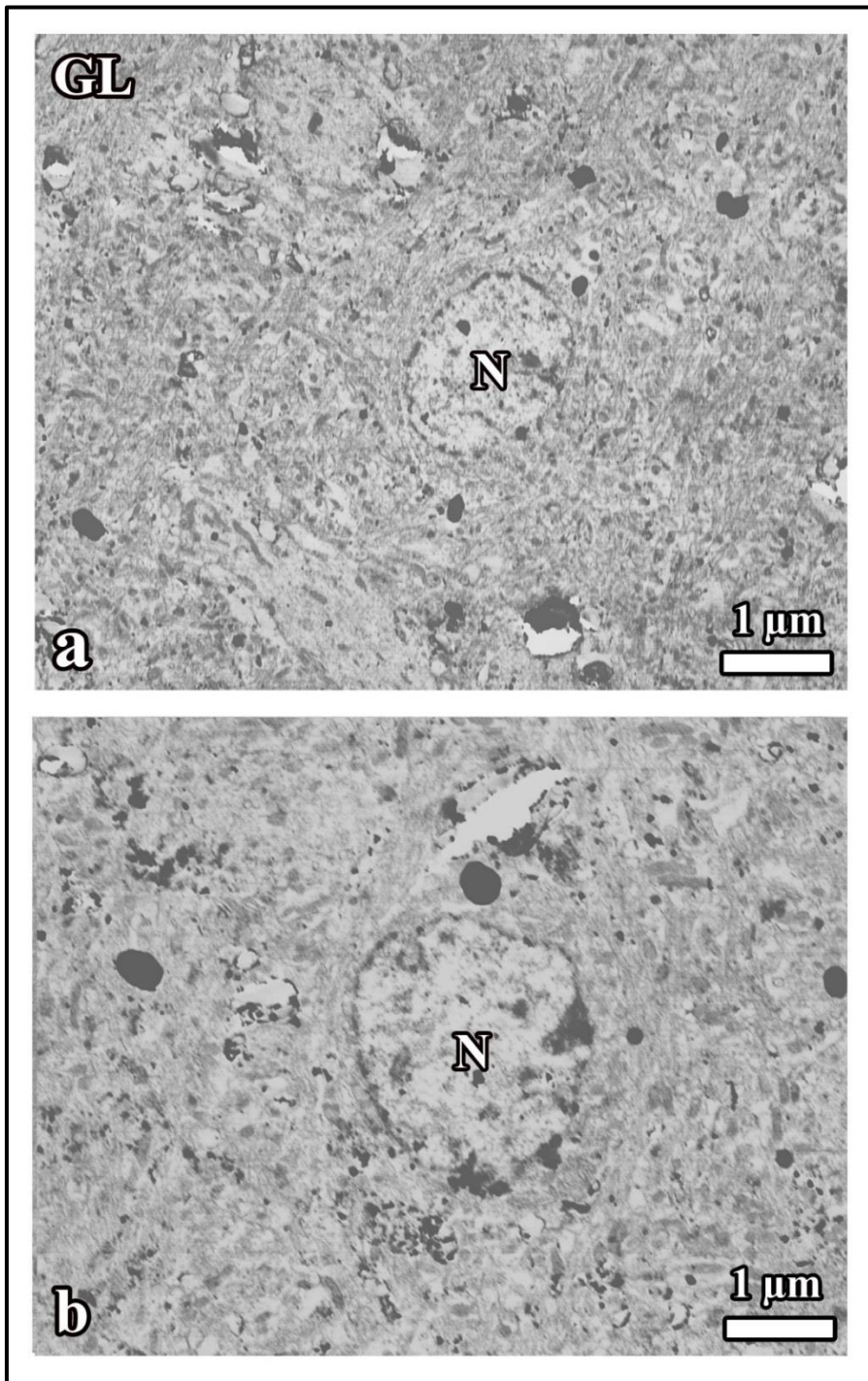


Figure 52. Electron microscopic images of the cerebellar cortex that belong to the GL group are shown. The ultrastructure of the cells in the cerebellum is seen normal. The border of nuclei is clearly observed. Euchromatic nuclei are observed. Nucleus (N)

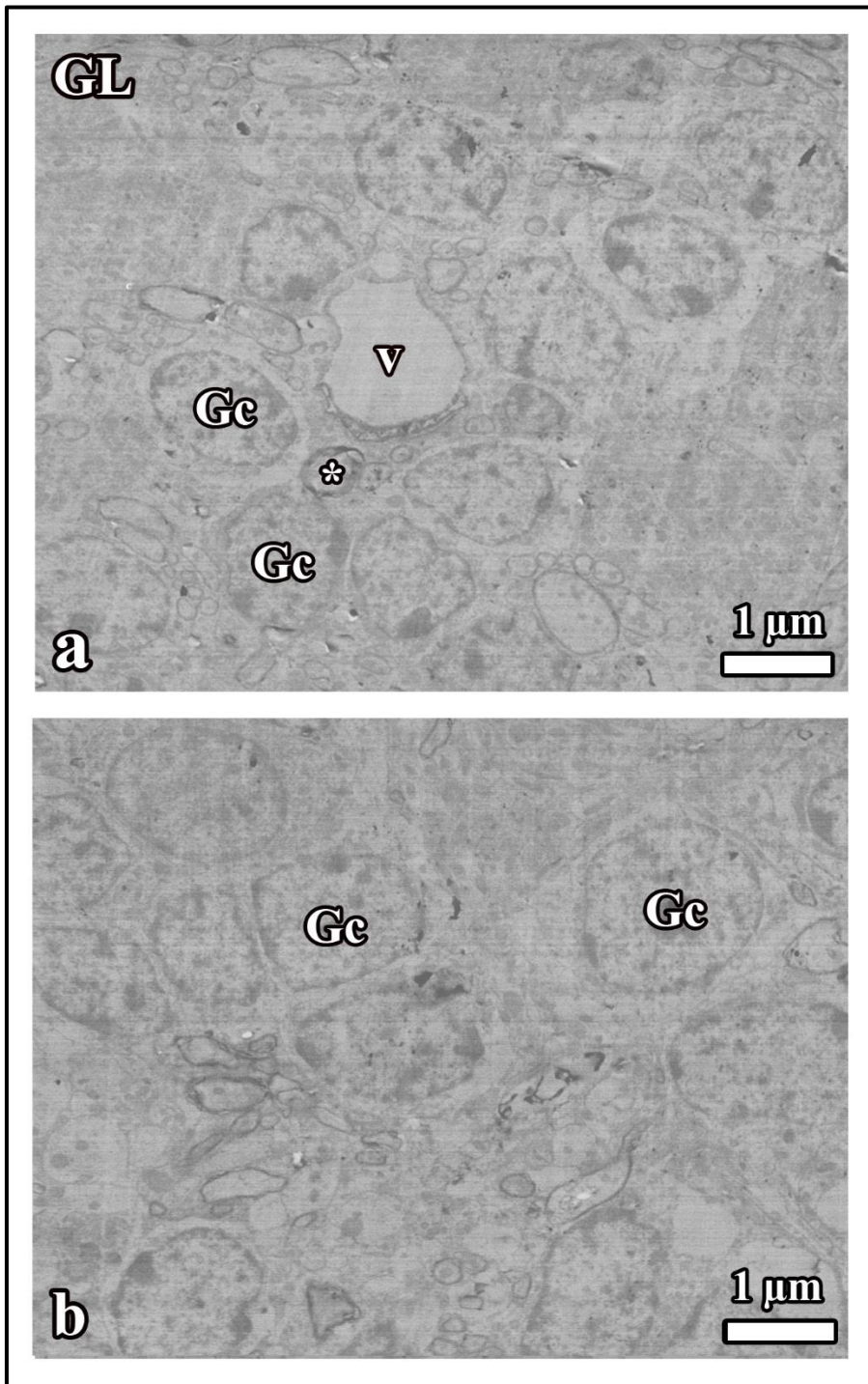


Figure 53. (a, b) Electron microscopic images of the cerebellar cortex that belong to the GL group are shown. The ultrastructure of granular cells in the cerebellum looks normal. The density and integrity of granular cells are also fine. Well-preserved myelinated axons, cell and nuclei borders are clearly seen. Granular cell (Gc); Axon (*); Vessel (v)

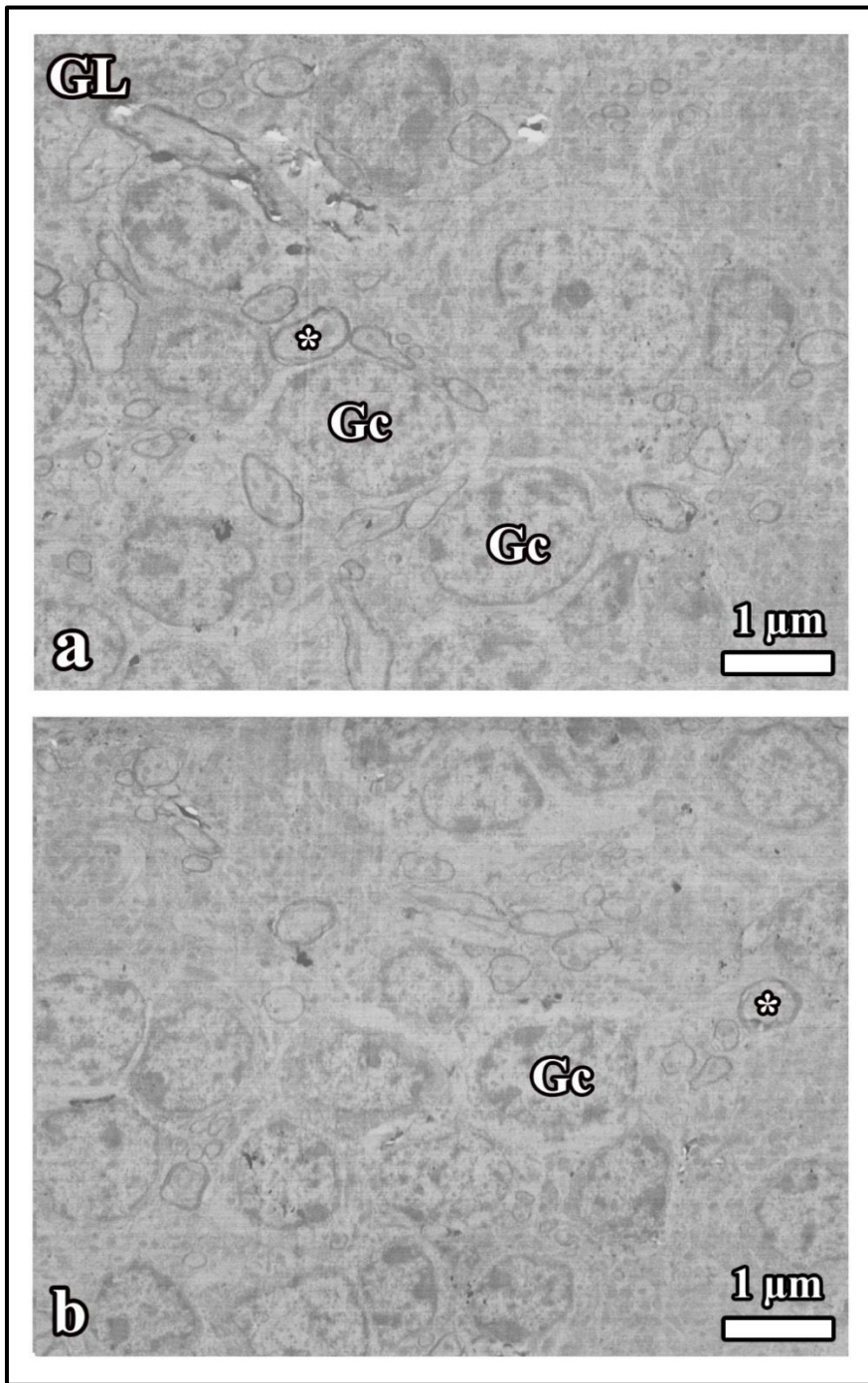


Figure 54. (a, b) Electron microscopic image of the cerebellar cortex that belong to the GL group is seen. A normal density of granular cells as well as normal integrity of them are observed. The structure of the myelinated axons looks fine (*). Granular cell (Gc); Axon (*)

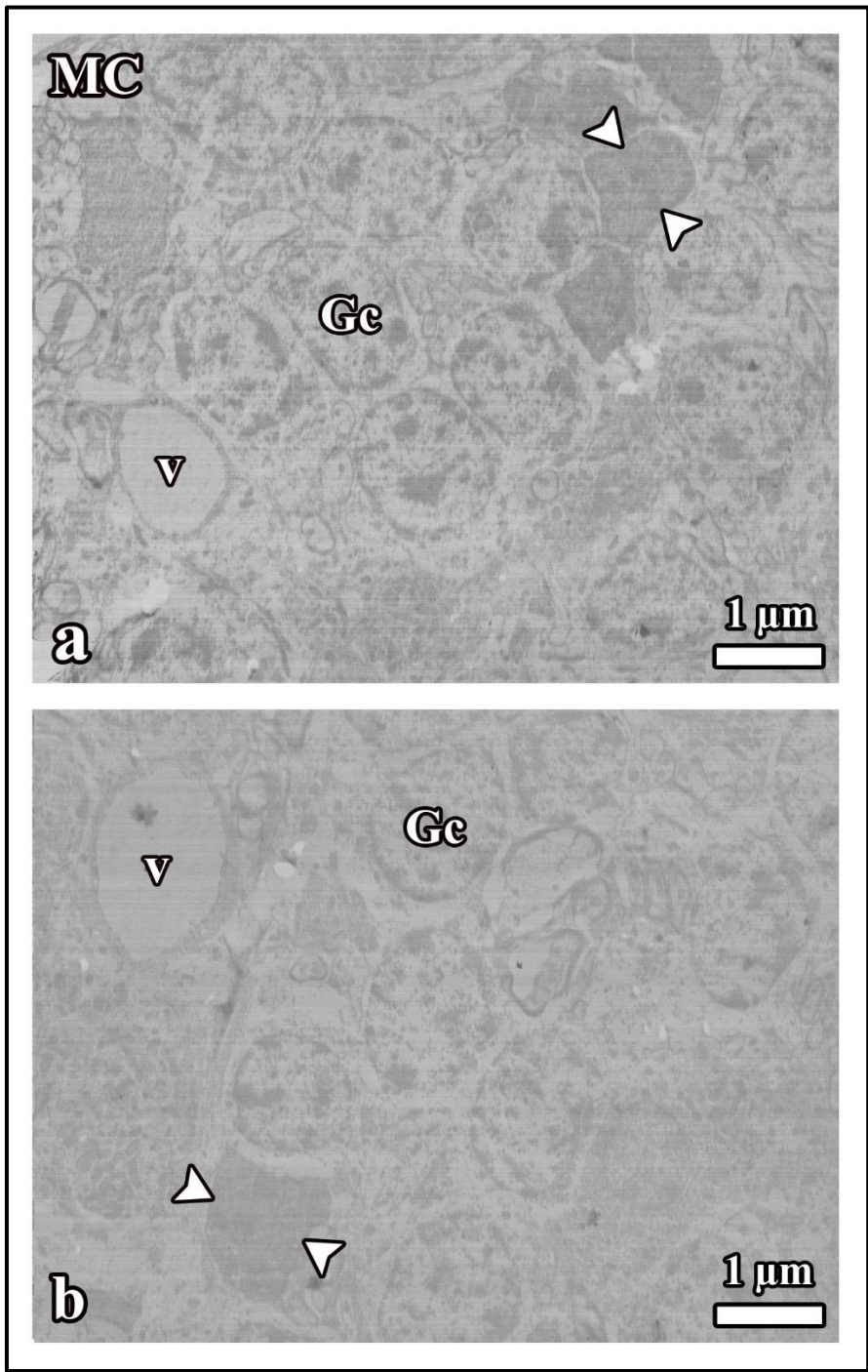


Figure 55. (a, b) Electron microscopic images of the cerebellar cortex that belong to the MC group are shown. Although the general structure of the cerebellum looks fine, but some of the granular cells are shrunken and darkly stained, these dark structures might be degenerated cells (arrowheads). Granular cell (Gc); Vessel (v)

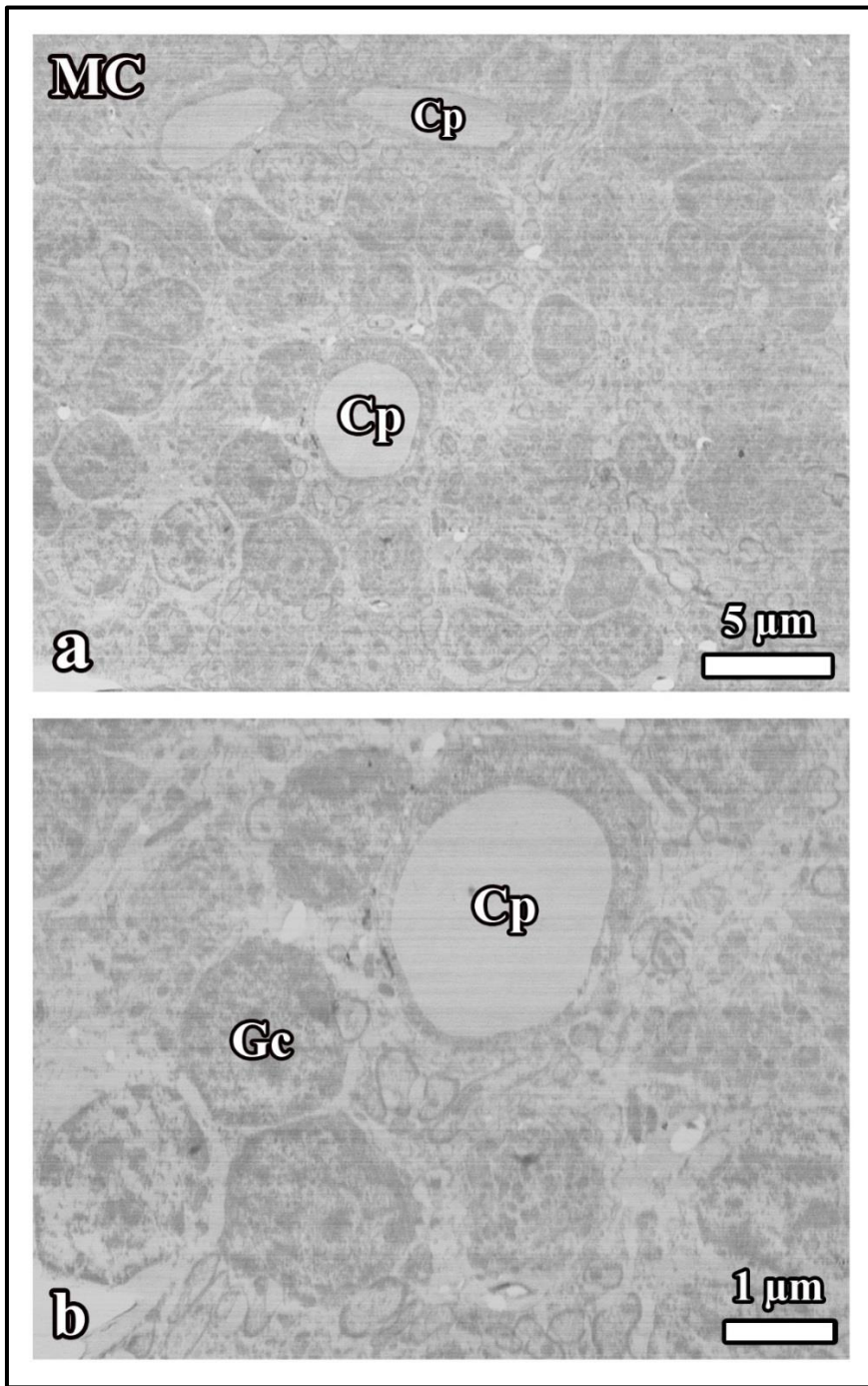


Figure 56. (a, b) Electron microscopic images of the cerebellar cortex that belong to the MC group are shown. The ultrastructure of granular cells in the cerebellum is normal. The structure of granular cells and their density are normal. Well-preserved capillaries are seen. Granular cell (Gc); Capillary (Cp)

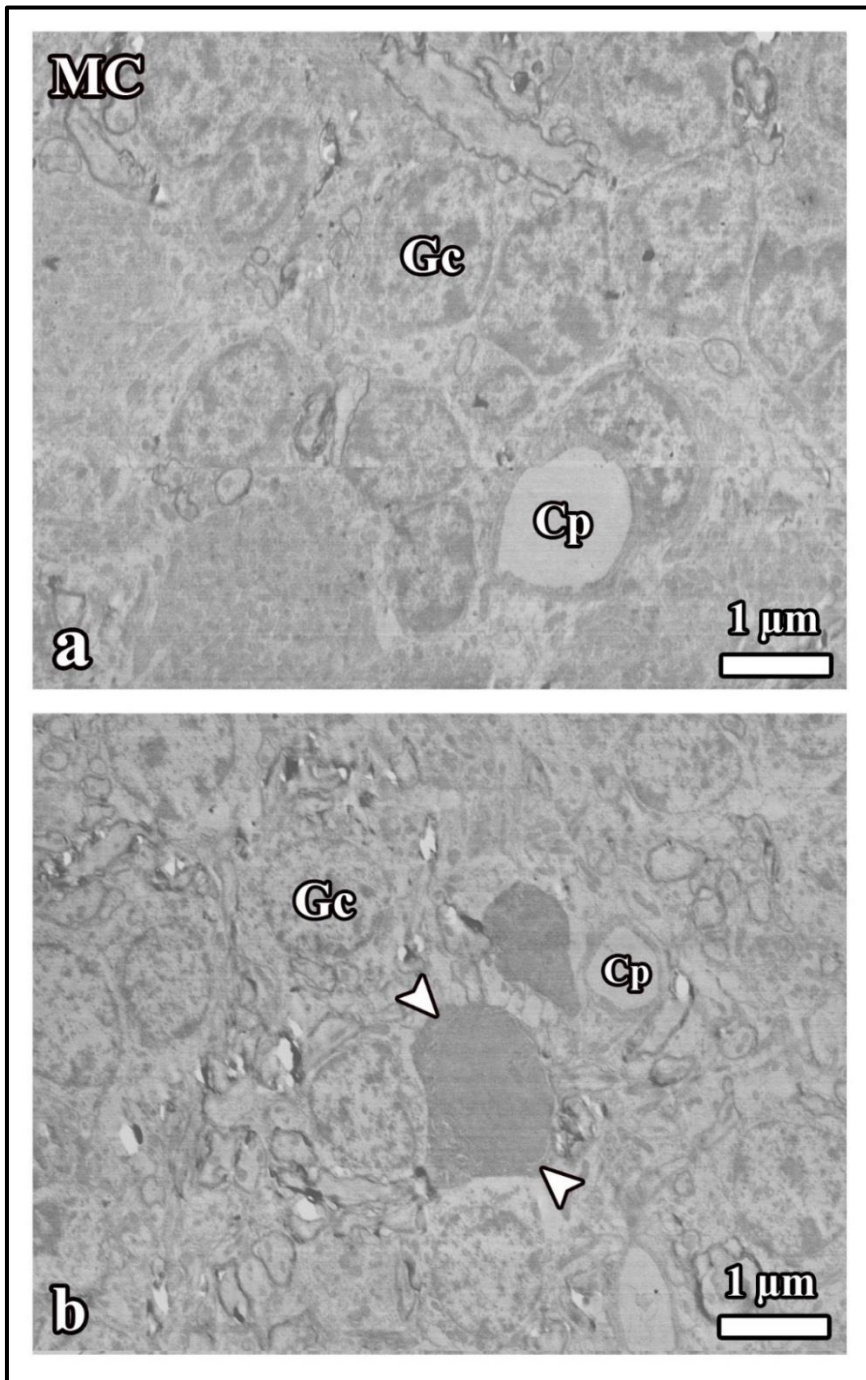


Figure 57. (a, b) Electron microscopic image of the cerebellar cortex that belong to the MC group is seen. The ultrastructure of granular cells in the cerebellum looks normal. (b) A darkly stained granular cell is seen (arrowheads) and a well-preserved capillaries are observed. Granular cell (Gc); Capillary (Cp)

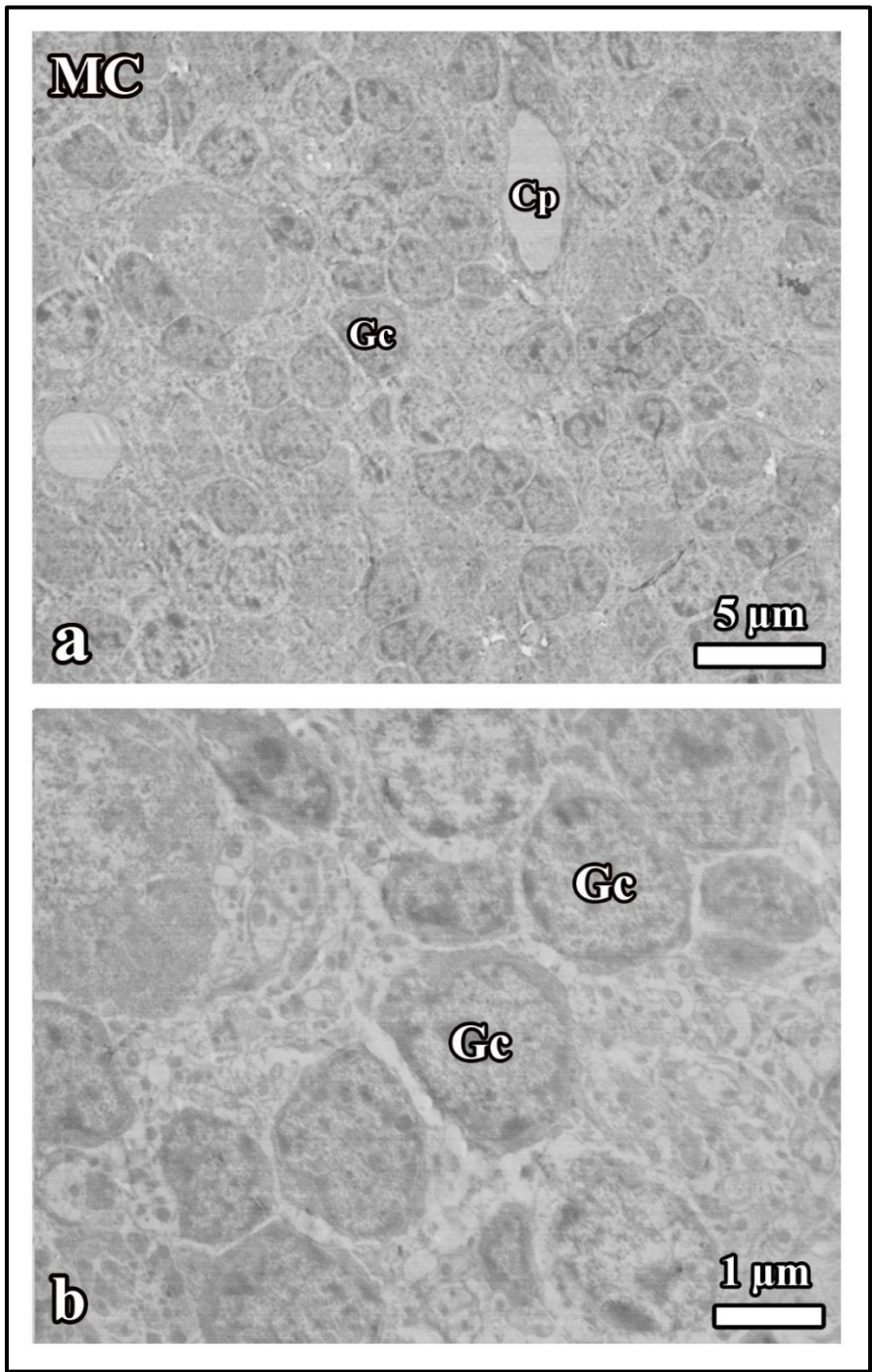


Figure 58. (a, b) Electron microscopic images of the cerebellar cortex that belong to the MC group are shown. The ultrastructure of granular cells and their density in the cerebellum looks normal. A capillary surrounded by healthy granular cells is seen (a). Granular cell (Gc); Capillary (Cp)

4.3. Biochemical Findings

4.3.1. Mean SOD Enzyme Activity for the Groups

SOD enzyme activity was measured in the serum samples taken from the rats of all groups. The findings are presented in the following table and figure (**Table 11; Figure 59**).

Table 11. SOD enzyme activity (U/ml (450 nm)) (mean \pm SD) values of all groups

Groups	SOD enzyme activity
Cont	23.48 \pm 3.52
Sham	26.10 \pm 1.16
EMF	23.24 \pm 1.35
EMF+GL	26.32 \pm 2.22
EMF+MC	27.79 \pm 0.29
EMF+GL+MC	29.03 \pm 0.33
GL	29.00 \pm 0.41
MC	28.72 \pm 0.46

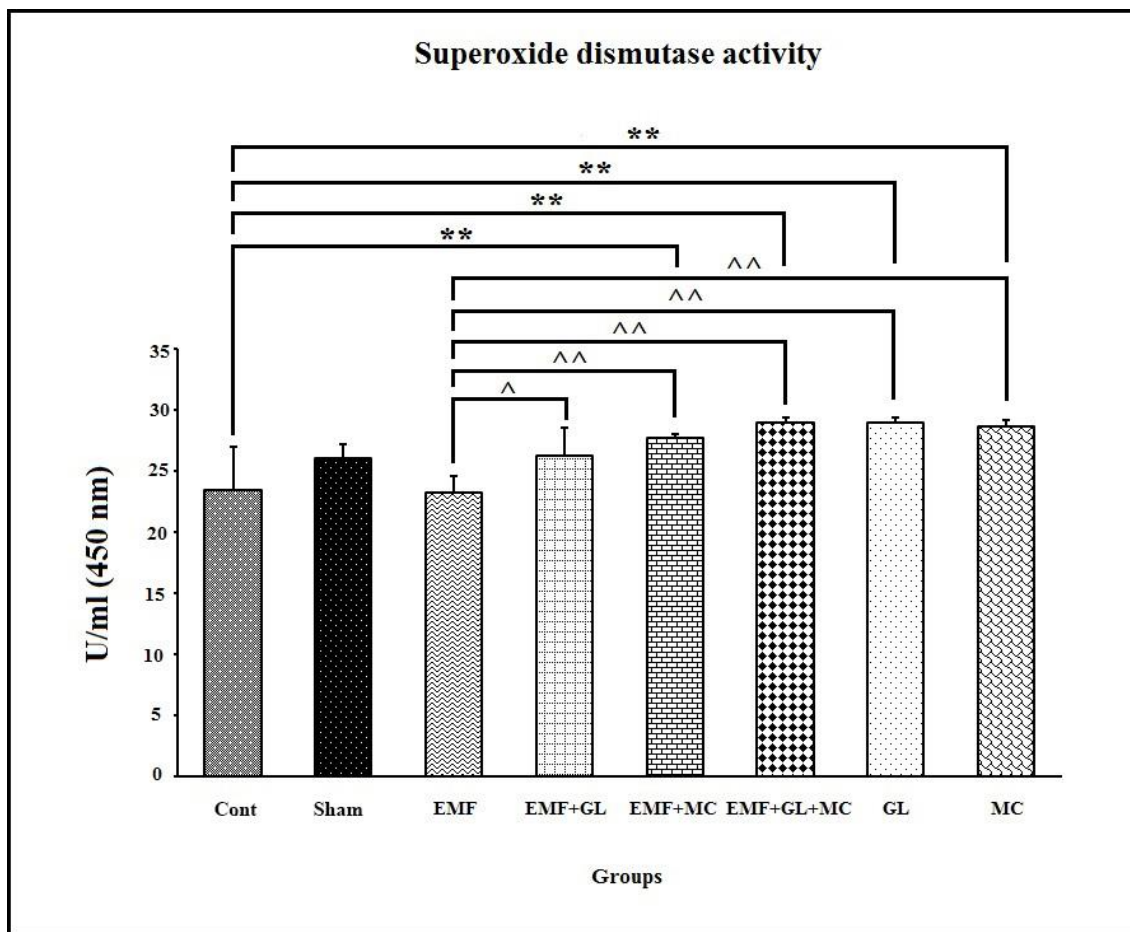


Figure 59. It shows the mean SOD enzyme activity values for all groups. Statistically significant difference at $p < 0.05$ was indicated by “^” while significant differences at $p < 0.01$ were indicated by “^^” and “**” (Mean \pm SD)

The statistical analysis of the SOD enzyme activity showed that the SOD enzyme activity in the EMF+MC and EMF+GL+MC groups was significantly higher than in the EMF group ($p < 0.01$). The SOD enzyme activity in the EMF+GL group significantly increased in comparison with the EMF group ($p < 0.05$). It was also found that the SOD enzyme activity decreased significantly in the EMF group compared to the GL and MC groups ($p < 0.01$), and that the GL and MC groups had significantly higher SOD enzyme activity than the Cont group ($p < 0.01$). There was no statistically significant difference in SOD enzyme activity when comparing the EMF group with Cont and sham groups ($p > 0.05$), also when comparing the sham group with the Cont group ($p > 0.05$) (**Table 12**).

Table 12. It shows the degree of significance among groups for the SOD enzyme activity

Comparison between groups	Significance
EMF with Cont group	1.000
EMF with Sham group	0.072
Cont with Sham group	0.124
EMF+GL with EMF group	0.040
EMF+MC with EMF group	0.000
EMF+GL+MC with EMF group	0.000
GL with EMF	0.000
MC with EMF	0.000
Cont with GL group	0.000
Cont with MC group	0.000

4.3.2. Mean CAT Enzyme Activity for the Groups

CAT enzyme activity was measured in the serum samples taken from the rats of all groups. The findings are presented in the following table and figure (**Table 13; Figure 60**).

Table 13. CAT enzyme activity (nmol/min/ml (540 nm)) (mean \pm SD) values for all groups

Groups	CAT enzyme activity
Cont	93.36 \pm 72.31
Sham	118.38 \pm 36.71
EMF	65.46 \pm 18.81
EMF+GL	100.19 \pm 34.74
EMF+MC	84.79 \pm 27.80
EMF+GL+MC	132.08 \pm 52.38
GL	205.55 \pm 57.75
MC	195.59 \pm 82.40

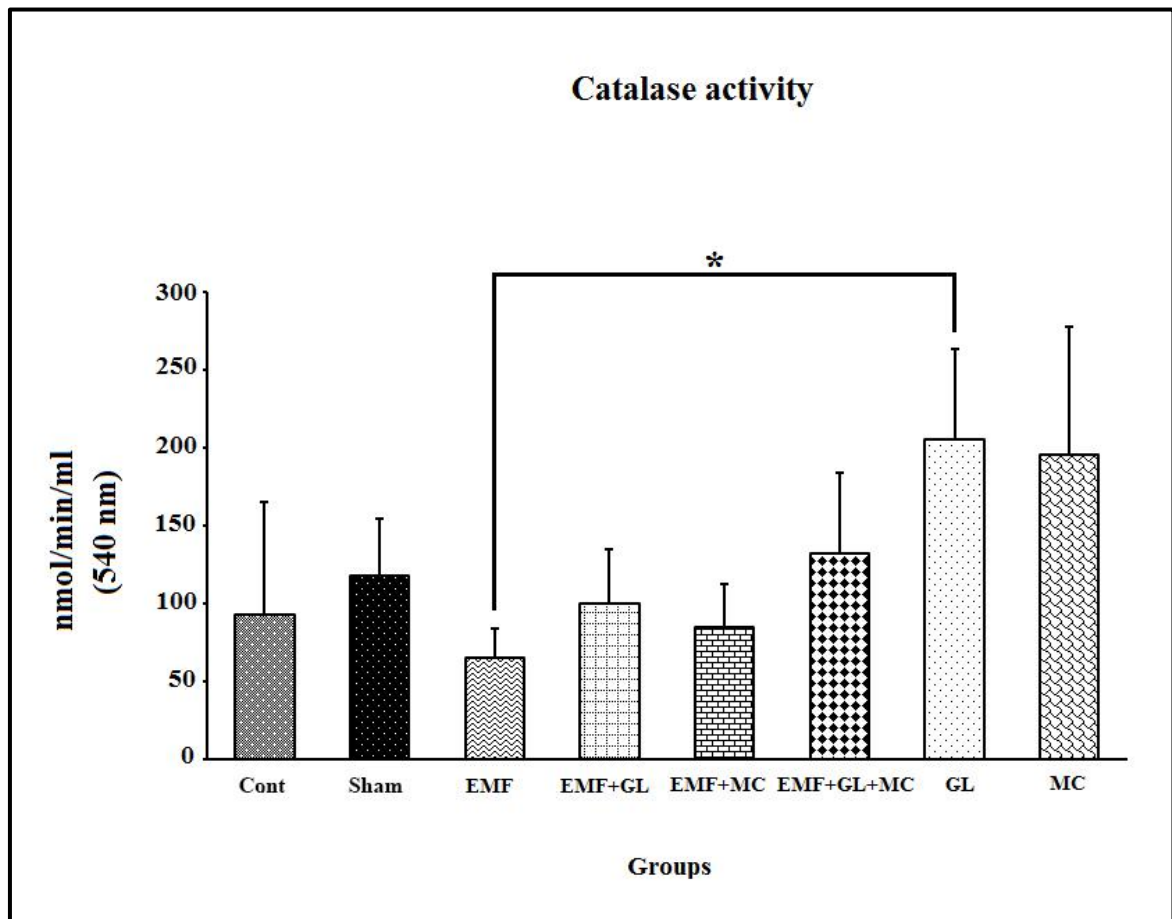


Figure 60. It shows the mean CAT enzyme activity values for all groups. “*” indicates statistically significant difference at $p < 0.05$, (Mean \pm SD)

The statistical analysis of the CAT enzyme activity showed that the CAT enzyme activity in the EMF group was significantly lower than in the GL group ($p < 0.05$) and there were no any significant differences between other groups ($p > 0.05$) (**Table 14**).

Table 14. It shows the degree of significance among groups for the CAT enzyme activity

Comparison between groups	Significance
EMF with Cont group	1.000
EMF with Sham group	0.346
Cont with Sham group	1.000
EMF+GL with EMF group	0.847
EMF+MC with EMF group	0.998
EMF+GL+MC with EMF group	0.507
GL with EMF	0.035
MC with EMF	0.263
Cont with GL group	0.341
Cont with MC group	0.732

4.4. Findings of Total Phenolic Content and Antioxidant Power

In the present study, the total phenolic content, ferric ion reduction antioxidant power (FRAP) and DPPH free radical scavenging effect of various solvent extracts from GL and MC were evaluated. The results are shown in (Table 15).

The total phenolic content of GL was 1068.75 mg/kg gallic acid equivalent (GAE), higher than that of MC 1003.125 mg/kg gallic acid equivalent (GAE). The FRAP of MC was 13.79 mmol/g torolox equivalent, higher than that of GL 2.78 mmol/g torolox equivalent. The DPPH free radical scavenging effect of GL was 7.61 mmol/g torolox equivalent, higher than that of MC 5.18 mmol/g torolox equivalent.

Table 15. It shows the total phenolic content, ferric ion reduction antioxidant power (FRAP) and DPPH free radical scavenging effect of GL and MC

Antioxidant	Total phenolic content, mg / kg, gallic acid equivalent (GAE)	FRAP, mmol/g torolox equivalent	DPPH free radical removal of mmol / g, torolox equivalent
GL	1068.75	2.78	7.61
MC	1003.125	13.79	5.18

5. DISCUSSION

In this study we aimed to know whether GL and/or MC are protective against the harmful effects of EMF on the cerebellum or not. We used the stereological techniques because they are unbiased tools commonly used in neuron counting.

There is no significant difference of mean total number of Purkinje cells was found between the Cont and EMF groups, and between the sham and EMF groups. On the other hand, the number of Purkinje cells in the EMF+MC group was greater than in the EMF exposed group, this may support the idea of neuroprotective role of MC. It was also observed that the mean total number of Purkinje cells in the EMF+GL+MC group was significantly higher than in the EMF exposed group, so it looks that giving both GL and MC protects the Purkinje cells from EMF exposure.

The mean total volume of the cerebellum for all groups has also been estimated. There was no significant difference in the volume of the cerebellum when comparing the EMF exposed group and Cont group, this means that the EMF exposure does not affect the volume of cerebellum.

Beside of those data, the mean total cell number and the volume of cerebellum, it was found that the numerical density of the Purkinje cells in the EMF group was significantly lower than in the Cont group. It was also noticed that the numerical density of cell in the sham group was significantly lower than in the Cont group. The cell density of the EMF+MC group and MC group was significantly higher than in the EMF group. On the other hand, the EMF+MC group had significantly lower cell density than in the Cont group. The cell density of EMF+GL group was not only significantly lower than the Cont group but also lower than the cell density of the GL group. On the other hand, the density of Purkinje cell in EMF+GL+MC group was significantly higher than the EMF group.

Histopathological assessment has been done for the cerebellum sections. According to this assessment, it was found that the 900 MHz EMF exposure leads to degeneration of the Purkinje cells in the cerebellum and the use of GL and/or MC has/have a protective effect on the Purkinje cells from the deleterious effect of EMF. According to the biochemical tests' findings, the SOD enzyme activity in each of the EMF+GL, EMF+MC and EMF+GL+MC groups was significantly higher than in the EMF group. Furthermore, the GL and MC groups

had significantly higher SOD activity than in EMF group, this means that the GL and/or MC could induce the SOD antioxidant enzyme and improve the body antioxidant defense system.

5.1. Electromagnetic Field and Cerebellum

In this study, it was found that the morphology of Purkinje cells as well as granular cells in the cerebellum was impaired as a result of 900 MHz EMF exposure that is equivalent to (GSM) mobile phone radiation. In a previous study, it was found a reduced number of Purkinje cells in the Sprague Dawley rats that was exposed to 2.45 GHz EMF during the fetal and postnatal period (Albert et al., 1981). Albert and co-workers have found that the mean Purkinje cell number in mm² of cerebellar cortical area had decreased after 2.45 GHz EMF exposure. The finding of present study about numerical density of Purkinje cell is parallel to that work even we have used lower frequency of EMF (900 MHz). Rağbetli et al. (2010) reported that the Purkinje cells had decreased significantly in the female offspring of Swiss albino mice due to exposure to EMF. Pregnant mice were exposed to mobile phone radiation at 890 to 915 MHz at SAR of 0.95 W/Kg, a mobile phone with external antenna was used in their experiment as a source of EMF and the optical fractionator method was used for Purkinje cell counting. In our study, adult male Wistar albino rats had been exposed to 900 MHz EMF using an EMF exposure system at the postnatal period and the physical disector technique was used for the estimation of cells' total number as well as their numerical density. Although numerical density results showed a reduction in the Purkinje cells' number in the EMF exposed group but total number estimation did not show a cell loss. In another study, adult female rats were exposed to 900 MHz EMF for 1 hour per day for a duration of 28 days and optical fractionator counting technique was used for cell number estimation. It was observed that the EMF exposure lead to Purkinje cells loss compared to the control group (Sonmez et al., 2010). Odacı et al. (2016) investigated the effect of prenatal exposure of EMF on the development of Purkinje cells in Sprague Dawley rats. They performed their study on female rat offspring sacrificed on the 32nd postnatal day. The stereological analysis was used for counting the Purkinje cells in the cerebellum and it was concluded that 900 MHz EMF exposure adversely affects the Purkinje cells number and morphology. In a study, the neuroprotective effect of some antioxidants such as melatonin and omega 3 against EMF

exposure was investigated. In the study, adult Wistar albino rats were exposed to 900 MHz for one hour daily for 15 days. EMF exposure caused biochemical and structural changes; number of the hippocampal neurons in the brain and Purkinje cells in the cerebellum were significantly lower than in other treated groups. It was also found a significant increase of antioxidant levels in EMF group. It was confirmed that melatonin and omega 3 might have a protective effect against EMF exposure in the cerebellum and hippocampal region (Altun et al., 2017). A similar study was done to investigate the possible neuroprotection of folic acid and *Boswellia sacra* against the side effect of 900 MHz EMF radiation on the cerebellum and hippocampus of male adult Wistar albino rats. The rats were exposed to EMF for 1 hour over a period of 21 days. Then stereological, biochemical and histological evaluations for the hippocampus and cerebellum were done. The numbers of pyramidal neurons in the hippocampus, granular cells in the dentate gyrus and Purkinje cells in the cerebellum were significantly less in the EMF group in comparison to the other groups. It looks that the folic acid and *Boswellia sacra* may have neuroprotective properties against EMF radiation (Kivrak et al., 2017b). Aslan et al. (2017) studied the effect of 900 MHz EMF exposure on the cerebellum in adolescent male Sprague Dawley rats. They did the experiment on the postnatal 21-day old rats and the EMF group were exposed to 900 MHz EMF for a duration of one hour daily for 25 days. Histopathological and stereological analyses were performed. It was found that the 900 MHz EMF exposure decreased significantly the number of Purkinje cells. Histopathological evaluation of this organ showed that there is intense-stained cytoplasm of many Purkinje cells in the cerebellum. Stereological and histological findings of our study are consistent with the previously mentioned works. A severe impairment of cell structure can be attributed to the oxidative stress caused by the 900 MHz EMF.

5.2. SOD and CAT activities

In the present study, a significant decrease in SOD enzyme activity was observed in the EMF group compared to the EMF+GL, EMF+MC, EMF+GL+MC, GL and MC groups; this means that the GL and MC induce the SOD enzyme and improve the antioxidant defense system in the rat body. In a previous study, the mobile phone (900 MHz) radiation caused a significant decrease in SOD and GPx activities in Wistar rat brain (Ilhan et al., 2004).

Although our study findings didn't show a difference in SOD activity between EMF and Cont groups, there was a significant decrease in SOD activity in EMF group compared to GL and MC groups. Another study was conducted on Sprague Dawley rats to investigate the protective effect of vitamin C from the effect of 900 MHz EMF emitted from base transceiver station on the cerebellum and encephalon. The experiment was done on four groups of animals: control, control-vitamin C, exposed group and exposed+vitamin C group. It was found that 900 MHz EMF radiation caused a decrease in the activity of SOD, CAT and GPx enzymes and increased lipid peroxidation, while vitamin C improved the activities of the antioxidant enzymes and decreased the lipid peroxidation significantly (Akbari et al., 2014). In our study, the GL and MC administration caused a significant increase in the activity of SOD enzyme when we compare EMF+GL, EMF+MC and EMF+GL+MC groups with EMF group, this finding is consistent with vitamin C study in that the GL and MC have antioxidant capabilities similar to vitamin C. In a study on pregnant mice, it was reported that total thiol content, SOD and CAT activities decreased significantly, while malondialdehyde (MDA) level significantly increased in exposed group of dams and offspring mice whose mothers were exposed to 900-1800 MHz EMF during pregnancy. The exposure was for 2 hours/day for 20 days (Bahreyni Toossi et al., 2018), while in our study we exposed adult male rats to 900 MHz for 1hour/day for 28 days. In another study, the 900 MHz electromagnetic field impact on the brain of guinea pigs has been investigated. The animals were divided into two groups control and treatment group; 7 animals in each. The treatment group of rats were exposed to 890-915 MHz for 12 hours/day for 30 days. Biochemical analysis was conducted in the brain tissue and serum samples. There was a significant decrease of GSH level and CAT activity and increase of MDA level in brain tissue, while levels of vitamins A, E and D were not affected in the brain tissues of exposed animals (Meral et al., 2007). In our findings, although CAT activity was lower in EMF group compared to Cont, this difference was not statistically significant. In addition, the CAT activity in EMF group was significantly lower than in GL group and there was no significant difference between GL and Cont groups. This leads us to the idea that the EMF may decrease the activity of CAT enzyme. There was no significant difference in CAT activity when comparing the EMF group with EMF+GL, EMF+MC and EMF+GL+MC groups, so the possibility of a supportive effect of GL and MC

on the antioxidant defense system regarding induction of CAT activity is not confirmed by the CAT assay findings in this study.

5.3. Garlic

In this study, the GL was used because of its antioxidant properties that were reported in many previous studies (Brunetti et al., 2009; Aminuddin et al., 2015; Xu et al., 2015; Zhang et al., 2016; Manoj Kumar et al., 2017; Becerril-Chávez et al., 2017). This study showed that there is no significant difference between the mean total Purkinje cell number of the EMF+GL group and the EMF group. This shows that the GL did not have a protective effect on the Purkinje cells that were exposed to 900 MHz EMF. To our knowledge, the GL has not been previously studied in rat cerebellum exposed to 900 MHz EMF.

In a previous study, it was found that black GL (fermented form of GL) extract has a protective effect on the rat cerebellum that treated with monosodium glutamate, a toxic substance. It was found that the total number of Purkinje cells of rats exposed to monosodium glutamate plus black GL was significantly high compared to rats exposed to monosodium glutamate only, concluding that black GL had caused this increase in Purkinje cell number (Aminuddin et al., 2015).

In addition, a study was carried out on the effect of administration of black GL extract on the spatial memory and hippocampus in rats exposed to monosodium glutamate. Although this substance creates an impairment of spatial memory in the rat, it did not have a side effect on the total number of hippocampal pyramidal cells. This result, no change in number of cells in hippocampus, was attributed to low dose of monosodium glutamate (Hermawati et al., 2015).

The protective effects of GL and ascorbic acid administration on the rat hippocampus that exposed to lead during prenatal life and lactation periods were studied. It was observed that the GL and ascorbic acid have a protective effect on the developing hippocampus. This comment was based on a decreased number of apoptotic neurons in the hippocampus (Ebrahimzadeh-Bideskan et al., 2016). It was suggested that treatment with GL reduces the learning and memory deficits caused by lead exposure during juvenile period of rat, this amelioration was explained by the antioxidant effect of GL (Ghasemi et al., 2017).

Nurmasitoh et al. (2018) reported that the ethanolic fermented GL extract could prevent the working memory deficit after monosodium glutamate administration. S-allyl-cysteine (organosulfur compound in GL) was detected to be an effective treatment in a model of multiple sclerosis, autoimmune encephalomyelitis. The neuroprotective effect of S-allyl-cysteine was due to its antioxidant activity (Escribano et al., 2018). In our study, the neuroprotection made by GL at least based on morphological protection is suggested to be due to its antioxidant capability through the following mechanisms: free radical scavenging, reduction of the ROS production and induction of SOD enzyme.

5.4. *Momordica charantia*

In this study, MC was used because of its antioxidant properties that were reported in previous studies (Semiz and Sen, 2007; Kubola and Siriamornpun, 2008; Thenmozhi and Subramanian, 2011; Kavitha et al., 2011; Ozusaglam and Karakoca, 2013; Duan et al., 2015; Gong et al., 2015).

A neuroprotective effect of MC against EMF exposure effect on the total Purkinje cell number was observed when the EMF+MC group compared with EMF group, and also the MC group compared with EMF group. These results show that MC has a protective feature since it was observed that after 900 MHz EMF exposure, a period of 28 days, the number of Purkinje cells in the cerebellum was higher in the EMF+MC group compared to EMF group. To our knowledge, MC has not been previously studied in rat cerebellum exposed to 900 MHz EMF.

The antioxidant activity of MC fruit extract on the stress-induced biochemical changes in albino rat brain was investigated. It was revealed that pretreatment with MC alleviated changes in the levels of monoamines and plasma corticosterone in different regions of brain such as cortex, hippocampus, and hypothalamus. Furthermore, the MC extract significantly inhibited lipid peroxidation in vitro (Kavitha et al., 2011). In another study, the MC supplementation was found to be able to protect the brain from the oxidative stress damage induced by high fat diet, and that the MC attenuated the changes in blood brain barrier (BBB) permeability associated with high fat diet. The MC extract also reduces the

neuroinflammatory cytokines. It can be concluded that the MC has a neuroprotective activity (Nerurkar et al., 2011).

Duan et al. (2015) demonstrated that polysaccharides found in MC could protect against intracerebral hemorrhage damage and found that MC inhibits the enzymes that induced by the intracerebral hemorrhage injury. Gong et al. (2015) reported that polysaccharides of MC could be a potential neuroprotective substance and this might be due to its antioxidant activities and suppression of JNK3 signaling cascades that stimulated during brain ischemic-reperfusion injury.

We strongly emphasize that there is no total cell number estimation using the stereological techniques that we used it. To our knowledge, there is no stereological study regarding the protective effect of MC on the Purkinje cell number in the cerebellum. Beside of this, the presented results agree with the previous reports on the positive effect of MC. As we stated previously the neuroprotective activity of MC could be explained by its antioxidant capacity via free radical scavenging, decreasing of the ROS production and SOD enzyme induction.

6. CONCLUSION AND RECOMMENDATIONS

6.1. Conclusion

1. A 900 MHz EMF exposure decreases the Purkinje cells in the cerebellum. By light microscopy, the damaged Purkinje cells appears dark blue stained.
2. Stress of the EMF exposure system without radiation affects the total number of the Purkinje cells and the morphology of these cells.
3. Natural substances such as GL and MC that have antioxidant properties may reduce the destructive effect of the EMF radiation on the Purkinje cells of the cerebellum by means of inhibiting generation of ROS and increasing the activities of the endogenous antioxidant enzymes.
4. GL alone did not protect the number of Purkinje cells in the cerebellum from the detrimental effect of the EMF exposure.
5. MC has a protective effect on the total number of Purkinje cells in the cerebellum that exposed to 900 MHz EMF radiation.
6. Using GL and MC together provides a pronounced protection of Purkinje cell number in the cerebellum against EMF radiation.
7. GL and MC have no toxic effect on the Purkinje cells of the cerebellum if compared with Cont and sham groups.
8. Even though we couldn't find a protective effect of GL on the cerebellum exposed to EMF radiation, our analysis showed that a high level of total phenolic content and antioxidant power are present in both substances, the GL and MC.

6.2. Recommendations

1. It would be recommended to take natural antioxidants in appropriate amounts, they would prevent or diminish the side effects of EMF radiation on the cerebellar neurons.
2. We recommend using a mobile phone headset and speaker to reduce the impact of mobile phone radiation on the body.
3. Children should be protected from exposure to EMFs emitted from the mobile phone.
4. The electronic devices should be developed in order to minimize their biological effects on human health.

REFERENCES

- Abalaka M, Inabo H, Onaolapo J, Olonitola O. Antioxidant capabilities of extracts and antimicrobial activities of chromatographic fractions of *Momordica charantia* L.(Cucurbitaceae). *Ferm Tech Bioeng* 2011;1:1-6.
- Ahlbom A, Bergqvist U, Bernhardt J, Cesarini J, Grandolfo M, Hietanen M, Mckinlay A, Repacholi M, Sliney DH, Stolwijk JA. Guidelines for limiting exposure to time-varying electric, magnetic, and electromagnetic fields (up to 300 GHz). *Health Phys* 1998;74(4):494-521.
- Akbari A, Jelodar G, Nazifi S. Vitamin C protects rat cerebellum and encephalon from oxidative stress following exposure to radiofrequency wave generated by a BTS antenna model. *Toxicol Mech Methods* 2014;24(5):347-352.
- Albert EN, Sherif MF, Papadopoulos NJ, Slaby FJ, Monahan J. Effect of nonionizing radiation on the Purkinje cells of the rat cerebellum. *Bioelectromagnetics* 1981;2(3):247-257.
- Alkis ME, Bilgin HM, Akpolat V, Dasdag S, Yegin K, Yavas MC, Akdag MZ. Effect of 900-, 1800-, and 2100-MHz radiofrequency radiation on DNA and oxidative stress in brain. *Electromagn Biol Med* 2019;38(1):32-47.
- Altman J, Bayer SA. Embryonic development of the rat cerebellum. I. Delineation of the cerebellar primordium and early cell movements. *J Comp Neurol* 1985a;231(1):1-26.
- Altman J, Bayer SA. Embryonic development of the rat cerebellum. II. Translocation and regional distribution of the deep neurons. *J Comp Neurol* 1985b;231(1):27-41.
- Altman J, Bayer SA. Embryonic development of the rat cerebellum. III. Regional differences in the time of origin, migration, and settling of Purkinje cells. *J Comp Neurol* 1985c;231(1):42-65.
- Altun G, Kaplan S, Deniz OG, Kocacan SE, Canan S, Davis D, Marangoz C. Protective effects of melatonin and omega-3 on the hippocampus and the cerebellum of adult Wistar albino rats exposed to electromagnetic fields. *J Microsc Ultrastruct* 2017;5(4):230-241.
- Aminuddin M, Partadiredja G, Sari DC. The effects of black garlic (*Allium sativum* L.) ethanol extract on the estimated total number of Purkinje cells and motor coordination of male adolescent Wistar rats treated with monosodium glutamate. *Anat Sci Int* 2015;90(2):75-81.

- Ammari M, Gamez C, Lecomte A, Sakly M, Abdelmelek H, De Seze R. GFAP expression in the rat brain following sub-chronic exposure to a 900 MHz electromagnetic field signal. *Int J Radiat Biol* 2010;86(5):367-375.
- Aslan A, İkinci A, Bas O, Sonmez OF, Kaya H, Odaci E. Long-term exposure to a continuous 900 MHz electromagnetic field disrupts cerebellar morphology in young adult male rats. *Biotech Histochem* 2017;92(5):324-330.
- Aslan L, Meral I. Effect of oral vitamin E supplementation on oxidative stress in guinea-pigs with short-term hypothermia. *Cell Biochem Funct* 2007;25(6):711-715.
- Assady M, Farahnak A, Golestani A, Esharghian M. Superoxide dismutase (SOD) enzyme activity assay in *Fasciola* spp. parasites and liver tissue extract. *Iran J Parasitol* 2011;6(4):17.
- Aydin B, Akar A. Effects of a 900-MHz electromagnetic field on oxidative stress parameters in rat lymphoid organs, polymorphonuclear leukocytes and plasma. *Arch Med Res* 2011;42(4):261-267.
- Bahreyni Toossi MH, Sadeghnia HR, Mohammad Mahdizadeh Feyzabadi M, Hosseini M, Hedayati M, Mosallanejad R, Beheshti F, Alizadeh Rahvar Z. Exposure to mobile phone (900–1800 MHz) during pregnancy: tissue oxidative stress after childbirth. *J Matern Fetal Neonatal Med* 2018;31(10):1298-1303.
- Barrett KE, Barman SM, Boitano S, Brooks HL. *Ganong's review of medical physiology*. 24th Ed., New York, The McGraw-Hill Companies Inc. 2012;248-251.
- Bas O, Odaci E, Mollaoglu H, Ucok K, Kaplan S. Chronic prenatal exposure to the 900 megahertz electromagnetic field induces pyramidal cell loss in the hippocampus of newborn rats. *Toxicol Ind Health* 2009;25(6):377-384.
- Basch E, Gabardi S, Ulbricht C. Bitter melon (*Momordica charantia*): a review of efficacy and safety. *Am J Health Syst Pharm* 2003;60(4):356-359.
- Becerril-Chávez H, Colín-González AL, Villeda-Hernández J, Galván-Arzate S, Chavarría A, Eduarda de Lima M, Túnez I, Santamaría A. Protective effects of S-allyl cysteine on behavioral, morphological and biochemical alterations in rats subjected to chronic restraint stress: Antioxidant and anxiolytic effects. *J Funct Foods* 2017;35:105-114.
- Bisen PS, Emerald M. Nutritional and therapeutic potential of garlic and onion (*Allium* sp.). *Curr Nutr Food Sci* 2016;12(3):190-199.
- Block E, Naganathan S, Putman D, Zhao SH. Organosulfur chemistry of garlic and onion: recent results. *Pure Appl Chem* 1993;65(4):625-632.

- Bloem E, Haneklaus S, Schnug E. Influence of fertilizer practices on S-containing metabolites in garlic (*Allium sativum* L.) under field conditions. *J Agric Food Chem* 2010;58(19):10690-10696.
- Borek C. Antioxidant health effects of aged garlic extract. *J Nutr* 2001;131(3):1010S-1015S.
- Borlinghaus J, Albrecht F, Gruhlke MC, Nwachukwu ID, Slusarenko AJ. Allicin: chemistry and biological properties. *Molecules* 2014;19(8):12591-12618.
- Brunetti L, Menghini L, Orlando G, Recinella L, Leone S, Epifano F, Lazzarin F, Chiavaroli A, Ferrante C, Vacca M. Antioxidant effects of garlic in young and aged rat brain in vitro. *J Med Food* 2009;12(5):1166-1169.
- Budrat P, Shotipruk A. Extraction of phenolic compounds from fruits of bitter melon (*Momordica charantia*) with subcritical water extraction and antioxidant activities of these extracts. *Chiang Mai J Sci* 2008;35(1):123-130.
- Calcabrini C, Mancini U, De bellis R, Diaz AR, Martinelli M, Cucchiarini L, Sestili P, Stocchi V, Potenza L. Effect of extremely low-frequency electromagnetic fields on antioxidant activity in the human keratinocyte cell line NCTC 2544. *Biotechnol Appl Biochem* 2017;64(3):415-422.
- Capasso A. Antioxidant action and therapeutic efficacy of *Allium sativum* L. *Molecules* 2013;18(1):690-700.
- Colin-Gonzalez AL, Santana RA, Silva-Islas CA, Chanez-Cardenas ME, Santamaria A, Maldonado PD. The antioxidant mechanisms underlying the aged garlic extract- and S-allylcysteine-induced protection. *Oxid Med Cell Longev* 2012;2012.
- Cui K, Luo X, Xu K, Murthy MV. Role of oxidative stress in neurodegeneration: recent developments in assay methods for oxidative stress and nutraceutical antioxidants. *Prog Neuropsychopharmacol Biol Psychiatry* 2004;28(5):771-799.
- Davis DL, Kesari S, Soskolne CL, Miller AB, Stein Y. Swedish review strengthens grounds for concluding that radiation from cellular and cordless phones is a probable human carcinogen. *Pathophysiology* 2013;20(2):123-129.
- Deshmukh PS, Nasare N, Megha K, Banerjee BD, Ahmed RS, Singh D, Abegaonkar MP, Tripathi AK, Mediratta PK. Cognitive impairment and neurogenotoxic effects in rats exposed to low-intensity microwave radiation. *Int J Toxicol* 2015;34(3):284-290.
- Devrim E, Ergüder İB, Kılıçoğlu B, Yaykaşlı E, Çetin R, Durak İ. Effects of electromagnetic radiation use on oxidant/antioxidant status and DNA turn-over enzyme activities in erythrocytes and heart, kidney, liver, and ovary tissues from rats: possible protective role of vitamin C. *Toxicol Mech Methods* 2008;18:679-683.

- Duan ZZ, Zhou XL, Li YH, Zhang F, Li FY, Su-Hua Q. Protection of Momordica charantia polysaccharide against intracerebral hemorrhage-induced brain injury through JNK3 signaling pathway. *J Recept Signal Transduct Res* 2015;35(6):523-529.
- Dubey RB, Hanmandlu M, Gupta SK. Risk of brain tumors from wireless phone use. *J Comput Assist Tomogr* 2010;34(6):799-807.
- Ebrahimzadeh-Bideskan AR, Hami J, Alipour F, Haghiri H, Fazel AR, Sadeghi A. Protective effects of ascorbic acid and garlic extract against lead-induced apoptosis in developing rat hippocampus. *Metab Brain Dis* 2016;31(5):1123-1132.
- Erdem koç G, Kaplan S, Altun G, Gümüş H, Gülsüm Deniz Ö, Aydın I, Emin Onger M, Altunkaynak Z. Neuroprotective effects of melatonin and omega-3 on hippocampal cells prenatally exposed to 900 MHz electromagnetic fields. *Int J Radiat Biol* 2016;92(10):590-595.
- Escribano BM, Agüera E, Aguilar-Luque M, Luque E, Feijóo M, Latorre M, Giraldo AI, Galván-Jurado A, Caballero-Villarraso J, García-Maceira FI, Santamaría A, Túnez I. Neuroprotective effect of S-allyl cysteine on an experimental model of multiple sclerosis: Antioxidant effects. *J Funct Foods* 2018;42:281-288.
- Fang EF, Zhang CZY, Fong WP, Ng TB. RNase MC2: a new Momordica charantia ribonuclease that induces apoptosis in breast cancer cells associated with activation of MAPKs and induction of caspase pathways. *Apoptosis* 2012a;17(4):377-387.
- Fang EF, Zhang CZY, Zhang L, Fong WP, Ng TB. In vitro and in vivo anticarcinogenic effects of RNase MC2, a ribonuclease isolated from dietary bitter melon, toward human liver cancer cells. *Int J Biochem Cell Biol* 2012b;44(8):1351-1360.
- Fernandes NP, Lagishetty CV, Panda VS, Naik SR. An experimental evaluation of the antidiabetic and antilipidemic properties of a standardized Momordica charantia fruit extract. *BMC Complement Altern Med* 2007;7(1):29.
- Friedman J, Kraus S, Hauptman Y, Schiff Y, Seger R. Mechanism of short-term ERK activation by electromagnetic fields at mobile phone frequencies. *Biochem J* 2007;405(3):559-568.
- Fuangchan A, Sonthisombat P, Seubnukarn T, Chanouan R, Chotchaisuwat P, Sirigulsatien V, Ingkaninan K, Plianbangchang P, Haines ST. Hypoglycemic effect of bitter melon compared with metformin in newly diagnosed type 2 diabetes patients. *J Ethnopharmacol* 2011;134(2):422-428.
- Gao X, Björk L, Trajkovski V, Uggla M. Evaluation of antioxidant activities of rosehip ethanol extracts in different test systems. *J Sci Food Agric* 2000;80(14):2021-2027.

- Ghasemi S, Hosseini M, Feizpour A, Alipour F, Sadeghi A, Vafae F, Mohammadpour T, Soukhtanloo M, Ebrahimzadeh Bideskan A, Beheshti F. Beneficial effects of garlic on learning and memory deficits and brain tissue damages induced by lead exposure during juvenile rat growth is comparable to the effect of ascorbic acid. *Drug Chem Toxicol* 2017;40(2):206-214.
- Glaser R. Are thermoreceptors responsible for “non-thermal” effects of RF fields. *Edition Wissenschaft* 2005;G14515(21):2-13.
- Gong J, Sun F, Li Y, Zhou X, Duan Z, Duan F, Zhao L, Chen H, Qi S, Shen J. Momordica charantia polysaccharides could protect against cerebral ischemia/reperfusion injury through inhibiting oxidative stress mediated c-Jun N-terminal kinase 3 signaling pathway. *Neuropharmacology* 2015;91:123-134.
- Goraca A, Ciejka E, Piechota A. Effects of extremely low frequency magnetic field on the parameters of oxidative stress in heart. *J Physiol Pharmacol* 2010;61(3):333-338.
- Gray H, Standring S. *Gray's Anatomy: The anatomical basis of clinical practice*. 40th Ed., London, Churchill Livingstone Elsevier. 2008;527-529.
- Gundersen H, Bendtsen TF, Korbo L, Marcussen N, Møller A, Nielsen K, Nyengaard J, Pakkenberg B, Sørensen FB, Vesterby A. Some new, simple and efficient stereological methods and their use in pathological research and diagnosis. *APMIS* 1988b;96(1-6):379-394.
- Gundersen H, Jensen E. The efficiency of systematic sampling in stereology and its prediction. *J Microsc* 1987;147(3):229-263.
- Gundersen HJG. Notes on the estimation of the numerical density of arbitrary profiles: the edge effect. *J Microsc* 1977;111(2):219-223.
- Gundersen HJG, Bagger P, Bendtsen T, Evans S, Korbo L, Marcussen N, Møller A, Nielsen K, Nyengaard J, Pakkenberg B. The new stereological tools: disector, fractionator, nucleator and point sampled intercepts and their use in pathological research and diagnosis. *APMIS* 1988a;96(7-12):857-881.
- Gundersen HJG, Jensen EBV, Kieu K, Nielsen J. The efficiency of systematic sampling in stereology-reconsidered. *J Microsc* 1999;193(3):199-211.
- Habicht SD, Kind V, Rudloff S, Borsch C, Mueller AS, Pallauf J, Yang R, Krawinkel MB. Quantification of antidiabetic extracts and compounds in bitter melon varieties. *Food Chem* 2011;126(1):172-176.

- Hagan CE, Bolon B, Keene CD. Nervous system. In: Treuting PM, Dintzis SM, editors. Comparative anatomy and histology: a mouse and human atlas. 1st Ed., London, Academic Press Elsevier. 2012;339-362.
- Haghani M, Shabani M, Moazzami K. Maternal mobile phone exposure adversely affects the electrophysiological properties of Purkinje neurons in rat offspring. *Neuroscience* 2013;250:588-598.
- Hall JE. Guyton and Hall Textbook of Medical Physiology. 13th Ed., Philadelphia, Elsevier Inc. 2016;722-727
- Halliwell B. How to characterize an antioxidant: an update. *Biochem Soc Symp* 1995;61:73-101.
- Halliwell B. Role of free radicals in the neurodegenerative diseases: therapeutic implications for antioxidant treatment. *Drugs Aging* 2001;18(9):685-716.
- Hardell L, Carlberg M. Mobile phone and cordless phone use and the risk for glioma-Analysis of pooled case-control studies in Sweden, 1997–2003 and 2007–2009. *Pathophysiology* 2015;22(1):1-13.
- Hardell L, Carlberg M, Mild KH. Pooled analysis of two case–control studies on use of cellular and cordless telephones and the risk for malignant brain tumours diagnosed in 1997–2003. *Int Arch Occup Environ Health* 2006;79(8):630-639.
- Hardell L, Carlberg M, Söderqvist F, Hansson Mild K. Meta-analysis of long-term mobile phone use and the association with brain tumours. *Int J Oncol* 2008;32(5):1097-1103.
- Hardell L, Sage C. Biological effects from electromagnetic field exposure and public exposure standards. *Biomed Pharmacother* 2008;62:104-109.
- Hardell LO, Carlberg M, Söderqvist F, Mild KH, Morgan LL. Long-term use of cellular phones and brain tumours-increased risk associated with use for > 10 years. *Occup Environ Med* 2007;64(9):626-632.
- Heinrich S, Thomas S, Heumann C, Von Kries R, Radon K. The impact of exposure to radio frequency electromagnetic fields on chronic well-being in young people - a cross-sectional study based on personal dosimetry. *Environ Int* 2011;37(1):26-30.
- Hermawati E, Sari C, Partadiredja G. The effects of black garlic ethanol extract on the spatial memory and estimated total number of pyramidal cells of the hippocampus of monosodium glutamate-exposed adolescent male Wistar rats. *Anat Sci Int* 2015; 90(4):275-286.

- Horax R, Hettiarachchy N, Islam S. Total phenolic contents and phenolic acid constituents in 4 varieties of bitter melons (*Momordica charantia*) and antioxidant activities of their extracts. *J Food Sci* 2005;70(4):C275-C280.
- Horníčková J, Kubec R, Cejpek K, Velišek J, Ovesna J, Stavěliková H. Profiles of S-alk(en)ylcysteine sulfoxides in various garlic genotypes. *Czech J Food Sci* 2010;28(4):298-308.
- Husna RN, Noriham A, Nooraain H, Azizah AH, Amna OF. Acute oral toxicity effects of *Momordica charantia* in sprague dawley rats. *Int J Biosci Biochem Bioinforma* 2013;3(4):408-410.
- Idrus NM, Napper RM. Acute and long-term Purkinje cell loss following a single ethanol binge during the early third trimester equivalent in the rat. *Alcohol Clin Exp Res* 2012;36(8):1365-1373.
- Ilhan A, Gurel A, Armutcu F, Kamisli S, Iraz M, Akyol O, Ozen S. Ginkgo biloba prevents mobile phone-induced oxidative stress in rat brain. *Clin Chim Acta* 2004;340(1-2):153-162.
- Jabbes N, Arnault I, Auger J, Dridi BAM, Hannachi C. Agro-morphological markers and organo-sulphur compounds to assess diversity in Tunisian garlic landraces. *Sci Hortic* 2012;148:47-54.
- Kavitha N, Babu SM, Rao ME. Influence of *Momordica charantia* on oxidative stress-induced perturbations in brain monoamines and plasma corticosterone in albino rats. *Indian J Pharmacol* 2011;43(4):424-428.
- Khurana VG, Hardell L, Everaert J, Bortkiewicz A, Carlberg M, Ahonen M. Epidemiological evidence for a health risk from mobile phone base stations. *Int J Occup Environ Health* 2010;16(3):263-267.
- Kivrak EG, Altunkaynak BZ, Alkan I, Yurt KK, Kocaman A, Onger ME. Effects of 900-MHz radiation on the hippocampus and cerebellum of adult rats and attenuation of such effects by folic acid and *Boswellia sacra*. *J Microsc Ultrastruct* 2017b;5(4):216-224.
- Kivrak EG, Yurt KK, Kaplan AA, Alkan I, Altun G. Effects of electromagnetic fields exposure on the antioxidant defense system. *J Microsc Ultrastruct* 2017a;5(4):167-176.
- Kocaman A, Altun G, Kaplan AA, Deniz ÖG, Yurt KK, Kaplan S. Genotoxic and carcinogenic effects of non-ionizing electromagnetic fields. *Environ Res* 2018;163:71-79.

- Kopec A, Piatkowska E, Leszczynska T, Sikora E. Healthy properties of garlic. *Curr Nutr Food Sci* 2013;9(1):59-64.
- Kristiansen SLB, Nyengaard JR. Digital stereology in neuropathology. *APMIS* 2012; 120(4):327-340.
- Kubola J, Siriamornpun S. Phenolic contents and antioxidant activities of bitter gourd (*Momordica charantia* L.) leaf, stem and fruit fraction extracts in vitro. *Food Chem* 2008;110(4):881-890.
- Lahkola A, Salminen T, Raitanen J, Heinävaara S, Schoemaker M, Christensen HC, Feychting M, Johansen C, Klæboe L, Lönn S. Meningioma and mobile phone use - a collaborative case-control study in five North European countries. *Int J Epidemiol* 2008;37(6):1304-1313.
- Lanzotti V, Scala F, Bonanomi G. Compounds from *Allium* species with cytotoxic and antimicrobial activity. *Phytochem Rev* 2014;13(4):769-791.
- Lobo V, Patil A, Phatak A, Chandra N. Free radicals, antioxidants and functional foods: Impact on human health. *Pharmacogn Rev* 2010;4(8):118.
- Lucas EA, Dumancas GG, Smith BJ, Clarke SL, Arjmandi BH. Health benefits of bitter melon (*Momordica charantia*). In: Watson RR, Preedy VR, editors. *Bioactive Foods in Promoting Health: Fruits and Vegetables*. 1st Ed., London, Academic Press Elsevier 2010;525-549.
- Madeo F, Fröhlich E, Ligr M, Grey M, Sigrist SJ, Wolf DH, Fröhlich KU. Oxygen stress: a regulator of apoptosis in yeast. *J Cell Biol* 1999;145(4):757-767.
- Manikonda PK, Rajendra P, Devendranath D, Gunasekaran B, Aradhya RSS, Sashidhar RB, Subramanyam C. Influence of extremely low frequency magnetic fields on Ca^{2+} signaling and NMDA receptor functions in rat hippocampus. *Neurosci Lett* 2007;413(2):145-149.
- Manoj Kumar V, Henley AK, Nelson CJ, Indumati O, Rao YP, Rajanna S, Rajanna B. Protective effect of *Allium sativum* (garlic) aqueous extract against lead-induced oxidative stress in the rat brain, liver, and kidney. *Environ Sci Pollut Res Int* 2017;24(2):1544-1552.
- Martínez-Sámano J, Torres-Durán PV, Juárez-Oropeza MA, Elías-Viñas D, Verdugo-Díaz L. Effects of acute electromagnetic field exposure and movement restraint on antioxidant system in liver, heart, kidney and plasma of Wistar rats: a preliminary report. *Int J Radiat Biol* 2010;86(12):1088-1094.

- Martínez-Sámano J, Torres-Durán PV, Juárez-Oropeza MA, Verdugo-Díaz L. Effect of acute extremely low frequency electromagnetic field exposure on the antioxidant status and lipid levels in rat brain. *Arch Med Res* 2012;43(3):183-189.
- Martins D, English AM. Catalase activity is stimulated by H₂O₂ in rich culture medium and is required for H₂O₂ resistance and adaptation in yeast. *Redox Biol* 2014;2:308-313.
- Martins N, Petropoulos S, Ferreira IC. Chemical composition and bioactive compounds of garlic (*Allium sativum* L.) as affected by pre- and post-harvest conditions: A review. *Food Chem* 2016;211:41-50.
- Maskey D, Kim M, Aryal B, Pradhan J, Choi IY, Park KS, Son T, Hong SY, Kim SB, Kim HG. Effect of 835 MHz radiofrequency radiation exposure on calcium binding proteins in the hippocampus of the mouse brain. *Brain Res* 2010;1313:232-241.
- Mausset-Bonnefont AL, Hirbec H, Bonnefont X, Privat A, Vignon J, De Seze R. Acute exposure to GSM 900-MHz electromagnetic fields induces glial reactivity and biochemical modifications in the rat brain. *Neurobiol Dis* 2004;17(3):445-454.
- Mausset AL, De Seze R, Montpeyroux F, Privat A. Effects of radiofrequency exposure on the GABAergic system in the rat cerebellum: clues from semi-quantitative immunohistochemistry. *Brain Res* 2001;912(1):33-46.
- Meral I, Mert H, Mert N, Deger Y, Yoruk I, Yetkin A, Keskin S. Effects of 900-MHz electromagnetic field emitted from cellular phone on brain oxidative stress and some vitamin levels of guinea pigs. *Brain Res* 2007;1169:120-124.
- Mescher AL. Junqueira's basic histology: text and atlas. 13th Ed., New York, McGraw-Hill Education. 2013;175-177.
- Moulder JE. Power-frequency fields and cancer. *Crit Rev Biomed Eng* 1998;26(1-2):1-116.
- Nakagawa S, Masamoto K, Sumiyoshi H, Harada H. Acute toxicity test of garlic extract. *J Toxicol Sci* 1984;9(1):57-60.
- Neltner TG, Kulkarni NR, Alger HM, Maffini MV, Bongard ED, Fortin ND, Olson ED. Navigating the US food additive regulatory program. *Compr Rev Food Sci Food Saf* 2011;10(6):342-68.
- Nerurkar PV, Johns LM, Buesa LM, Kipyakwai G, Volper E, Sato R, Shah P, Feher D, Williams PG, Nerurkar VR. *Momordica charantia* (bitter melon) attenuates high-fat diet-associated oxidative stress and neuroinflammation. *J Neuroinflammation* 2011;8(1):64.

- Nerurkar PV, Lee YK, Motosue M, Adeli K, Nerurkar VR. Momordica charantia (bitter melon) reduces plasma apolipoprotein B-100 and increases hepatic insulin receptor substrate and phosphoinositide-3 kinase interactions. *Br J Nutr* 2008;100(4):751-759.
- Niki E, Noguchi N, Tsuchihashi H, Gotoh N. Interaction among vitamin C, vitamin E, and beta-carotene. *Am J Clin Nutr* 1995;62(6):1322S-1326S.
- Nillert N, Pannangrong W, Welbat JU, Chaijaroonkhanarak W, Sripanidkulchai K, Sripanidkulchai B. Neuroprotective Effects of Aged Garlic Extract on Cognitive Dysfunction and Neuroinflammation Induced by β -Amyloid in Rats. *Nutrients* 2017;9(1):24.
- Noorafshan A, Asadi-Golshan R, Abdollahifar MA, Karbalay-Doust S. Protective role of curcumin against sulfite-induced structural changes in rats' medial prefrontal cortex. *Nutr Neurosci* 2015;18(6):248-255.
- Nurmasitoh T, Sari DCR, Partadiredja G. The effects of black garlic on the working memory and pyramidal cell number of medial prefrontal cortex of rats exposed to monosodium glutamate. *Drug Chem Toxicol* 2018;41(3):324-329.
- Odaci E, Bas O, Kaplan S. Effects of prenatal exposure to a 900 MHz electromagnetic field on the dentate gyrus of rats: a stereological and histopathological study. *Brain Res* 2008;1238:224-229.
- Odaci E, Hanci H, İkinci A, Sonmez OF, Aslan A, Şahin A, Kaya H, Çolakoğlu S, Bas O. Maternal exposure to a continuous 900-MHz electromagnetic field provokes neuronal loss and pathological changes in cerebellum of 32-day-old female rat offspring. *J Chem Neuroanat* 2016;75:105-110.
- Ozra A, Jafar SR, Moradi L, Saki G. Ultrastructural change of cerebellum in exposed rats to 3mT electromagnetic field. *J Biol Sci* 2010;10(6):526-530.
- Ozusaglam MA, Karakoca K. Antimicrobial and antioxidant activities of Momordica charantia from Turkey. *Afr J Biotechnol* 2013;12(13):1548-1558.
- Park JH, Park YK, Park E. Antioxidative and antigenotoxic effects of garlic (*Allium sativum* L.) prepared by different processing methods. *Plant Foods Hum Nutr* 2009; 64(4):244-249.
- Pawlina W, Ross MH. *Histology: a text and atlas with correlated cell and molecular biology.* 7th Ed., Philadelphia, Wolters Kluwer Health. 2016;400-401.
- Peltola V, Huhtaniemi I, Ahotupa M. Antioxidant enzyme activity in the maturing rat testis. *J Androl* 1992;13(5):450-455.

- Pişkin A, Altunkaynak BZ, Tümentemur G, Kaplan S, Yazıcı ÖB, Hökelek M. The beneficial effects of *Momordica charantia* (bitter melon) on wound healing of rabbit skin. *J Dermatolog Treat* 2014;25(4):350-357.
- Prasad V, Jain V, Girish D, Dorle AK. Wound-healing property of *Momordica charantia* L. fruit powder. *J Herb Pharmacother* 2006;6(3-4):105-115.
- Preece AW. Effect of a 915-MHz simulated mobile phone signal on cognitive function in man. *Int J Radiat Biol* 1999;75(4):447-456.
- Rabinkov A, Miron T, Konstantinovski L, Wilchek M, Mirelman D, Weiner L. The mode of action of allicin: trapping of radicals and interaction with thiol containing proteins. *Biochim Biophys Acta* 1998;1379(2):233-244.
- Rafati A, Noorafshan A, Jahangir M, Hosseini L, Karbalay-Doust S. Vitamin E can improve behavioral tests impairment, cell loss, and dendrite changes in rats' medial prefrontal cortex induced by acceptable daily dose of aspartame. *Acta Histochem* 2018;120(1):46-55.
- Rafati A, Nourzei N, Karbalay-Doust S, Noorafshan A. Using vitamin E to prevent the impairment in behavioral test, cell loss and dendrite changes in medial prefrontal cortex induced by tartrazine in rats. *Acta Histochem* 2017;119(2):172-180.
- Rağbetli MC, Aydinlioğlu A, Koyun N, Rağbetli C, Bektas Ş, Ozdemir S. The effect of mobile phone on the number of Purkinje cells: a stereological study. *Int J Radiat Biol* 2010;86(7):548-554.
- Rağbetli MC, Aydinlioğlu A, Koyun N, Rağbetli C, Karayel M. Effect of prenatal exposure to mobile phone on pyramidal cell numbers in the mouse hippocampus: a stereological study. *Int J Neurosci* 2009;119(7):1031-1041.
- Rahman MS. Allicin and other functional active components in garlic: health benefits and bioavailability. *Int J Food Prop* 2007;10(2):245-268.
- Ray B, Chauhan NB, Lahiri DK. Oxidative insults to neurons and synapse are prevented by aged garlic extract and S-allyl-L-cysteine treatment in the neuronal culture and APP-Tg mouse model. *J Neurochem* 2011;117(3):388-402.
- Rekowska E, Skupień K. The influence of selected agronomic practices on the yield and chemical composition of winter garlic. *Veg Crops Res Bull* 2009;70:173-182.
- Rubtsova N, Perov S, Belaya O, Kuster N, Balzano Q. Near-field radiofrequency electromagnetic exposure assessment. *Electromagn Biol Med* 2015;34(3):180-182.

- Salehi I, Komaki A, Karimi SA, Sarihi A, Zarei M. Effect of garlic powder on hippocampal long-term potentiation in rats fed high fat diet: an in vivo study. *Metab Brain Dis* 2018;33(3):725-731.
- Salford LG, Brun AE, Eberhardt JL, Malmgren L, Persson BR. Nerve cell damage in mammalian brain after exposure to microwaves from GSM mobile phones. *Environ Health Perspect* 2003;111(7):881-883.
- Santos AK, Costa JG, Menezes IR, Cansancao IF, Santos KK, Matias EF, Coutinho HD. Antioxidant activity of five Brazilian plants used as traditional medicines and food in Brazil. *Pharmacogn Mag* 2010;6(24):335-338.
- Sato E, Kohno M, Hamano H, Niwano Y. Increased anti-oxidative potency of garlic by spontaneous short-term fermentation. *Plant Foods Hum Nutr* 2006;61(4):157-160.
- Semiz A, Sen A. Antioxidant and chemoprotective properties of *Momordica charantia* L.(bitter melon) fruit extract. *Afr J Biotechnol* 2007;6(3):273-277.
- Sepehrimanesh M, Nazifi S, Saeb M, Kazemipour N. Effect of 900MHz radiofrequency electromagnetic field exposure on serum and testicular tissue antioxidant enzymes of rat. *Onl J Vet Res* 2016;20(9):617-624.
- Singh UP, Maurya S, Singh A. Phenolic acids in some Indian cultivars of *Momordica charantia* and their therapeutic properties. *J Med Plant Res* 2011;5(15):3558-3560.
- Singleton VL, Rossi JA. Colorimetry of total phenolics with phosphomolybdic-phosphotungstic acid reagents. *Am J Enol Viticult* 1965;16(3):144-158.
- Sinnatamby CS. *Last's Anatomy: regional and applied*. 12th Ed., London, Churchill Livingstone Elsevier. 2011;488-489.
- Sonmez OF, Odaci E, Bas O. & Kaplan, S. Purkinje cell number decreases in the adult female rat cerebellum following exposure to 900 MHz electromagnetic field. *Brain Res* 2010;1356:95-101.
- Staebler P. *Human exposure to electromagnetic fields: from extremely low frequency (ELF) to radiofrequency*. 1st Ed., UK and USA, ISTE Ltd and John Wiley & Sons Inc. 2017; 10-37.
- Sterio D. The unbiased estimation of number and sizes of arbitrary particles using the disector. *J Microsc* 1984;134(2):127-136.
- Tan ES, Abdullah A, Maskat MY. Effect of drying methods on total antioxidant capacity of bitter gourd (*momordica charantia*) fruit. *AIP Conf Proc* 2013;1571(1):710-716.

- Tan SP, Kha TC, Parks SE, Roach PD. Bitter melon (*Momordica charantia* L.) bioactive composition and health benefits: a review. *Food Rev Int* 2016;32(2):181-202.
- Tang J, Zhang Y, Yang L, Chen Q, Tan L, Zuo S, Feng H, Chen Z, Zhu G. Exposure to 900 MHz electromagnetic fields activates the mep-1/ERK pathway and causes blood-brain barrier damage and cognitive impairment in rats. *Brain Res* 2015;1601:92-101.
- Terzi M, Ozberk B, Deniz OG, Kaplan S. The role of electromagnetic fields in neurological disorders. *J Chem Neuroanat* 2016;75:77-84.
- Thenmozhi AJ, Subramanian P. Antioxidant Potential of *Momordica Charantia* in Ammonium Chloride-Induced Hyperammonemic Rats. *Evid Based Complement Alternat Med* 2011;2011:1-7.
- Treuting PM, Dintzis SM, Montine KS. Comparative anatomy and histology: a mouse, rat, and human atlas. 2nd Ed., London, Academic Press Elsevier. 2017;403-412.
- Tural S, Koca I. Physico-chemical and antioxidant properties of cornelian cherry fruits (*Cornus mas* L.) grown in Turkey. *Sci Hortic* 2008;116(4):362-366.
- Ukeda H, Kawana D, Maeda S, Sawamura M. Spectrophotometric assay for superoxide dismutase based on the reduction of highly water-soluble tetrazolium salts by xanthine-xanthine oxidase. *Biosci Biotechnol Biochem* 1999;63(3):485-488.
- Van Rongen E, Croft R, Juutilainen J, Lagroye I, Miyakoshi J, Saunders R, De Seze R, Tenforde T, Verschaeve L, Veyret B. Effects of radiofrequency electromagnetic fields on the human nervous system. *J Toxicol Environ Health B Crit Rev* 2009;12(8):572-597.
- Viggiano A, Viggiano D, Viggiano A, Luca BD. Quantitative histochemical assay for superoxide dismutase in rat brain. *J Histochem Cytochem* 2003;51(7):865-871.
- Wang X, Liu C, Ma Q, Feng W, Yang L, Lu Y, Zhou Z, Yu Z, Li W, Zhang L. 8-oxoG DNA glycosylase-1 inhibition sensitizes Neuro-2a cells to oxidative DNA base damage induced by 900 MHz radiofrequency electromagnetic radiation. *Cell Physiol Biochem* 2015;37(3):1075-1088.
- West M, Slomianka L, Gundersen HJG. Unbiased stereological estimation of the total number of neurons in the subdivisions of the rat hippocampus using the optical fractionator. *Anat Rec* 1991;231(4):482-497.
- Xu XH, Li GL, Wang BA, Qin Y, Bai SR, Rong J, Deng T, Li Q. Diallyl trisulfide protects against oxygen glucose deprivation -induced apoptosis by scavenging free radicals via the PI3K/Akt -mediated Nrf2/HO-1 signaling pathway in B35 neural cells. *Brain Res* 2015;1614:38-50.

Zhang SX, Niu YL, Tian ZQ, He GR, Wang LJ, Wang JP. Diallyl Sulfide Attenuates Iminodipropionitrile Provoked Oxidative Neuropathy in a Rat Model. *Lat Am J Pharm* 2016;35(5):991-1000.



APPENDICES

Ethical Committee Approval Certificate



GİZLİ
T.C.
ONDOKUZ MAYIS ÜNİVERSİTESİ
Hayvan Deneyleri Yerel Etik Kurulu



Sayı : 68489742-604.01.02-E.8235
Konu : HADYЕК izin Onayı Hk.

04/04/2017

DOÇ.DR. BERRİN ZUHAL ALTUNKAYNAK

ETİK KURUL KARARI

KARAR NO: 2017/11

Proje No 2017/11

KARAR TARİHİ: 31.03.2017

PROJE BAŞLIĞI: 900 MHz elektromanyetik alana maruz kalmış sıçan beyinciği üzerine *Momordica charantia* ve sarımsağın muhtemel etkilerinin araştırılması
YÜRÜTÜCÜ: Doç. Dr. Berrin Zuhall ALTUNKAYNAK
E-POSTA: zuhal.altunkaynak@omu.edu.tr
KURUM: Ondokuz Mayıs Üniversitesi

TC NO: 13253133708
MOBİL TEL: 05067723379
İÇ HAT TEL NO: 2268

ARAŞTIRICILAR: (Yürütücü dışındakiler)

1.Arş.Gör. Fathelrahman Ali Ondokuz Mayıs Üniversitesi
2.Arş.Gör. Gamze ALTUN Ondokuz Mayıs Üniversitesi

- Yukarıda tanımlanan Denev Hayvanları ile yapılan çalışmayı; belirtilen araştırmacılar ile gerçekleştireceğini, ekip dışında başka kişileri HADYЕК ten izin almadan iştirak ettirmeyeceğini, çalışmanın başından sonuna kadar başkaları ile paylaşmayacağını ve yayın haline dönüştüğünde belirtilen katkı sırasına göre yayınlayacağını,
- Üniversitemiz WEB sayfasında güncel hali yayınlanan, Ondokuz Mayıs Üniversitesi Hayvan Deneyleri Yerel Etik Kurulu Yönergesine uygun olarak çalışacağını,
- Onay alınmış Projede belirtilen Denev Hayvanları Kullanımına müsaade edilen kişilerin haricinde başkalarına hayvanlarda herhangi bir Deneysel işlem yaptırmayacağını ve Proje sürecinde işlemlerde ve çalışma ekibinde yapılacak değişiklikler için HADYЕК'e izin başvurusunda bulunacağını ve onay gelinceye kadar çalışmalarını durduracağını,
- Proje onay tarihinden itibaren her 6(altı) ay sonrasında HADYЕК'e gelişim raporu vereceğini ve Proje bitim tarihini müteakiben 3 ay içerisinde çalışma sonucunu HADYЕК'e bildireceğini, Bu Proje süresince, Ondokuz Mayıs Üniversitesi Hayvan Deneyleri Yerel Etik Kurulu Yönergesinde yer alan etik ilkelerle uyumsuz veya beklenmeyen ters bir etki veya olay olduğunda derhal Yerel Etik Kurul'a bildireceğini Kabul ve taahhüt eden kimlik ve iletişim bilgileri yukarıda yazılı yürütücünün Araştırma Projesi, Etik Kurul Üyeleri tarafından OMU HADYЕК yönergesi kapsamında Hayvan Hakları ve Denev Etik İlkelerine UYGUN bulunmuştur.

e-imzadır

Prof. Dr. Ferişt Kolbakır
HADYЕК

Curriculum Vitae

Full Name: Fathelrahman Idris Gasmelseed ALI

Place of Birth: Bahri-Khartoum State-Sudan

Date of Birth: 01/11/1988

Marital Status: Single

Nationality: Sudanese

Educational Status (Institution and Year):

MBBS: Faculty of Medicine- University of Khartoum 2005-2011 Khartoum, Sudan

Ph.D.: Department of Histology and Embryology- Faculty of Medicine- Ondokuz Mayıs
University 2013-2019 Samsun, Turkey

E-mail: fathelrahman@uofk.edu or fathelrahman.234@gmail.com